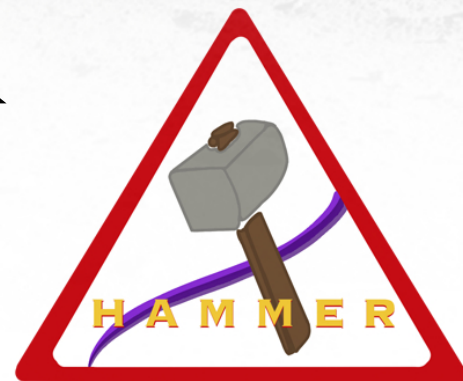


# HAMMER

*Human Assisted Martian Moons  
Explore and Return*

## **Space Pirates**

*The University of Texas at Austin  
Cockrell School of Engineering*

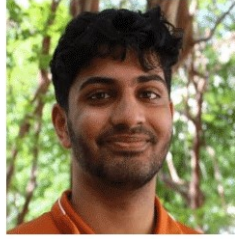




**AIAA#:** 1357840

*Reece Appel*

Reece Appel



**AIAA#:** 1357857

*Teja Gorantla*

Teja Gorantla



**AIAA#:** 981791

*Nick Delurgio*

Nick Delurgio



**AIAA#:** 1357950

*Christian Hinton*

Christian Hinton



**AIAA#:** 1357006

*Jhereg Jones*

Jhereg Jones



**AIAA#:** 1357839

*Pete Lealiiee Jr*

Pete Lealiiee Jr



**AIAA#:** 1357897

*Shea Popov*

Shea Popov



**AIAA#:** 1357004

*Shannon Scott*

Shannon Scott



**AIAA#:** 1357585

*Nils Schlautmann*

Nils Schlautmann



**AIAA#:** 1326022

*Rye Seekins*

Rye Seekins



**Faculty Advisor**

*Adam Nokes*

Adam Nokes

# Table of Contents

|          |  |           |
|----------|--|-----------|
| <b>1</b> | <b>Executive Summary</b>                                     | <b>1</b>  |
| 1.1      | Concept of Operations . . . . .                              | 2         |
| 1.2      | Environment . . . . .  | 3         |
| 1.3      | EEV Design . . . . .   | 3         |
| 1.4      | Payload and Sampling . . . . .                               | 4         |
| 1.5      | Deep Space Transport . . . . .                               | 5         |
| <b>2</b> | <b>Mission Overview</b>                                      | <b>6</b>  |
| 2.1      | Analysis of Needs . . . . .                                  | 6         |
| 2.2      | System Level Requirements . . . . .                          | 6         |
| 2.3      | Mission Objectives of the EEV . . . . .                      | 7         |
| 2.4      | Scientific Objectives of HAMMER . . . . .                    | 8         |
| <b>3</b> | <b>Mission Architecture</b>                                  | <b>10</b> |
| 3.1      | Concept of Operations . . . . .                              | 10        |
| 3.2      | Trajectory Design and Space Logistics Optimization . . . . . | 14        |
| 3.2.1    | Mars Transfer Optimization . . . . .                         | 14        |
| 3.2.2    | Parking Orbit . . . . .                                      | 15        |
| 3.2.3    | Inbound Orbit Logistics Optimization . . . . .               | 16        |
| 3.2.4    | $\Delta V$ Budget . . . . .                                  | 19        |
| 3.3      | Landing Location Assessment . . . . .                        | 20        |
| 3.4      | Phobos and Deimos Space Environment . . . . .                | 21        |
| 3.4.1    | Surface Qualities . . . . .                                  | 21        |
| 3.4.2    | Gravity And Its Implications . . . . .                       | 21        |
| 3.4.3    | Electrostatic Environment . . . . .                          | 22        |
| 3.5      | Resupplying with the DST . . . . .                           | 23        |
| 3.5.1    | Logistics of Resupplying . . . . .                           | 23        |
| 3.5.2    | Logistics of Refueling . . . . .                             | 24        |
| <b>4</b> | <b>Exploration Excursion Vehicle</b>                         | <b>26</b> |
| 4.1      | EEV Overview . . . . .                                       | 26        |
| 4.1.1    | Mass and Power Budget . . . . .                              | 29        |
| 4.1.2    | Launch Vehicle Selection . . . . .                           | 32        |
| 4.2      | Guidance, Navigation, and Control . . . . .                  | 32        |
| 4.2.1    | System Architecture . . . . .                                | 32        |
| 4.2.2    | Navigation Sensors . . . . .                                 | 34        |
| 4.2.3    | Reaction Control System . . . . .                            | 35        |
| 4.2.4    | Maneuvers . . . . .  | 38        |
| 4.3      | Command and Data Handling . . . . .                          | 39        |
| 4.3.1    | System Architecture . . . . .                                | 40        |

|          |  |           |
|----------|--|-----------|
| 4.3.2    | Risk and Risk Mitigation . . . . .   | 42        |
| 4.4      | Propulsion . . . . .   | 42        |
| 4.4.1    | Propulsion Requirements . . . . .  | 43        |
| 4.4.2    | Propulsion Design . . . . .  | 44        |
| 4.4.3    | Propulsion Fluids System . . . . .   | 48        |
| 4.5      | Structures . . . . .   | 49        |
| 4.5.1    | Structures Design . . . . .  | 49        |
| 4.5.2    | Landing Legs Analysis . . . . .  | 51        |
| 4.6      | Payload & Sampling Systems . . . . .   | 51        |
| 4.6.1    | Sampling Procedures and Sample Containment . . . . .                         | 51        |
| 4.6.2    | Coring Sampling System Architecture (C-Sampling) . . . . .                   | 53        |
| 4.6.3    | Excavation/Encapsulating Sampling System Architecture (E-Sampling) . . . . . | 56        |
| 4.6.4    | Additional Scientific Instruments and Imagers . . . . .                      | 58        |
| 4.7      | Environmental Control and Life Support System . . . . .                      | 60        |
| 4.7.1    | Requirements and Consumables . . . . .                                       | 60        |
| 4.7.2    | ECLSS Architecture . . . . .   | 60        |
| 4.8      | Communications . . . . .   | 67        |
| 4.8.1    | System Requirements & Architecture . . . . .                                 | 67        |
| 4.8.2    | EEV Communications Trade Study . . . . .                                     | 68        |
| 4.9      | Power . . . . .  | 74        |
| 4.9.1    | System Requirements Overview . . . . .                                       | 74        |
| 4.9.2    | Design And Sizing . . . . .  | 74        |
| 4.9.3    | Modes . . . . .  | 76        |
| 4.9.4    | Human Safety Design Considerations . . . . .                                 | 77        |
| 4.10     | Thermal Control . . . . .  | 78        |
| 4.10.1   | TCS Calculations & Environmental Conditions . . . . .                        | 78        |
| 4.10.2   | TCS Subsystem Architecture . . . . .   | 78        |
| 4.10.3   | Thermal Heater Architecture . . . . .  | 80        |
| <b>5</b> | <b>Deep Space Transport</b>  | <b>81</b> |
| 5.1      | DST Requirements . . . . .   | 81        |
| 5.2      | Refuelling in Space . . . . .  | 81        |
| 5.3      | Communications . . . . .   | 83        |
| <b>6</b> | <b>Mission Management</b>  | <b>84</b> |
| 6.1      | Research, Development & Integration Schedule . . . . .                       | 84        |
| 6.2      | Cost Analysis . . . . .  | 85        |
| <b>7</b> | <b>Conclusions</b>   | <b>87</b> |
| 7.1      | Compliance Matrix . . . . .  | 88        |
|          | <b>Appendix A Definitions</b>  | <b>v</b>  |

# List of Figures

|      |   |    |
|------|---|----|
| 2.1  | System Level Requirements . . . . .   | 7  |
| 3.1  | Visualization of phases of EEV operations that occur before landing. . . . .  | 12 |
| 3.2  | Phases of EEV operations during landing . . . . .   | 13 |
| 3.3  | Porkchop Diagrams which indicate the Departure (left) and Arrival (right) $\Delta V$ for the Earth-Mars Transfer . . . . .                                    | 14 |
| 3.4  | Comparison demonstrating the similarity between the calculated solution (left) and the NASA Ames Trajectory Browser (right) . . . . .                         | 15 |
| 3.5  | 5 Sol Orbit that the DST will be in for the duration of the mission, and where the EEV will be at the beginning of the mission. . . . .                       | 16 |
| 3.6  | Schedule and $\Delta V$ for each maneuver. . . . .  | 19 |
| 3.8  | Illustration of solar wind impacting a perfect sphere - reflects an electrostatic charged environment via solar wind. . . . .                                 | 22 |
| 3.9  | Expected propellant mass transfer for each refueling event. . . . .   | 24 |
| 3.10 | Proposed system architecture of the refueling system . . . . .  | 25 |
| 4.1  | Rendered views of the full Exploration Excursion Vehicle (EEV) . . . . .  | 26 |
| 4.2  | Service module internal views . . . . .   | 27 |
| 4.3  | Crew module internal views . . . . .  | 28 |
| 4.4  | Payload Module Internal View labelled. . . . .  | 29 |
| 4.5  | Power Budget. . . . .   | 32 |
| 4.6  | High-Level Architecture for the GNC System. Includes all the sensors and actuators that will be used on the vehicle. . . . .                                  | 33 |
| 4.7  | Chosen Navigation Sensors for the EEV. . . . .  | 35 |
| 4.8  | Design decision matrix used to select the actuator type for this mission. . . . .   | 36 |
| 4.9  | Configuration of the Reaction Control System. . . . .   | 37 |
| 4.10 | Plots demonstrating the effectiveness of the RCS controller in reducing body rates and restoring a desired attitude. . . . .                                  | 38 |
| 4.11 | Decision Matrix: Propulsion System Propellant choice [29] [31] [32] . . . . .   | 45 |
| 4.12 | CAD Model of the main engine, created using reference material from Aerojet Rocketdyne [35] and other references on liquid rocket engines [31] [34] . . . . . | 47 |
| 4.13 | CAD Model of the R-4D-11, created using reference material from Aerojet Rocketdyne [35]. . . . .  | 47 |
| 4.14 | Structural Analysis done on the Landing Leg in Solidworks . . . . .   | 51 |
| 4.15 | Robotic Arms for Excavation Sampler Interface (left) and Coring Drill (right) . . . . .   | 53 |
| 4.16 | Sample Collection Tube and Hermetic Seal Cap . . . . .  | 54 |
| 4.17 | Core Sample Containment Racks . . . . .   | 56 |
| 4.18 | Excavation Arm Interface, Encapsulation Sphere Connector, and Encapsulation Sphere . . . . .  | 57 |
| 4.19 | Excavation Sample Sphere Containment Cylinders . . . . .  | 57 |
| 4.20 | The EEV Life Support System Architecture . . . . .  | 61 |

|      |   |    |
|------|---|----|
| 4.21 | The Air Revitalization Subsystem Architecture . . . . .   | 62 |
| 4.22 | Chosen components for Air Revitalization System (ARS) . . . . .   | 63 |
| 4.23 | Soyuz-Inspired Waste Receptacle . . . . .   | 66 |
| 4.24 | The EEV Life Support System in LiSTOT . . . . .   | 67 |
| 4.25 | Proposed System Architecture . . . . .  | 68 |
| 4.26 | Antenna Type Descision Matrix . . . . .   | 70 |
| 4.27 | Proposed Communication System Architecture . . . . .  | 70 |
| 4.28 | Parabolic Dish Array CAD . . . . .  | 71 |
| 4.29 | EEV to DST Link Budget . . . . .  | 72 |
| 4.30 | Times of EEV-to-DST-to-DSN Communications Link (green), and Communications Blackout<br>Events (Black) . . . . . | 73 |
| 4.31 | Fluid Cooling Loop Architecture . . . . .   | 79 |
| 4.32 | Thermal Coating and Insulation Architecture . . . . .   | 79 |
| 4.33 | Thermal Heater Architecture Diagram . . . . .   | 80 |
| 5.1  | Refueling Apparatus . . . . .   | 82 |
| 5.2  | DST to DSN Down-Link Budget with Design Considerations . . . . .  | 83 |
| 6.1  | Development and Operations Schedule for the EEV. . . . .  | 85 |
| 6.2  | Advanced Mission Cost Model Results . . . . .   | 86 |

# List of Tables

|      |   |    |
|------|---|----|
| 4.1  | Integrated system mass budget for EEV . . . . .   | 29 |
| 4.2  | Data for EEV Propulsion System, Scaled from AJ-10 [34] . . . . .                                      | 46 |
| 4.3  | Propulsion Fluids Tank Data . . . . .   | 49 |
| 4.4  | Phobos - Max and Expected Collection Masses for each Sampling System . . . . .                        | 52 |
| 4.5  | Deimos - Max and Expected Collection Masses for each Sampling System . . . . .                        | 52 |
| 4.6  | Both Moons - Max and Expected Collection Masses for each Sampling System . . . . .                    | 52 |
| 4.7  | <i>Perseverance</i> v EEV Drilling . . . . .  | 55 |
| 4.8  | List of Payload Scientific Instruments NOT Used for Mass Collection . . . . .                         | 58 |
| 4.9  | Consumables Required by the Crew on the Life Support System . . . . .                                 | 60 |
| 4.10 | Parameters of the Cabin Atmosphere . . . . .  | 61 |
| 5.1  | Requirements for the DST . . . . .  | 81 |
| 7.1  | Compliance Matrix showing adherence to all Design Requirements and Constraints from the RFP . . . . . | 88 |
| 7.2  | Location of all deliverables required by the RFP . . . . .  | 88 |

# Chapter 1

## Executive Summary

This proposal was written by a team of ten students at the University of Texas at Austin. The project was to develop a mission to the Martian moons of Phobos and Deimos and to design an Exploration Excursion Vehicle (EEV) capable of transferring crew to and from the moons while conducting scientific research and collecting samples from Phobos and Deimos.

There has been interest in sending humans to the surface of Mars for decades. Such an achievement would be a remarkable demonstration of human engineering and scientific capabilities, and bring increased public support and funding to private space enterprise and government agencies. It is critical to the future of the space industry that a human landing on Mars be safely achieved. However, current space capabilities do not allow for such a mission. A number of issues including deep space habitation, safe autonomous landing, and communication delay planning must be addressed before sending humans to the surface of Mars.

Through a mission to the moons of Mars, several of these challenges will be addressed. Due to the micro-gravity environment present around the moons, a human-rated mission to Phobos and Deimos is significantly lower risk than one to Mars, and would allow a demonstration of the technology necessary to support future Mars missions. This mission, named HAMMER (Human Assisted Martian Moons Explore and Return), would provide invaluable heritage to achieve the ultimate goal of landing humans on Mars.

There are three main goals that HAMMER aims to achieve. First, HAMMER seeks to enhance human understanding of both moons through sample collection and scientific investigation, learning about the moons' origins and material compositions. Second, HAMMER aims to demonstrate safe, autonomous landing and takeoff capabilities on a human-rated spacecraft. This will support future entry, descent, and landing (EDL) and takeoff activities on Mars. Finally, HAMMER intends to provide a baseline for human-in-the-loop



operations with substantial Earth communication delay. Portions of HAMMER are not autonomous and require crew intervention. A successful completion of mission objectives with delayed Earth communication will set a useful precedent for future Mars missions.

## 1.1 Concept of Operations

The EEV will be launched in October 2039 on a Falcon Heavy launch vehicle. Upon arriving in orbit around Mars in June 2040, the EEV inserts itself into a 5-sol, high eccentricity orbit and awaits the arrival of the Deep Space Transport (DST). The DST is a second spacecraft carrying three astronauts. The DST will deliver two crew members to the EEV; the vehicle is assumed in the concept of operations, but it is not designed in this proposal.

When the DST arrives, the EEV will autonomously dock with the DST and pick up the two crew members. A third crew member will remain on the DST for the duration of the mission. After refueling (see section 1.5) and transferring the crew, the EEV will travel to Phobos for nine days for science and sampling at four locations. The vehicle will then return to the DST to refuel and resupply. The EEV will proceed to Deimos, where it will remain for 4.9 days. After collecting samples at two locations, the EEV will return the crew and samples to the DST. This completes the primary phase of the mission, which will take roughly 30 days. The majority of maneuvers during HAMMER will be autonomous; however, all landing and traversal maneuvers across the surfaces of the moons will be piloted by a crew member. An autonomous landing is deemed to pose unacceptable risks to the crew.

The DST will transport the crew and samples back to Earth. Meanwhile, a final and optional phase of the mission will commence. The EEV will be refueled one last time before the DST departs to Earth. The EEV will then return to Phobos, where it will act as a communication relay and perform long-term science until it perishes. This final sequence will include a higher risk autonomous landing such that HAMMER demonstrates an autonomous landing on a human-rated vehicle, providing valuable heritage for future missions.

The total cost of the mission is estimated to be 996 million dollars using NASA's Project Cost Estimating Capability tool. This falls within the 1 billion dollar constraint, demonstrating the cost-effectiveness of a mission to Phobos to Deimos in comparison to a mission to Mars.

## 1.2 Environment

The surface environment on both moons is unique and heavily influenced the design of the EEV. The gravitational field on each moon is less than 0.1% of Earth's surface gravity. This makes landing on the moons like a rendezvous with another spacecraft rather than a landing. The low-gravity environment also makes a friction based maneuvering system infeasible. Although not much is known about the surface features of the moons, a mixture of dust and rocks is expected. Due to the low gravity, dust is a notable issue that the EEV must be able to mitigate. There is also unknowns with regard to the electrostatic environment on the moons. The EEV must operate successfully with regards to this uncertainty.

## 1.3 EEV Design

The EEV is a spacecraft capable of 2.4 km/s of  $\Delta V$ , and will transport two crew members to the surface of Phobos and Deimos. The vehicle is equipped with a bipropellant engine and 24 bipropellant reaction control thrusters, all using monomethyl hydrazine and nitrogen tetroxide (MMH/NTO) fuel pressurized by nitrogen ( $N_2$ ). The EEV spacecraft has a total mass of 7658.6 kg with margin and divided into three regions: the Crew Module, the Service Module, and the Payload Module.

### Crew Module

The Crew Module is the capsule where a two astronauts will reside, and is the only pressurized section of the EEV. Contained within are seats, windows, control panels, consumables, life support equipment, and all scientific equipment that will be handled by the crew. The crew module is in between the payload and service modules and is oriented such that the crew will have a direct line of sight to the moons' surfaces.

### Service Module

The Service Module contains the MMH and NTO fuel tanks,  $N_2$  pressurant tanks, oxygen, nitrogen, and water life support tanks, and batteries for the spacecraft. The main engine, three circular solar panels, a communication dish, four reaction control (RCS) assemblies, and several navigation sensors are also mounted

on the surface. Three landing legs will be attached to the bottom of the service module, right above the crew module.

## **Payload Module**

The Payload Module contains the majority of scientific equipment on the spacecraft. Four RCS assemblies, several navigation sensors, two robotic arms, and the sampling storage system are located in this module.

The docking adapter between the EEV and DST is also located in the center of this section.

## **1.4 Payload and Sampling**

The scientific objectives of the HAMMER mission are completed through the payload and sampling subsystem. This subsystem is used to collect a variety of surface and subsurface samples from Phobos and Deimos. These samples will allow scientists to analyze and understand the origins, surface processes, and composition of Phobos and Deimos. The Payload subsystem is comprised of two key sub-subsystems: the coring (subsurface minerals) and excavation (surface and subsurface minerals) sampling systems, which are described below.

### **Coring Sampling System (Subsurface Minerals)**

The coring sampling system is heavily influenced by the *Perseverance* mission's drill docking and bit carousel methods; However, HAMMER has up-scaled the drill to support adequate material collection rates with adjusted powers and masses. HAMMER's drill, like *Perseverance*'s, uses a model of Honeybee's ROPEC drill to core the surface of the moons. After coring, the drill docks at a deposition and processing station on the EEV to hand-off the sample bit to the interior robotic systems. The interior robotic systems then transport the sample bit to a core containment service rack which is retrieved by the crew during the next rendezvous with the DST. After dropping off the bit at the deposition and processing station, the drill docks at the dispenser station to acquire another bit to collect further samples. This sampling system, with consideration of failure modes and micro-gravity effects, expects (at 80% Max Potential) to collect a 64 kg and 58 kg of material from Phobos and Deimos, respectively.

## **Excavation Sampling System (Surface Minerals)**

The excavation sampling system is an effective and simple method of acquiring surface and subsurface samples and rocks on the moons. The excavation sampling system utilizes an "encapsulating sphere" which consist of two independent sphere halves that wrap around and enclose loose gravel or rocks with the help of a robotic arm. An interfacing connector of the robotic arm is specific to screwing open and close the encapsulating sphere halves. The sphere itself was designed to be the capture and containment unit for samples in order to persist sample collection in micro-gravity. The empty spheres are initially stored independently on the outside of the EEV. Once loaded with minerals and rocks, the encapsulation sphere is moved to its storage cylinder - where it stays until cylinders containing all encapsulating spheres are collected by the DST during rendezvous. This sampling system, with consideration of failure modes, micro-gravity effects, and volume usage, expects (at 50% Max Potential) to collect a 57.9 kg and 45.6 kg of material from Phobos and Deimos, respectively.

## **1.5 Deep Space Transport**

The DST plays a critical role in completing the mission. It will include a docking port sized appropriately to fit international space docking standards. The EEV will also adhere to these standards. The DST will act as a communication relay between the EEV and the Deep Space Network (DSN). This enables the EEV's communication dish to be much smaller, and a higher up-time of communication between the EEV and Earth as the DST doesn't experience the same communication blackouts the EEV will. This is further discussed later in the paper.

The DST will also act as a propellant depot for the EEV, allowing the EEV to have a reduced  $\Delta V$  capacity, minimizing the mass of the vehicle. This requires the DST to have a refueling arm, which has been designed and will be used to transfer fuel to the EEV.

# Chapter 2

## Mission Overview

This section reviews the objectives and design requirements for the mission ***HAMMER: Human Assisted Martian Moons Explore and Return.*** Design constraints identified in the mission brief are also discussed below.

### 2.1 Analysis of Needs

Mars is the newest frontier of space travel, and as a result has provided a need to prove a crewed mission can successfully make the long journey to and from the red planet. To support future long endurance, crewed missions to the Martian surface, NASA and international partners are looking to develop large scale descent systems. The largest payload to land on Mars is currently the Perseverance Rover; to support a human crew on a martian mission, the payload mass capability must increase by orders of magnitude. In preparation for the development of a descent system that can land on the surface of Mars, NASA has proposed the exploration of the Martian moons: Phobos and Deimos. A low cost, commercially procured, Martian Moon Exploration Excursion Vehicle (EEV) would create a bridge between Martian orbits and surface landings. The EEV would provide knowledge about operating crew missions away from Earth's sphere of influence and preparing for Martian surface missions in the future.

### 2.2 System Level Requirements

The following requirements are derived from the RFP. The mission was designed around ensuring that all these requirements were met.

| ID    | Requirement   | Rationale  | Parent ID |
|-------|---|--|-----------|
| DR-01 | The EEV shall visit both Phobos and Deimos  | In Proposal  |           |
| DR-02 | The EEV shall support a sample retrieval from each destination. The retrieved mass from each moon shall be no less than 50kg.   | In Proposal  | DR-01     |
| DR-03 | The Mission Duration shall be less than 30 days, including transit time from the DST vehicle and back.  | In Proposal  |           |
| DR-04 | The EEV shall have the capability to support 2 crew members.  | In Proposal  | DR-01     |
| DR-05 | The DST shall deliver two crew members to a 5-sol Martian Orbit in the Summer of 2040.  | In Proposal  |           |
| DR-06 | The EEV shall have the ability for two crew members to conduct exploration and expirementation of the moons   | In Proposal  |           |
| DR-07 | The collected samples shall be quarantined to prevent any contamination chemical, biological or physical until they reach Earth   | In Proposal. To ensure veracity of data collected from those samples | DR-02     |
| DR-08 | the EEV shall be in Martian 5-sol orbit before January 1, 2040  | In Proposal  |           |
| DR-09 | The EEV shall autonomously dock with the DST  | In Proposal  | DR-05     |
| DR-10 | The budget for the vehicle shall be no more than \$1 Billion US Dollar (in FY21), including the launch cost   | In Proposal  |           |
| DR-11 | The EEV shall be able to land on and later escape both of the moons   | In Proposal  | DR-01     |
| DR-12 | The EEV shall have to the ability to maneuver around the surfaces of Phobos & Deimos  | In Proposal  |           |
| DR-13 | The required science equipment for exploration shall be transported to Mars aboard the EEV. Up to 200kg of further science equipment may be delivered to the EEV together with the Crew aboard the DST. | In Proposal  |           |
| DR-14 | The mission shall deploy technologies within the NASA technology development portfolio or demonstrated on previous programs.  | In Proposal  |           |

Figure 2.1: System Level Requirements

## 2.3 Mission Objectives of the EEV

The primary objective of the Martian Moon EEV is to successfully bring two crew members to Phobos and Deimos, collect samples, and safely return to the Deep Space Transport (DST). In addition to the primary objective, several secondary objectives are listed below that are relevant to the long-term goal of supporting a crewed mission on Mars.

1. **Establish a foundation of scientific understanding of Phobos and Deimos:** a dedicated mission to Phobos and Deimos would allow for better understanding of the properties, resources, and origins of the unexplored moons.
2. **Develop and test technologies for future, long-term space missions:** The novel solutions

required for this mission to be successful will be useful to future deep space missions, particularly those involving low gravity bodies.

3. **Design and set a precedent for trajectory design around Mars and its Moons:** Given the novelty of this mission and the time and mass constraints, the precedent this mission sets will be important to future manned mission trajectory design around Mars.
4. **Conduct experimentation to improve human and autonomous activities in extremely low-G surface environments:** Phobos and Deimos both have extremely low surface gravity that would make it dangerous to perform an EVA when landed. Experimentation in these environments can be done to further improve spacecraft operation and human presence on their surface.
5. **Demonstrate feasibility of landing and launching craft from Deimos and Phobos:** Phobos and Deimos provide a middle point between the Martian orbit and its surface. In order to successfully use Phobos and Deimos as a bridge it is important to have landing and takeoff capabilities from both moons' surfaces.

## 2.4 Scientific Objectives of HAMMER

The primary scientific objectives of the HAMMER mission are described below:

1. **Investigate surface processes and composition of Phobos and Deimos:** The surface weathering will be investigated, primarily, through the comparison between samples returned from the Coring and Excavation samplers (with comparison between surface and subsurface material compositions). Additionally, Cosmic-Ray and Solar Wind exposure ages will be determined via the relative and absolute abundances and isotopic compositions of noble gases - providing valuable information about the localization of small particles and surface terrains on the moons [1] [2] [3] [4]. Finally,  $^{39}\text{Ar} - ^{40}\text{Ar}$  ages of returned samples can give insight to the timing of the formation of surface terrains and can be subsequently compared with age estimates from crater counter. [5] [6]
2. **Investigate the moons' origins from isotope concentrations in surface and subsurface minerals:** The two popular ideas for the formation of the moons (especially Phobos) are that they were

formed either through Mars' capture of an asteroid or when an asteroid impacted Mars [1]. To collaborate the idea that the moons' origins lie in asteroid capture, the moons' mineralogical and petrological information can permit the direct comparison between the moon surface compositions and known meteorite groups such as CM, Ci and CR chondrites [1]. To collaborate the idea that the moons' formations come from asteroid impact with Mars, the mineralogical and petrology of the samples will be studied for the presence/absence of absorption of  $\approx 0.7$  and  $2.7 \mu\text{m}$  indicative of hydrated minerals and at  $\approx 3.4 \mu\text{m}$  for macro molecular organic solids [7]. Non-mass dependent isotopic compositions of elements such as Oxygen, Calcium, Titanium, and Chromium can be used to characterize the source material where collected samples have been formed and possibly their location of origin [1].

- 3. Investigate moon surface and subsurface minerals to determine evolution of surface processes on Mars:** Martian materials have been predicted to be ejected throughout the entire history of Mars, and the collection of materials on Phobos and Deimos can provide evidence for the evolution of Mars. Additionally, formation ages determined by  $^{39}\text{Ar} - ^{40}\text{Ar}$ ,  $^{87}\text{Rb} - ^{87}\text{Sr}$ , and  $^{238,235}\text{U} - ^{206,207}\text{Pb}$  from surface materials collected on the moon could be useful for determining Mars' surface evolution throughout time [1]. The Hydrogen isotopic compositions of phosphate and hydrous materials (containing hydroxyl and  $\text{H}_2\text{O}$ ) can provide information about how the surface water and atmosphere of Mars were lost [8]. Also, Because Martian meteorites typically underwent shock metamorphism to  $>5 \text{ GPa}$  (resetting any remanent magnetism [9]), materials ejected to the moons with lower shock pressures could provide clues to better understand the possible evolution of the Martian magnetic field [1] [9].



# Chapter 3

## Mission Architecture

### 3.1 Concept of Operations

The HAMMER mission begins in **October 2039**, with the launch of the Exploration Excursion Vehicle (EEV) on a SpaceX Falcon Heavy during the low-energy transfer window to Mars. Due to the high performance of the SpaceX Falcon Heavy's upper stage, the EEV can be directly inserted into a Mars transfer orbit.

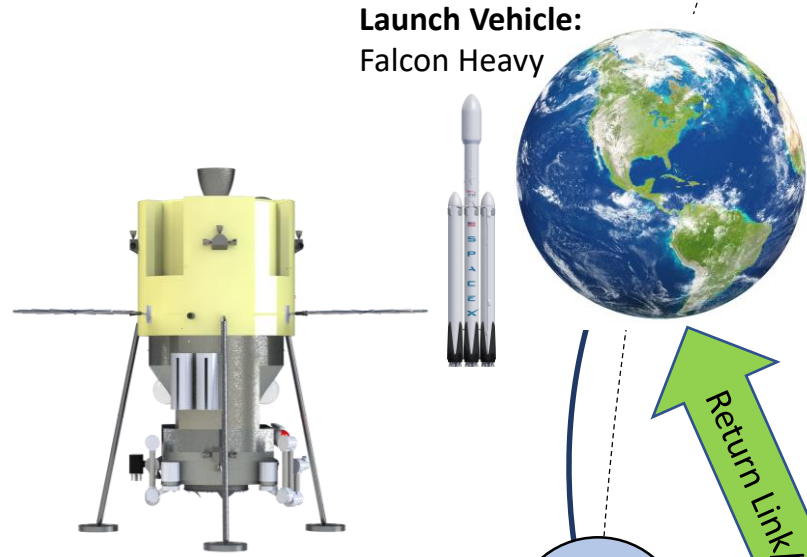
Once the EEV arrives at Mars in June 2040, it will use its main propulsion system to perform an Orbital Insertion Burn (OIB) into a 6,000 x 100,000 km 5-sol parking orbit. Here, the EEV awaits the arrival of the Deep Space Transport (DST) vehicle and its crew. A few days prior to the DST's arrival, the EEV is pressurized and heated to ensure habitable conditions.

Upon arrival at Mars at the end of June 2040, the DST performs an OIB into the same 5-sol orbit in which EEV is waiting for it. Once complete, the EEV will perform an automated rendezvous and docking sequence with the DST. After docking, the DST will be used to refuel the EEV, which has burned a large amount of its fuel during the Mars OIB. To do this, the refueling arm attached to the DST will be employed.

After refueling of the EEV is complete, the crew will open the airlock from the DST to the EEV. Once complete, the Crew will transfer about 75kg of science equipment and supplies to the EEV through the International Docking Adapter (IDA) which connects the EEV to the DST. This equipment is safely secured in the storage compartments located on the sides of the EEV Crew Module. After loading of science equipment, the crew moves to the EEV, which then detaches from the DST for the first sortie of the mission.

# Concept of Operations

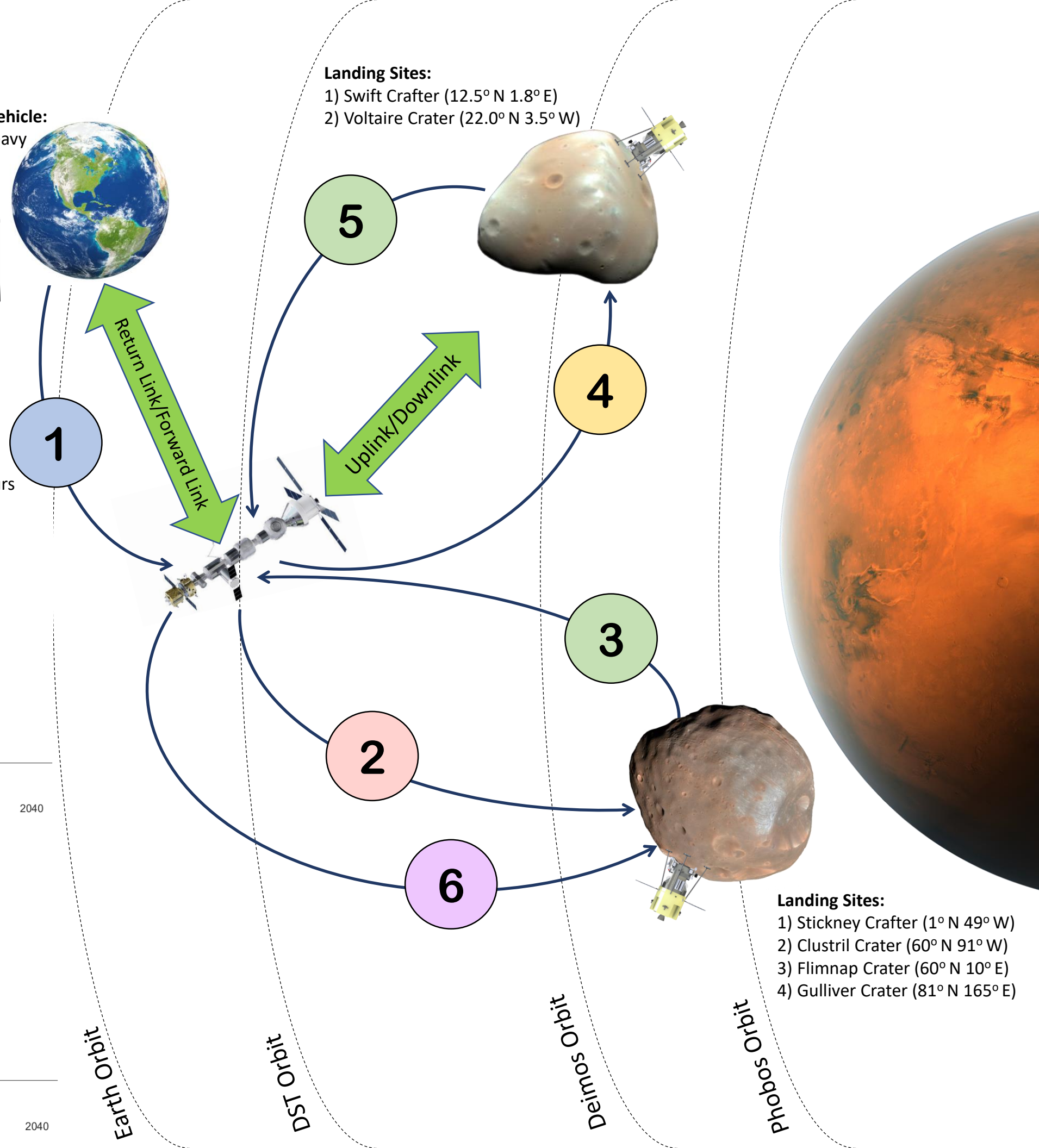
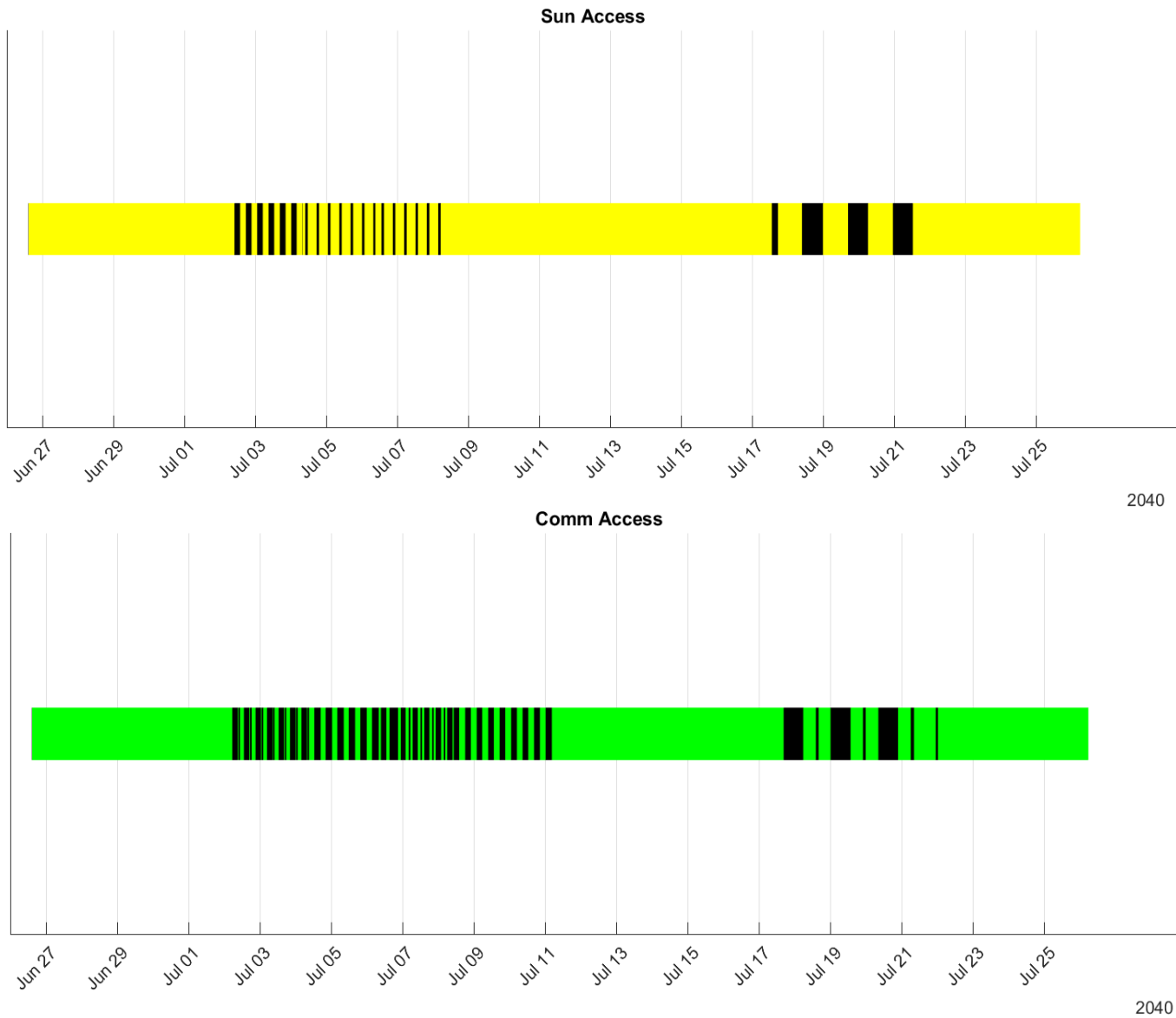
|                        | MISSION EVENT                | DATE / DURATION / INFO |
|------------------------|------------------------------|------------------------|
| Uncrewed               | <b>1) Launch Baseline</b>    | <b>Oct 9, 2039</b>     |
|                        | Launch Vehicle               | Falcon Heavy           |
|                        | Transfer Time                | 256 days               |
|                        | EEV Mars Orbital Insertion   | Jun 22, 2040           |
|                        | DST Mars Orbital Insertion   | Jun 27, 2040           |
| Crewed                 | <b>2) Transfer to Phobos</b> | <b>Jul 2, 2040</b>     |
|                        | Phobos Rendezvous            | Jul 3, 2040            |
|                        | Phobos Science               | 9.2 days               |
|                        | Landing Sites                | 4                      |
|                        | <b>3) Return to DST</b>      | <b>Jul 12, 2040</b>    |
| Docking                | Jul 12, 2040                 |                        |
| Resupply Time          | 2.5 days                     |                        |
| Uncrewed               | <b>4) Transfer to Deimos</b> | <b>Jul 15, 2040</b>    |
|                        | Deimos Rendezvous            | Jul 18, 2040           |
|                        | Deimos Science               | 4.9 days               |
|                        | Landing Sites                | 2                      |
|                        | <b>5) Return to DST</b>      | <b>Jul 23, 2040</b>    |
| Docking                | Jul 27, 2040                 |                        |
| Resupply Time          | 11 days                      |                        |
| DST Departure to Earth | Next Available Launch Window |                        |
| Uncrewed               | <b>6) Transfer to Phobos</b> | <b>Aug 7, 2040</b>     |
|                        | Phobos Rendezvous            | Aug 7, 2040            |
|                        | Phobos Science               | Until Failure          |

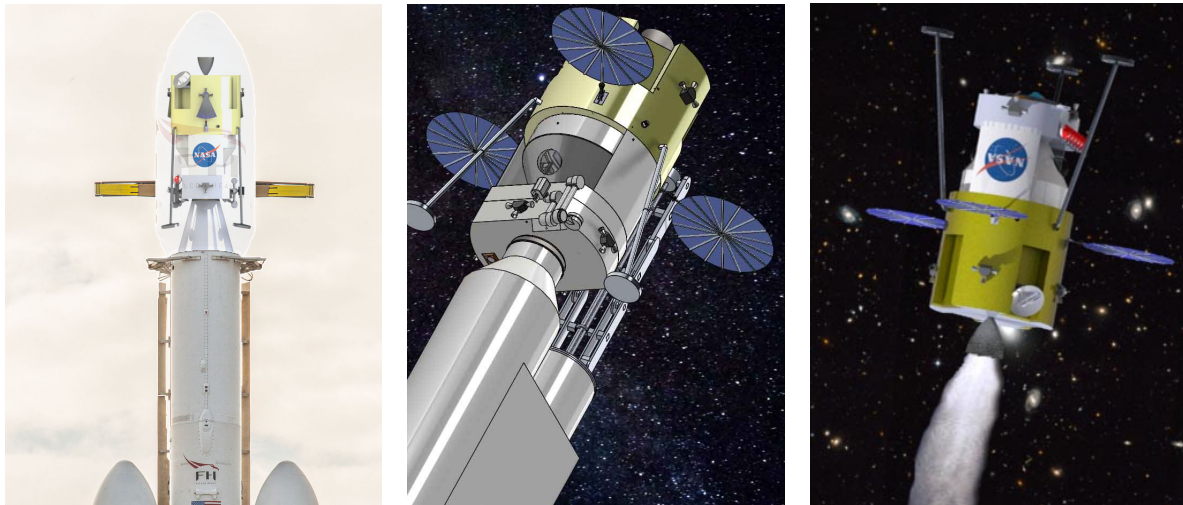


**Longest Eclipse: 14 hours**  
**Longest Comm Blackout: 13 hours**

**Landing Sites:**  
1) Swift Crafter (12.5° N 1.8° E)  
2) Voltaire Crater (22.0° N 3.5° W)

**Landing Sites:**  
1) Stickney Crafter (1° N 49° W)  
2) Clustril Crater (60° N 91° W)  
3) Flimnap Crater (60° N 10° E)  
4) Gulliver Crater (81° N 165° E)





(a) The EEV in Launch Configuration inside Falcon Heavy fairing (b) The EEV Docking with the DST (c) The EEV performing a transfer burn from the DST to Phobos

Figure 3.1: Visualization of phases of EEV operations that occur before landing.

After detaching, the EEV performs a sequence of maneuvers to arrive at **Phobos**, the first Martian Moon visited during the mission. This transfer will take approximately 12 hours to complete. Upon arrival, the crew of the EEV will validate the pre-assessment performed on the landing sites prior to crew arrival. Based on this, the crew will choose a final landing site and perform a rendezvous on Phobos in the micro-g environment. After landing, the crew will collect samples from the moon and perform a number of experiments (see section 4.6). Once the first site has been adequately explored after two days, the vehicle will transfer to three other landing sites on Phobos, each where additional samples are stored and measurements are taken for two days. In total, the EEV will conduct science on Phobos for nine days.

After completing their science objectives on Phobos, the EEV again performs several maneuvers in order to transfer back into the 5-sol waiting orbit, where the DST is waiting for its arrival. After an autonomous rendezvous and docking sequence, the crew is able to transfer the collected samples from Deimos to the DST. Subsequently, the crew resupplies the EEV with about 125kg of science equipment and consumables, and the DST then refuels the EEV once again. The EEV takes about 2.5 days to complete the rendezvous and resupply with the DST.

After completing its resupply, the crew once again transfers to the EEV and separates from the DST. Next, the EEV maneuvers to **Deimos** within about 4 days. Here, the approach is chosen analog to **Phobos**

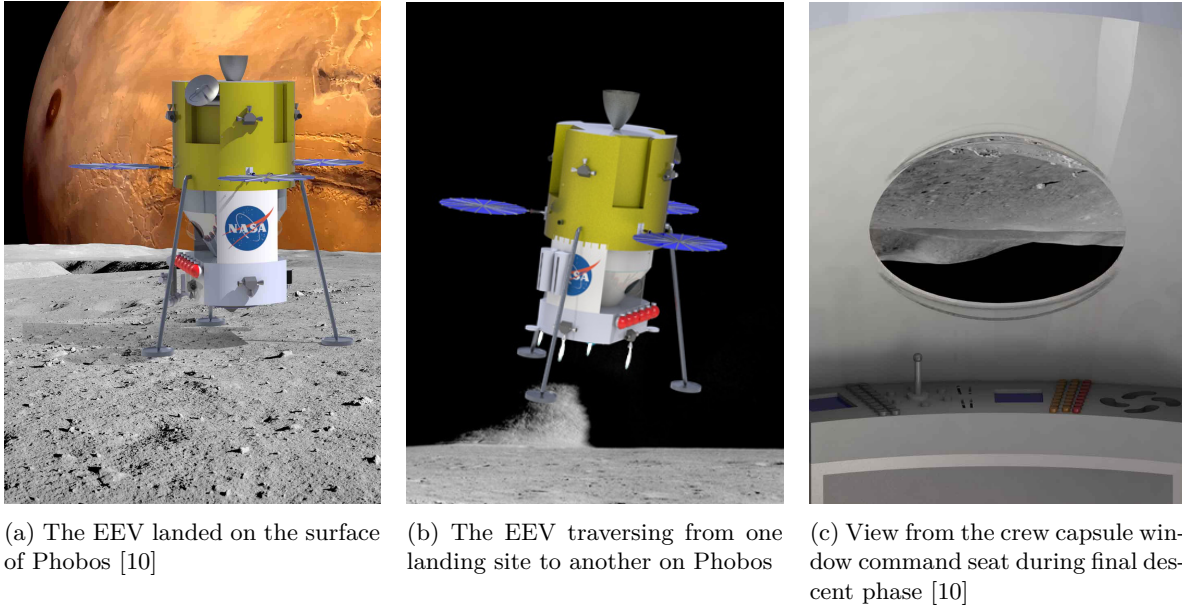


Figure 3.2: Phases of EEV operations during landing

to conduct the required science experiments. In contrast to Deimos, the time spent on Phobos is shorter, at about 5 days. In total, 2 landing sites will be visited on the smaller moon to help collect a sample mass.

After completing their science objectives on Deimos, the EEV once again transfers back into the 5-sol waiting orbit, where it autonomously docks with the DST again. Following docking, the crew transfers back to the DST. With it, the crew moves the newly collected collected samples and science back to the DST. The EEV is refuelled one last time. After the crew has transferred to the DST and closed the EEV hatch, the EEV detaches from the DST. At this point, the DST returns to Earth with the crew and samples at the next available launch window, completing the primary 30-day phase of the mission.

After a final detachment from the DST, the EEV performs a number of maneuvers to transfer back to Phobos. Once arrived, an experimental autonomous landing will be performed on the tidally locked, Mars facing side of the Moon. Here, the EEV will serve as a science station on the Moon for years past the departure of the crew. On Phobos, it can be used to take detailed images of Mars, serve as a communication relay around the planet for future missions and perform additional, long term science. This helps to maximize the scientific value of the vehicle at the end of its life.

## 3.2 Trajectory Design and Space Logistics Optimization

The EEV and DST will be launched separately by different launch vehicles and will meet at Mars in the Summer of 2040. As required, the total time of the crewed mission once arriving at Mars will not exceed 30 days. Therefore, the crew must be transferred back to the DST within that time frame with all main mission objectives being completed. Significant effort was made to reduce the total  $\Delta V$  of the trajectory given the constraints of the logistics problem.

### 3.2.1 Mars Transfer Optimization

A Lambert solver was used for estimation of the optimal launch date for the EEV to insert the vehicle into Martian orbit. A patched conics model was used for this preliminary investigation. Porkchop Diagrams for the Departure and Arrival  $\Delta V$ s are shown below.

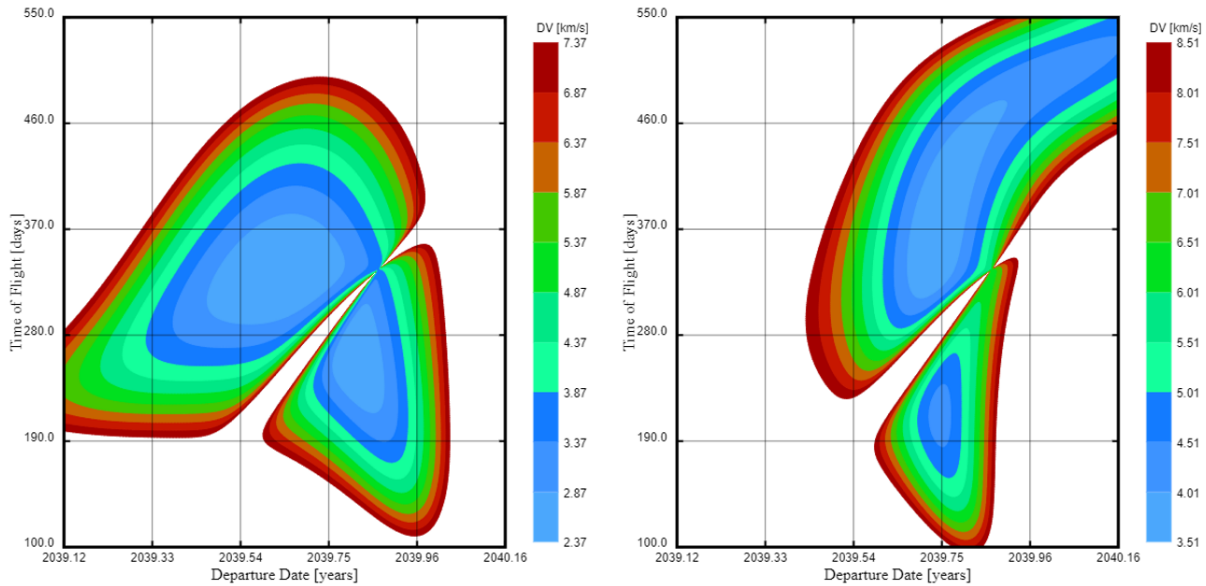


Figure 3.3: Porkchop Diagrams which indicate the Departure (left) and Arrival (right)  $\Delta V$  for the Earth-Mars Transfer

These diagrams were used to bound the optimization problem inherent in balancing the tradeoff between  $\Delta V$  and transfer time. To do this analysis, an in-house solar system model was developed using SPICE

ephemeris data and an automation wrapper for a Lambert solver was created in MATLAB. Using this software, an optimal transfer orbit between the time bounds is determined and provided by Figure 3.4.

The automation scripts use a simple search algorithm that discretizes and evaluates the entire solution space to find the optimal initial conditions for the cost function. A more efficient solver is unnecessary for this problem due to the reasonably small solution space. Once the optimal trajectory was determined, the solution was checked against the NASA Ames Trajectory Browser [11] to verify the results.

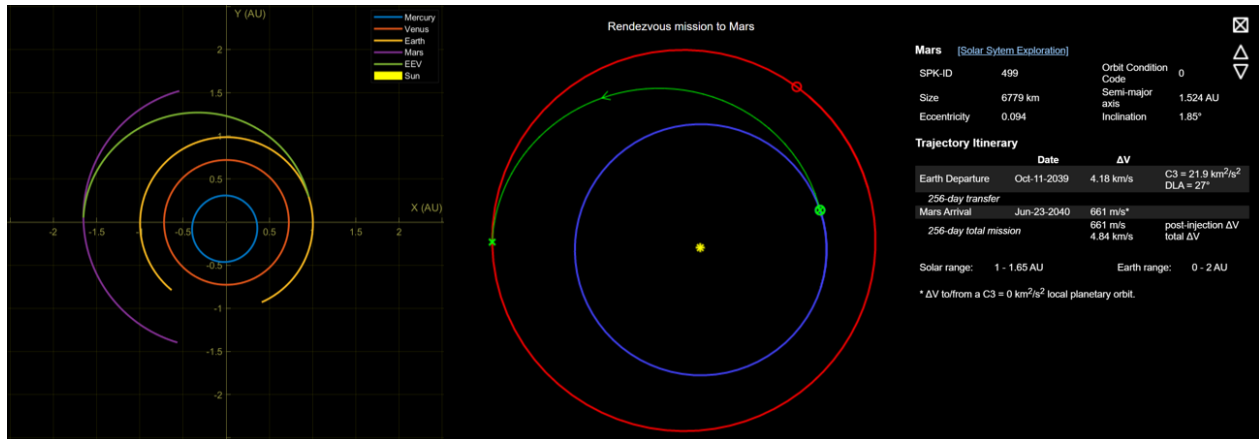


Figure 3.4: Comparison demonstrating the similarity between the calculated solution (left) and the NASA Ames Trajectory Browser (right)

A transfer date of October 11, 2039 was selected, which is preceded by LEO insertion on October 9th. This launch date was selected using the automated design tool described above and it represents the most favorable trade-off between  $\Delta V$  and transfer time, which are 4.13 km/s and 256 days, respectively.

After the selection, this trajectory was input into Systems Tool Kit (STK) to take advantage of the high fidelity orbit propagator. The rest of the trajectory design for this mission was done in STK.

### 3.2.2 Parking Orbit

The EEV will be placed in a high eccentricity orbit, which reduces the total  $\Delta V$  required for orbital maneuvers due to the higher orbit energy. Although this reduces the orbital insertion, a high-energy inclination change is also performed such that the parking orbit is in plane with Phobos and Deimos. This orbital insertion requires 1.74 km/s of  $\Delta V$ . Five days after insertion, the DST arrives in an identical orbit such that the EEV can autonomously dock.

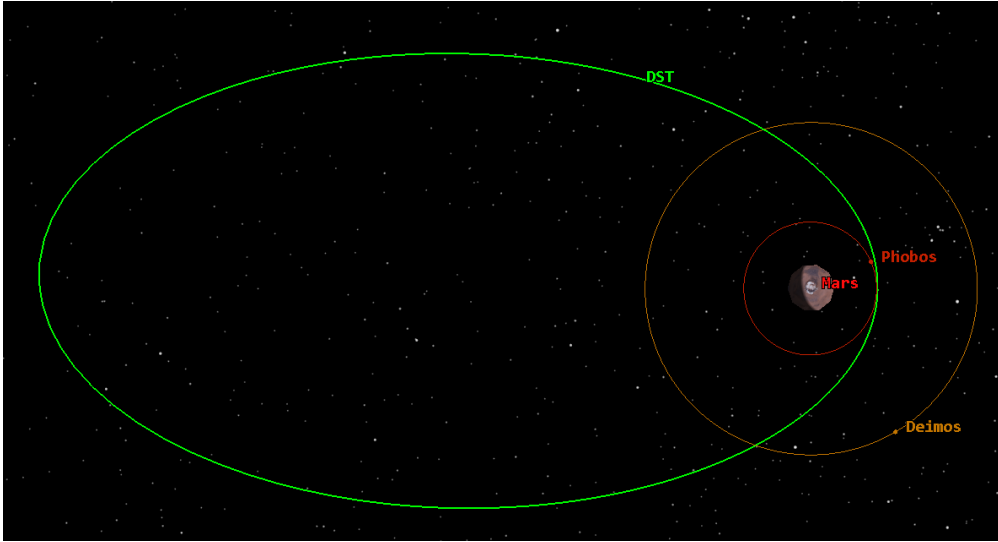


Figure 3.5: 5 Sol Orbit that the DST will be in for the duration of the mission, and where the EEV will be at the beginning of the mission.

### 3.2.3 Inbound Orbit Logistics Optimization

The inbound trajectory solution space for this mission is substantial. Due to the presence of the DST, there are four main logistics options for a rendezvous with both moons. One could either start with Phobos, start with Deimos, or do so with a rendezvous and refueling event at the DST between moons. There are advantages and disadvantages to all these options, which can be quantified in the following optimization variables:

1. **EEV propellant mass:** This quantity is derived from the required  $\Delta V$  capabilities of the EEV using the rocket equation. It is of interest to keep this value low to reduce the size and complexity of the EEV, and therefore is weighted highly in the cost function.
2. **DST propellant payload:** If the DST is used for refueling, it must carry additional fuel as payload. This extra capacity must be considered as to not place an unacceptable requirement on the DST. However, as this fuel does not place burden on the EEV, it is weighted significantly lower than **1** at a tenth the cost.
3. **Time on Phobos:** The longer the EEV stays on Phobos, the more science and sample collection can

be done. This metric is critical in evaluating mission effectiveness due to the 30 day mission constraint, and therefore is weighted very highly in the cost function.

4. **Time on Deimos:** Similar to **3**. However, in the recently released Decadal Survey [12], there appears to be greater scientific interest in Phobos over Deimos. This is due to its potential to have transitioned between a ring and a moon multiple times. The survey also mentions that the Martian Moons eXploration (MMX) mission intends to bring samples back from Phobos, but not Deimos. Therefore, the time on Deimos is weighted at three quarters of the time on Phobos.

In order to solve this logistics problem, some constraints were added. The DST parking orbit was fixed for this analysis, and only minimal or near-minimal  $\Delta V$  transfer orbits were considered. This made the solution space significantly smaller and allowed for the use of STK to evaluate the optimization variables above for each trajectory.

Several trajectories for each of the four logistics architectures were designed, analyzed, and had their objective functions evaluated. **Foldout 2** contains the details of this analysis. Four of the many trajectories designed are analyzed in this foldout, and the details of the trajectory selected for this mission are also provided.

As mentioned above, the EEV will refuel using the DST, requiring that it will rendezvous with the vehicle between operations at Phobos and Deimos. This trajectory established a schedule for the mission and approximate times and  $\Delta V$  for each maneuver. This schedule also includes different landing sites for the mission (see Section 3.3).



# Mission Logistics Optimization

**Objective:** Find Trajectory that minimizes the cost function:

$$J = S_1 m_{EEV} + S_2 m_{DST} - S_3 t_{Phobos} - S_4 t_{Deimos}$$

- Rocket Eqn. used to convert  $\Delta V$  to mass.
- Four example trajectories (not entire solution space) below
- **Trajectory #2 was selected for this mission**

$m_{EEV}$  – Required propellant capacity of the EEV

$m_{DST}$  – Required propellant from the DST

$t_{Phobos}$  – Science time on Phobos (days)

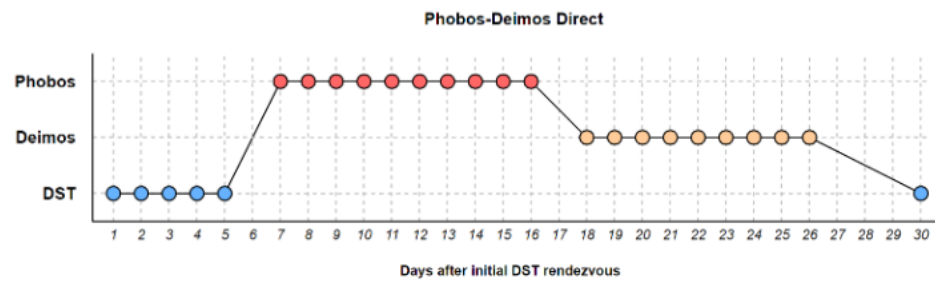
$t_{Deimos}$  – Science time on Deimos (days)

$$S_1 = 1$$

$$S_2 = 0.1$$

$$S_3 = 400$$

$$S_4 = 300$$



1. Phobos to Deimos, no stop at DST.  $J = 1,840$

$\Delta V = 2.20$  km/s

$m_{EEV} = 8,854$  kg

$m_{DST} = 0$  kg

$t_{Phobos} = 10.52$  days

$t_{Deimos} = 9.35$  days

2. Phobos to Deimos, refuel at DST.  $J = 1,536$

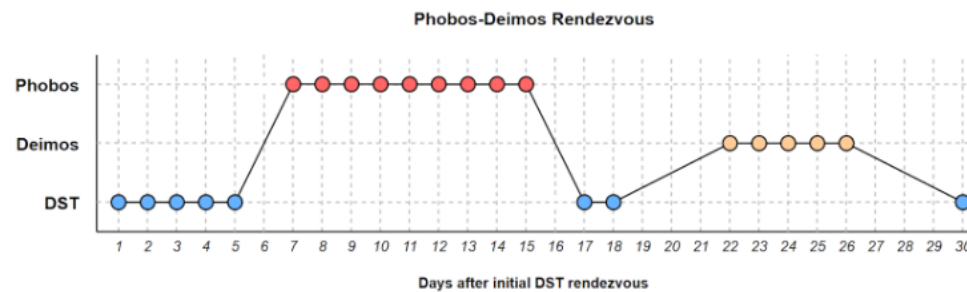
$\Delta V = 1.74$  km/s

$m_{EEV} = 6,419$  kg

$m_{DST} = 2851$  kg

$t_{Phobos} = 9.24$  days

$t_{Deimos} = 4.91$  days



3. Deimos to Phobos, no stop at DST.  $J = 3,308$

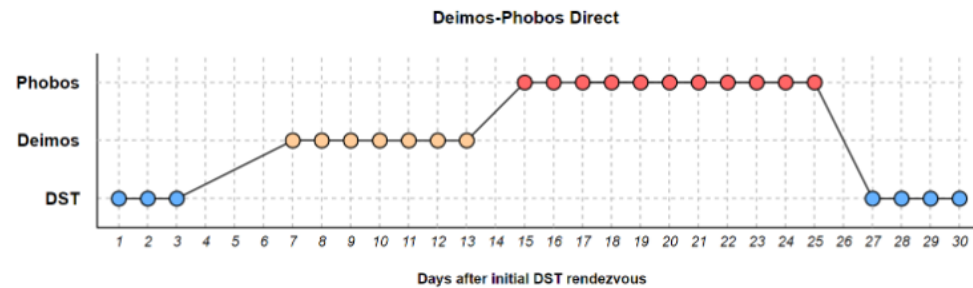
$\Delta V = 2.41$  km/s

$m_{EEV} = 10,103$  kg

$m_{DST} = 0$  kg

$t_{Phobos} = 11.32$  days

$t_{Deimos} = 7.56$  days



4. Deimos to Phobos, refuel at DST.  $J = 2,316$

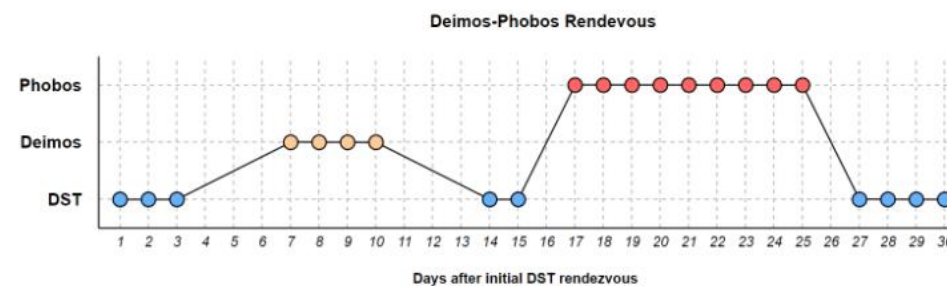
$\Delta V = 1.80$  km/s

$m_{EEV} = 6,727$  kg

$m_{DST} = 3,793$  kg

$t_{Phobos} = 9.25$  days

$t_{Deimos} = 3.63$  days

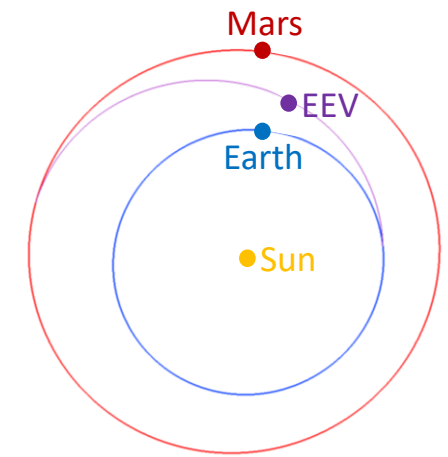


## 1. Transfer Arc to Mars

Launch Date: Oct 9, 2039

Transfer Time: 256 Days

$\Delta V$ : 4.13 km/s



## 2. Parking Orbit Insertion

EEV Arrival Date: Jun 22, 2040

DST Arrival Date: Jun 27, 2040

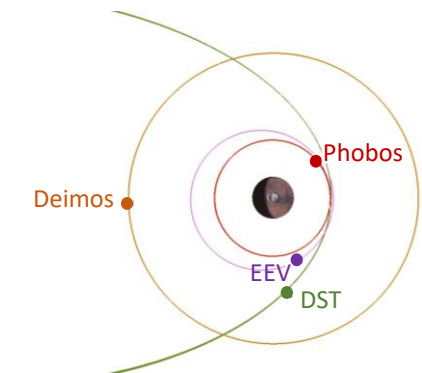
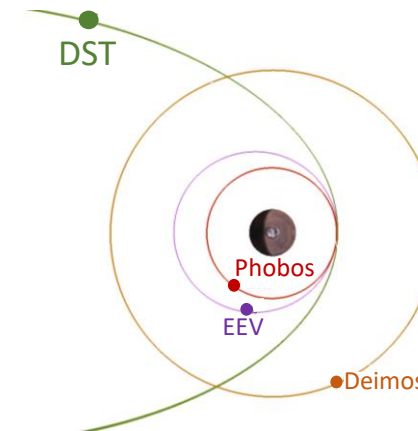
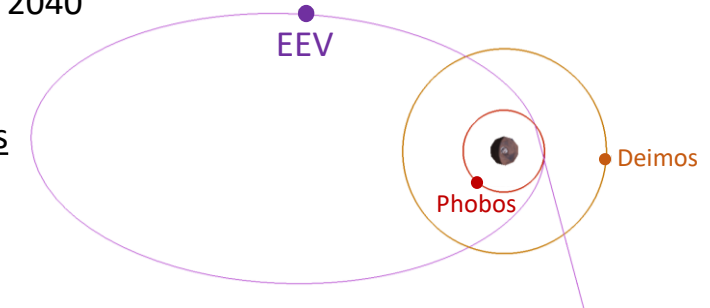
$\Delta V$ : 0.90 km/s

### Parking Orbit Parameters

Period: 5.0 days

Eccentricity: 0.84

SMA: 59000 km

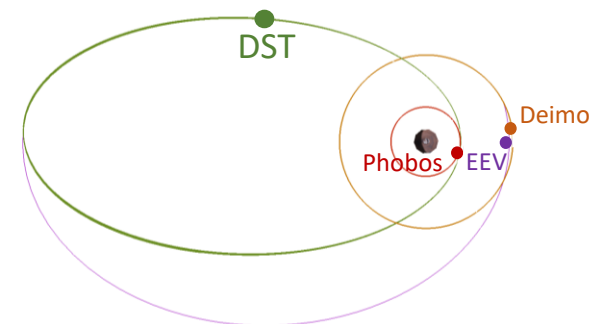


## 3. Transfer to Phobos

Transfer Date: Jul 2, 2040

Time on Phobos: 9.2 days

$\Delta V$ : 0.83 km/s

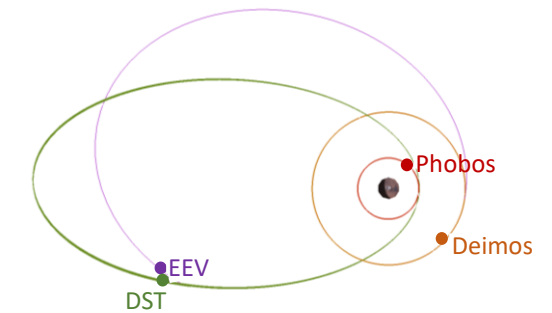


## 4. Return to DST

Transfer Date: Jul 12, 2040

Transfer Time: 11 hours

$\Delta V$ : 0.90 km/s



## 5. Transfer to Deimos

Transfer Date: Jul 15, 2040

Time on Deimos: 4.9 days

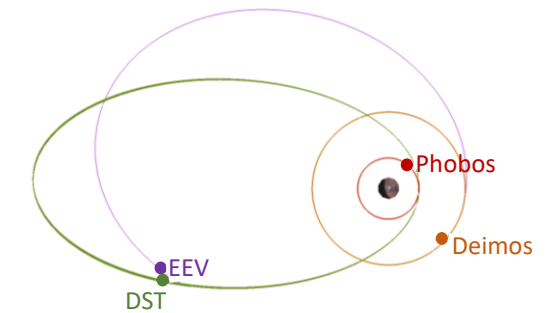
$\Delta V$ : 0.59 km/s

## 6. Return to DST

Transfer Date: Jul 26, 2040

Transfer Time: 4 days

$\Delta V$ : 0.63 km/s



| MISSION SEGMENT  | DATE               | EVENT ID | EVENT DESCRIPTION  | EEV LOCATION                      | DELTA-V (m/s) |
|------------------|--------------------|----------|--|-----------------------------------|---------------|
| TRANSFER TO MARS | 10/9/2039 0:00:00  | TKO-1    | Launch and insert into LEO   | Payload in Falcon Heavy           | 0             |
|                  | 10/11/2039 0:00    | ORB-1    | Burn to escape gravity of Earth & enter a transfer trajectory towards Mars | LEO                               | 4131.334      |
|                  | 6/22/2040 8:27:11  | ORB-2    | Mars Orbital Insertion/Insert into DST                                     | Near Mars Perigee                 | 1738.715      |
|                  | 6/24/2040 19:43:34 | ORB-3    | Optional Correction Maneuver   | In 5-sol Orbit                    | 15.8243       |
|                  | 6/27/2040 8:31:46  | DCK-1    | Dock with the DST  | Near DST                          | 5             |
|                  | 7/2/2040 10:00:00  | DCK-2    | Undock with the DST  | Docked to DST                     | 2             |
| PHOBOS OPS       | 7/2/2040 10:08:56  | ORB-4    | Lower Apogee   | Near DST, Periapse of 5-Sol Orbit | 553.016       |
|                  | 7/2/2040 15:42:16  | ORB-5    | Optional Correction Maneuver   | Apogee                            | 51.614        |
|                  | 7/2/2040 21:16:56  | ORB-6    | Insert into Phobos Orbit   | Near Phobos                       | 233.991       |
|                  | 7/2/2040 22:00:00  | LND-1    | Land on Phobos at Stickney Crater  | ~5 km above Phobos                | 20            |
|                  | 7/5/2040 1:00:00   | TKO-2    | Takeoff and transfer to Clustring Crater                                   | Stickney Crater                   | 20            |
|                  | 7/5/2040 2:00:00   | LND-2    | Land at Clustring Crater   | Above Clustring Crater            | 20            |
|                  | 7/7/2040 2:00:00   | TKO-3    | Takeoff and transfer to Flimnap Crater                                     | Clustring Crater                  | 20            |
|                  | 7/7/2040 3:00:00   | LND-3    | Land at Flimnap Crater   | Above Flimnap Crater              | 20            |
|                  | 7/9/2040 3:00:00   | TKO-4    | Takeoff and transfer to Gulliver Crater                                    | Flimnap Crater                    | 20            |
|                  | 7/9/2040 4:00:00   | LND-4    | Land at Gulliver Crater  | Above Gulliver Crater             | 20            |
|                  | 7/12/2040 3:00:00  | TKO-5    | Takeoff from Phobos  | At Gulliver Crater                | 20            |
|                  | 7/12/2040 3:02:32  | ORB-7    | Raise Apoapse to rendezvous with DST                                       | Near Phobos                       | 163.988       |
|                  | 7/12/2040 8:10:53  | ORB-8    | Optional Correction Maneuver   | Near apoapse                      | 27.697        |
|                  | 7/12/2040 13:43:43 | ORB-9    | Insert into DST Orbit  | Near DST                          | 711.35        |
|                  | 7/12/2040 14:00:00 | DCK-3    | Dock with the DST  | Near DST                          | 5             |
| DEIMOS OPS       | 7/15/2040 2:00:00  | DCK-4    | Undock with the DST  | Docked to DST                     | 2             |
|                  | 7/15/2040 2:07:12  | ORB-10   | Raise Periapse to match Deimos   | Near DST, Apogee of 5-Sol orbit   | 119.29        |
|                  | 7/18/2040 5:43:40  | ORB-11   | Insert into Deimos Orbit   | Near Deimos                       | 475.458       |
|                  | 7/18/2040 7:00:00  | LND-5    | Land on Deimos at Swift Crater   | ~5 km above Deimos                | 20            |
|                  | 7/20/2040 7:00:00  | TKO-6    | Takeoff and transfer to Voltaire Crater                                    | Swift Crater                      | 20            |
|                  | 7/20/2040 8:00:00  | LND-6    | Land at Voltaire Crater  | Above Voltaire Crater             | 20            |
|                  | 7/23/2040 2:00:00  | TKO-7    | Takeoff from Phobos  | At Voltaire Crater                | 20            |
|                  | 7/23/2040 3:31:29  | ORB-12   | Raise Apoapse to rendezvous with DST                                       | Near Deimos                       | 355.54        |
|                  | 7/26/2040 23:03:30 | ORB-13   | Insert into DST Orbit  | Periapse, Near DST                | 270.075       |
|                  | 7/26/2040 23:30:00 | DCK-5    | Dock with the DST  | Near DST                          | 5             |

Figure 3.6: Schedule and  $\Delta V$  for each maneuver.

### 3.2.4 $\Delta V$ Budget

The total mission  $\Delta V$  is 3.32 km/s. Since the vehicle is refueling, the EEV requires a minimum  $\Delta V$  capacity of 1.91 km/s (note that this number is slightly higher than the  $\Delta V$  in foldout 2 due to additional  $\Delta V$  being required to traverse the moons). This is in contrast to a hypothetical mission without refueling at the DST between moons, it would have a  $\Delta V$  of 2.60 km/s.

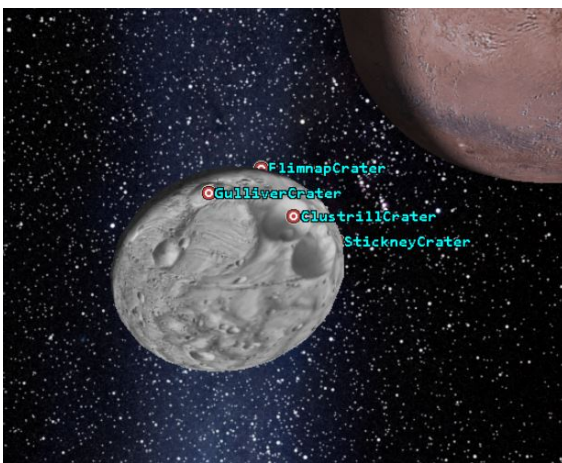
The vehicle is designed with significant fuel margin, and will be capable of 2.4 km/s. This provides it

with comfortable margin for the Phobos portion of the mission, and will allow for return to the DST using the Reaction Control System (RCS) in event of main engine failure.

### 3.3 Landing Location Assessment

On Phobos, four landings will be attempted in the nine days allotted to spend on the moon. Due to the time of year the mission will take place and its resultant availability of sunlight compared to the rest of the moon, three of the landings shall be attempted above sixty degrees north [13]. These sites will be Clustril Crater (60°N 91°W), Flimnap Crater (60°N 10°E), and Gulliver Crater (81°N 165°E). The fourth landing site has been designated as being near Stickney Crater (1°N 49°W) as it is the geographical feature of most interest on Phobos. Stickney will be visited first, and the other sites will be visited in ascending order of increasing latitudes. Each landing area will allow for a radius that extends five additional degrees in longitude and latitude.

On Deimos, two landings will be attempted in the five days allotted to spend on the moon. The first landing will be near Swift Crater (12.5°N 1.8°E). The second landing site will occur near Voltaire Crater (22°N 3.5°W) because it is the largest of the only named geological features of Deimos. The landing areas at these sites of interest will be the same dimensions as the ones on Phobos and the same inclination limit will be followed.



(a) Landing Areas of Interest on Phobos



(b) Landing Areas of Interest on Deimos

## 3.4 Phobos and Deimos Space Environment

### 3.4.1 Surface Qualities

Phobos and Deimos both have cold, dark, and rocky surfaces with albedos of 0.071 and 0.068, respectively. These make for dark surfaces which are difficult to photograph and by extension map from a distance. The average temperature of Phobos on the sunlit side is -4 Celsius, and -113 Celsius on the dark side. Temperature estimations are expected to be similar for Deimos.[13]

The moons are thought to be collections of smaller rocks that were lightly bonded together and then formed a crust. That crust has been bombarded by other objects since its formation and has created a variety of craters. The surface of this crust is very rough due to the craters, low gravity, and no smoothing erosion forces like wind. The non-spherical bodies create locations where the local gravity is not perpendicular to the surface by large margins of up to 45 degrees. This creates a risk during landing operations for the vehicle, it may land flat on the surface but be pulled over from a non-perpendicular gravity field. In order to mitigate this risk landing sites were chosen where the gravitational field is within 15 degrees of perpendicular to the surface.

### 3.4.2 Gravity And Its Implications

Surface gravity on both Phobos and Deimos is incredibly minute, on the scale of ten thousandths of Earth's gravity. Phobos, the larger of the two moons has a mean surface gravity of 0.006 meters per second squared while Deimos sits at 0.003 meter per second squared of acceleration on the surface. The escape velocities of Phobos and Deimos are 12 and 6 m/s respectively. Therefore, the force of the EEV on the moons is no more than a few hundred newtons.

The low gravity environment impacts space operations and the surface qualities of the moon. Firstly for the vehicle, it means that it can't rely on gravity to hold the EEV in place during sampling and it can't rely on friction with the surface to traverse the moons. In response to these difficulties, the EEV will anchor to the surface during sampling using RCS thrusters. Secondly, the low gravity environment makes Phobos and Deimos both have weakly linked minerals with little compaction. This worsens the dust environment

and excavation methods of the EEV. Lastly, the minimal gravity also impacts the trajectory and landing operations. The landings are better understood as rendezvous as the acceleration force is minimal.

### 3.4.3 Electrostatic Environment

Similar to Earth, Mars is protected from solar wind via its atmosphere and magnetosphere. The martian atmosphere is roughly 10.8 km in reach while the magnetosphere is considered a magnetic tail with random magnetic locations along Mars's surface. Since Phobos orbits Mars at an average distance of 6,000 km and Deimos orbits Mars at an average distance of 23,000 km, neither moon falls within scope of the martian atmosphere or magnetosphere. As a result, Phobos and Deimos are exposed to solar wind.

Solar wind is an electrically neutral collection of protons and electrons in a plasma state. As solar wind impacts the moon, the protons and electrons are absorbed into the moon's surface. The fluid behavior of solar wind on a planet can be modeled using a perfect sphere pictured below in figure 3.8.

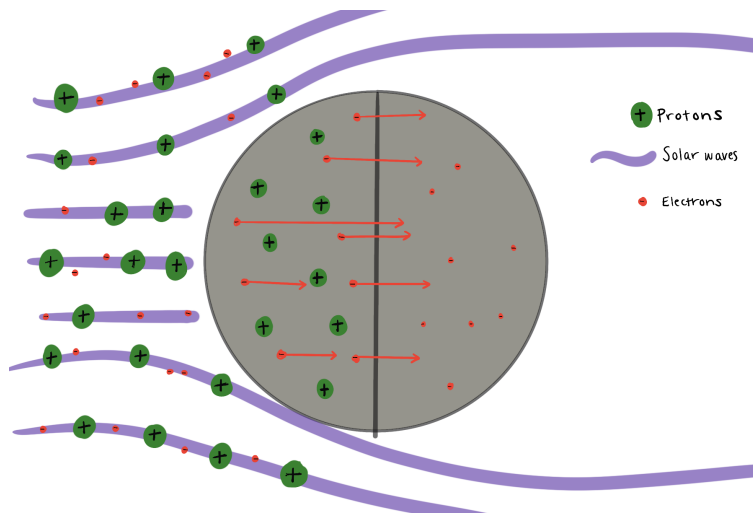


Figure 3.8: Illustration of solar wind impacting a perfect sphere - reflects an electrostatic charged environment via solar wind.

The back half of the moon/sphere has a void of charges. This is not a stable environment and as a result, the lighter in mass electrons rush to the uncharged half of the moon. This movement of electrons creates an environment with varying charge.

Since the shapes of Phobos and Deimos are not ideal spheres, electrostatic charges can build up along topographic features. This phenomenon must be considered when selecting landing sites on both Phobos and

Deimos. Electrostatic charges have the potential to interfere with the lander's electronics. Mitigation tactics are detailed in the command and data handling subsystem in chapter four.

## **3.5 Resupplying with the DST**

Resupplying with the DST comes with several advantages and challenges. Such advantages include a smaller Delta-V requirement, the ability to offload waste and samples at the DST, the ability to swap on board scientific equipment between sorties, and a significant reduction in the total mass of the EEV. These listed benefits of resupplying the DST, and the subsequent challenges to implementing their use in the mission, are detailed in this section.

### **3.5.1 Logistics of Resupplying**

By opting for a mission that includes resupplying the EEV with the DST, it is necessary to assess the viability of transferring consumables from one craft to another in the micro-G environment. Fortunately, resupplying a craft in space with consumables necessary for human survival has extensive heritage with the International Space Station [14]. The ISS resupplies its food, water, air tanks, scientific equipment, and other miscellaneous items necessary for crew survival and comfort by transporting the needed cargo through an airlock between the two spacecrafts. Similarly, the EEV will be resupplied by docking with the DST and transferring all the needed on board cargo through an airlock.

Some consumables, such as food, will be transferred through the airlock. All water, oxygen, and nitrogen will be brought on the EEV and does not need to be transferred. At the end of each sortie, waste and core samples will be offloaded by the crew. Three encapsulation spheres (see section 4.6.3) will be transferred to the DST by the crew using the robotic arm.

The amount of time spent resupplying the EEV is estimated to be 2 hours. This takes into account the total mass that needs to be transferred, the mobility of the crew in the micro-G environment, and the necessary breaks for the crew to rest.

### 3.5.2 Logistics of Refueling

While refueling the EEV with the DST offers many benefits to the mission, it does come with the cost of adding a layer of complexity to the overall mission. This additional complexity is made worse, as the transferring of fuel in a micro-G environment has little precedence in the history of crewed spaceflight. The proposed method of refueling is explored in this section.

The DST shall have the additional purpose of acting as a propellant depot for the mission. This means that in addition to carrying the amount of fuel necessary for the DST to perform all of its maneuvers, the DST shall also carry an extra **10,700 kg** of propellant for the EEV to refuel with. This extra amount of propellant is the amount necessary for the EEV to perform the remainder of its maneuvers for the second sortie to Deimos from the DST.

| Event Number                     | 1st Refueling | 2nd Refueling | 3rd Refueling         |
|----------------------------------|---------------|---------------|-----------------------|
| Next Mission Phase               | Phobos Ops    | Deimos Ops    | End of Life at Phobos |
| Remaining Delta-V Capacity (m/s) | 600           | 450           | 400                   |
| Propellant Mass Transferred (kg) | <b>3967</b>   | <b>2885</b>   | <b>3781</b>           |
| Final Delta-V Capacity (m/s)     | 2400          | 1700          | 2200                  |

Figure 3.9: Expected propellant mass transfer for each refueling event.

Due to the toxicity of the chosen propellant for the mission, it was deemed that a remotely operated refueling method would be employed for the refueling of the EEV. While little precedence of automated transfer of fuel between two spacecrafts exists, NASA has performed small scale tests of refueling in space with their Robotic Refueling Missions [15]. As such, the designed refueling apparatus between the DST and EEV shall have similar components with modifications necessary for the mission. The following figure details the proposed autonomous architecture for the transfer of propellant between the EEV and the DST.

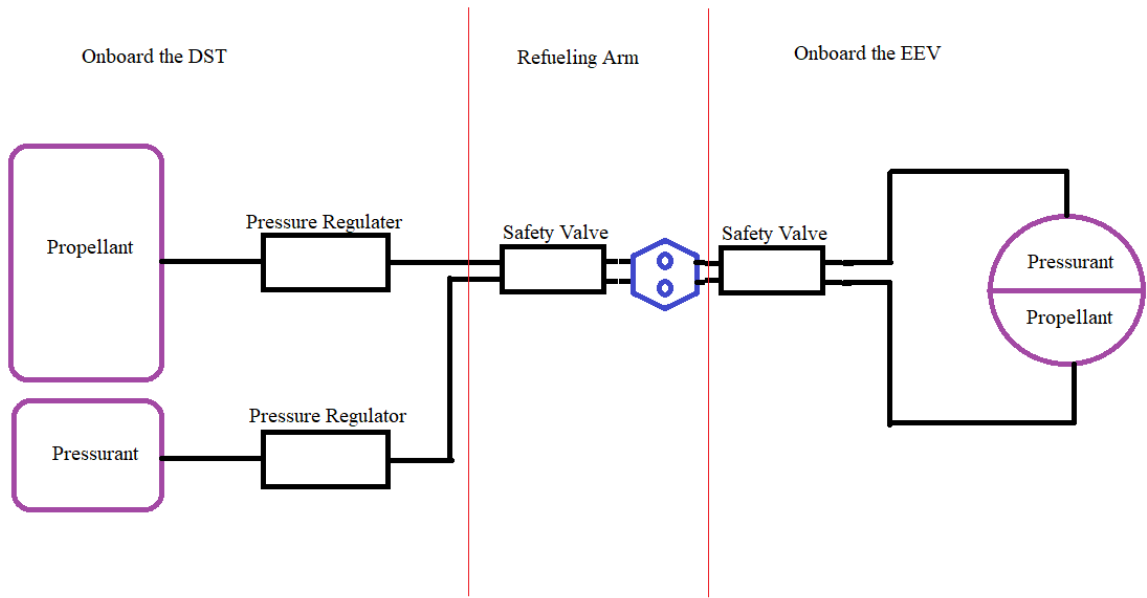


Figure 3.10: Proposed system architecture of the refueling system

As shown in Figure 3.10 above, the propellant will be transferred with an array of transfer lines, pumps, safety valves, and a robotic arm attached to the DST. Because the propellant for the EEV can be stored without cryogenic conditions, the temperature regulation for the entire system will mostly be passive methods. These methods shall include sufficient coating of insulation along any exterior pipe networks.



# Chapter 4

## Exploration Excursion Vehicle

### 4.1 EEV Overview

The Exploration Excursion Vehicle (EEV) is a human-rated spacecraft that will enable two astronauts to explore the surface of Phobos and Deimos. This chapter details the overall architecture of the EEV, details of its subsystems, and the EEV's reliance on a Deep Space Transport (DST) interface for portions of the mission.

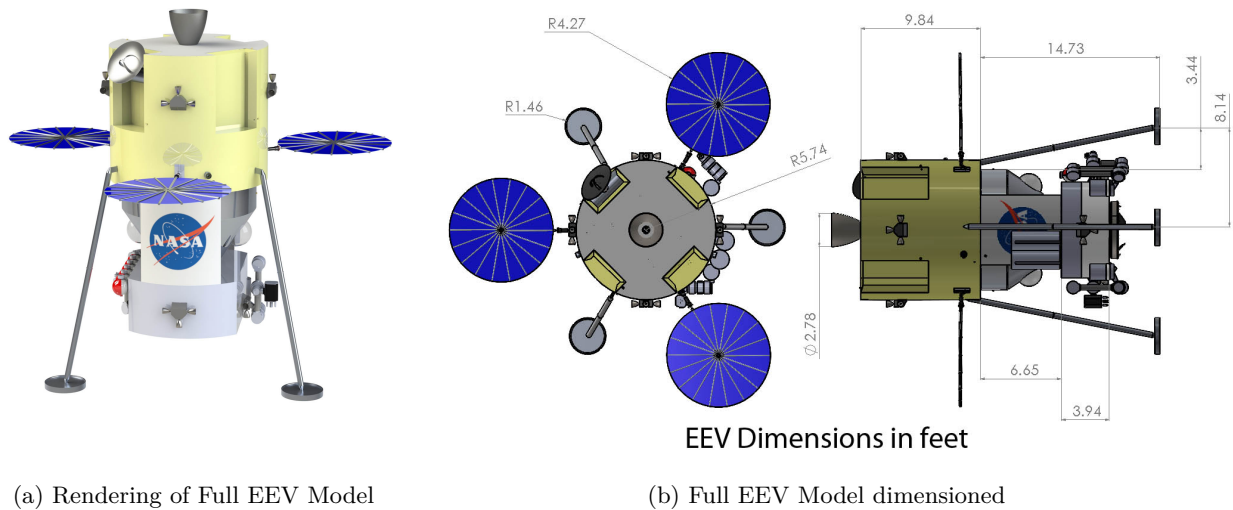


Figure 4.1: Rendered views of the full Exploration Excursion Vehicle (EEV)

There are three main sections of the EEV that are visible.

1. **Service Module (Top):** The Service Module contains the propellant tanks, life support tanks, and power system for the spacecraft. The main engines, solar panels, communication dish, four reaction

control (RCS) assemblies, and several navigation sensors are also mounted on the surface. Three landing legs will be mounted to the bottom of the service module.

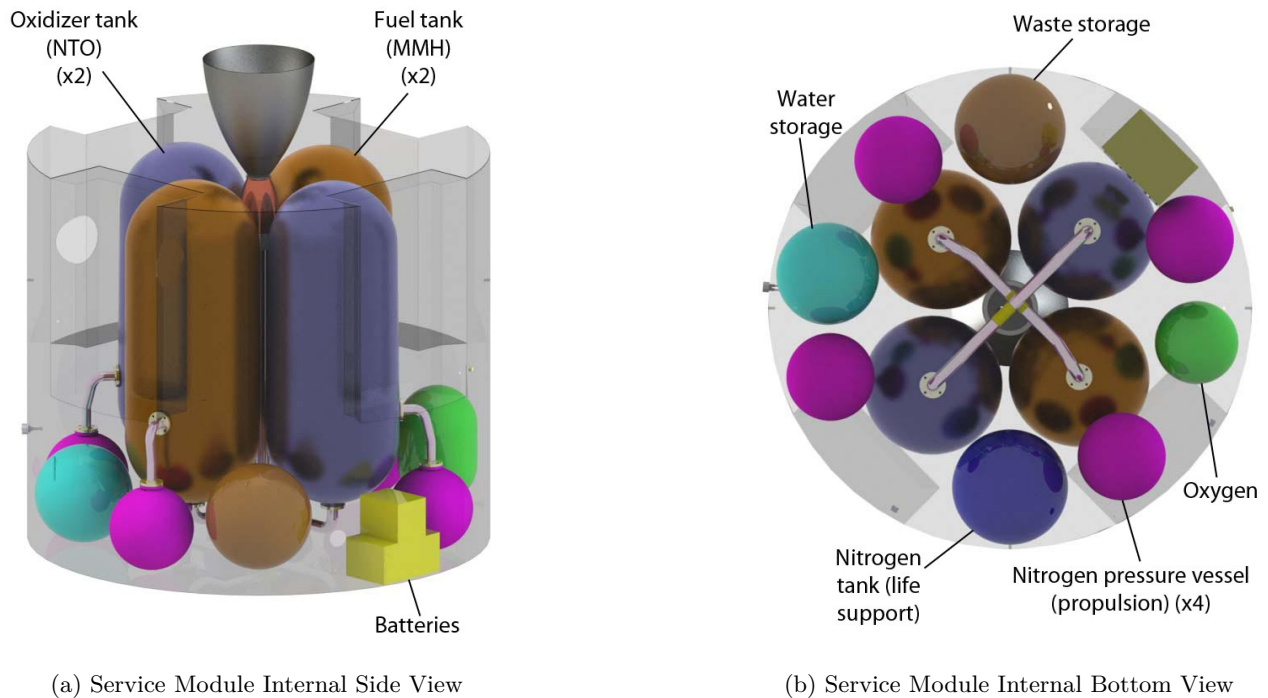


Figure 4.2: Service module internal views

**2. Crew Module (Middle):** The Crew Module is the capsule where a two person crew will reside for entirety of moon operations. The crew module is the only pressurized section of the EEV. Contained within are seats, windows, control panels, consumables, life support equipment, and all scientific equipment that will be handled by the crew.

The orientation of the crew module is inverted, with the crew positioned "upside down" relative to the moons' surfaces. This unconventional orientation is made possible by the micro-gravity environment and is preferable for two reasons. First, this allows the pilot a direct line of sight to the moons' surfaces during landing and visibility of the robotic arm during sample collections. Second, this orientation reduces the total pressurized volume, therefore reducing power requirements and thermal and life support system mass.

The crew module also has two semi-spherical windows, one for each crew member. This shape allows the crew to have increased situational awareness and improved visibility of the moons' surfaces and

EEV exterior. One downside of this design is that heat flux out of the capsule is slightly greater, increasing requirements for the thermal system.

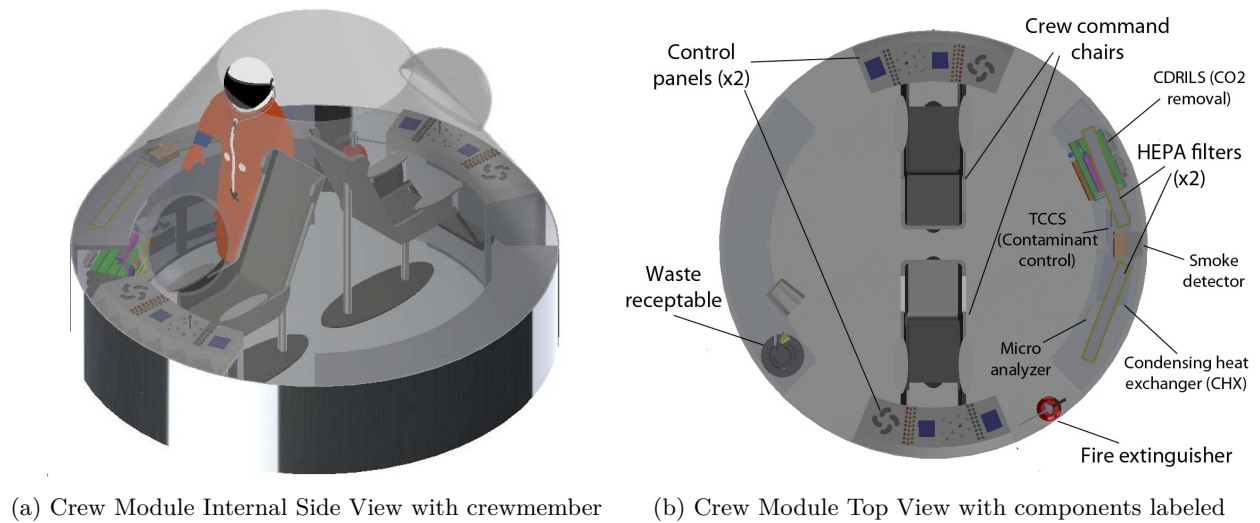


Figure 4.3: Crew module internal views

3. **Payload Module (Bottom):** The Payload Module is split into two parts - one being dedicated to the suite of the operational sensors and the other being composed of a choreographed core sample organization system which transports both coring sample bits and coring sample containment racks within the module so that they can be quarantined or shipment in and out of the module. A over-viewing visual of the scientific systems equipped to the payload module can be found in Figure 4.4 below:

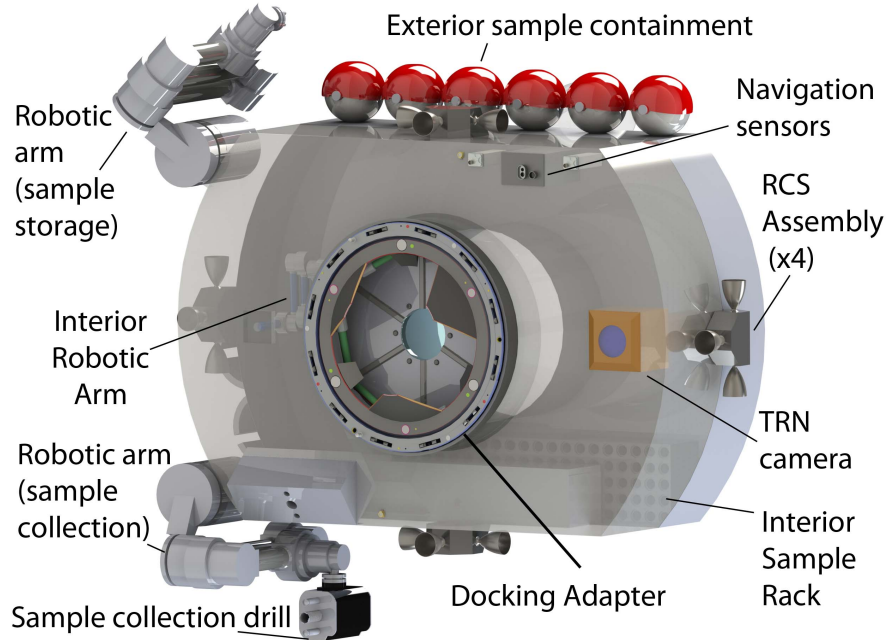


Figure 4.4: Payload Module Internal View labelled.

#### 4.1.1 Mass and Power Budget

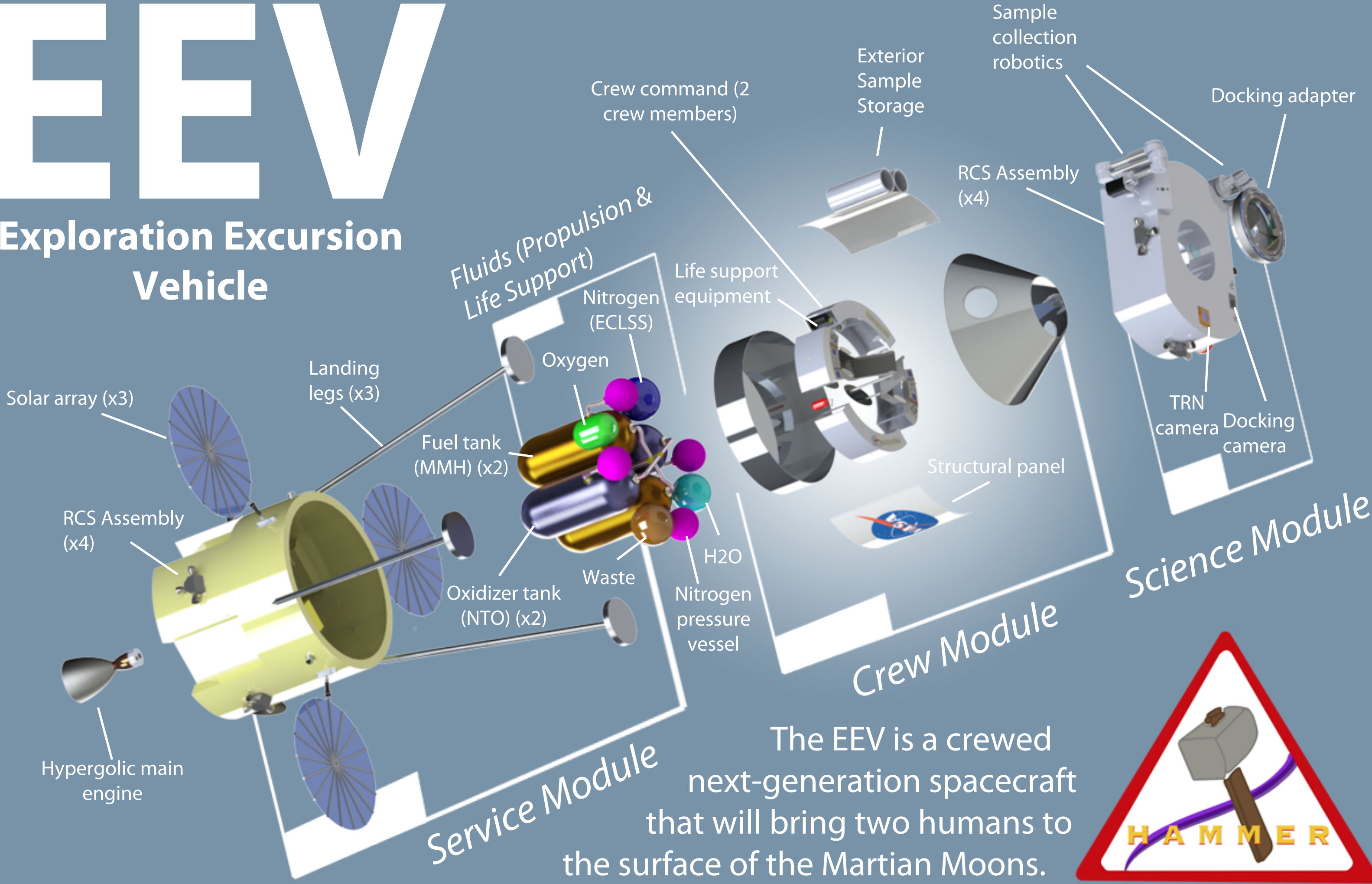
The mass budget for each system is estimated below to predict a total mass budget. Margin values were applied based on the new SMAD manual [16].

| Subsystem    | Mass [kg]      | Margin percentage | Margin mass [kg] | Allocated mass [kg] |
|--------------|----------------|-------------------|------------------|---------------------|
| GNC          | 121.12         | 10%               | 12.11            | 133.23              |
| C&DH         | 86.5           | 10%               | 8.65             | 95.15               |
| PROP         | 341.53         | 5%                | 17.08            | 358.61              |
| STRUC        | 3659.9         | 10%               | 366.0            | 4025.9              |
| PAY          | 1101.02        | 10%               | 110.10           | 1211.11             |
| ECLSS        | 739.57         | 10%               | 73.96            | 813.53              |
| COMM         | 60.7           | 10%               | 6.07             | 66.77               |
| POW          | 584.0          | 6.90%             | 40.3             | 624.3               |
| TCS          | 300.0          | 10%               | 30.0             | 330.0               |
| <b>Total</b> | <b>6994.34</b> |                   | <b>664.27</b>    | <b>7658.60</b>      |

Table 4.1: Integrated system mass budget for EEV

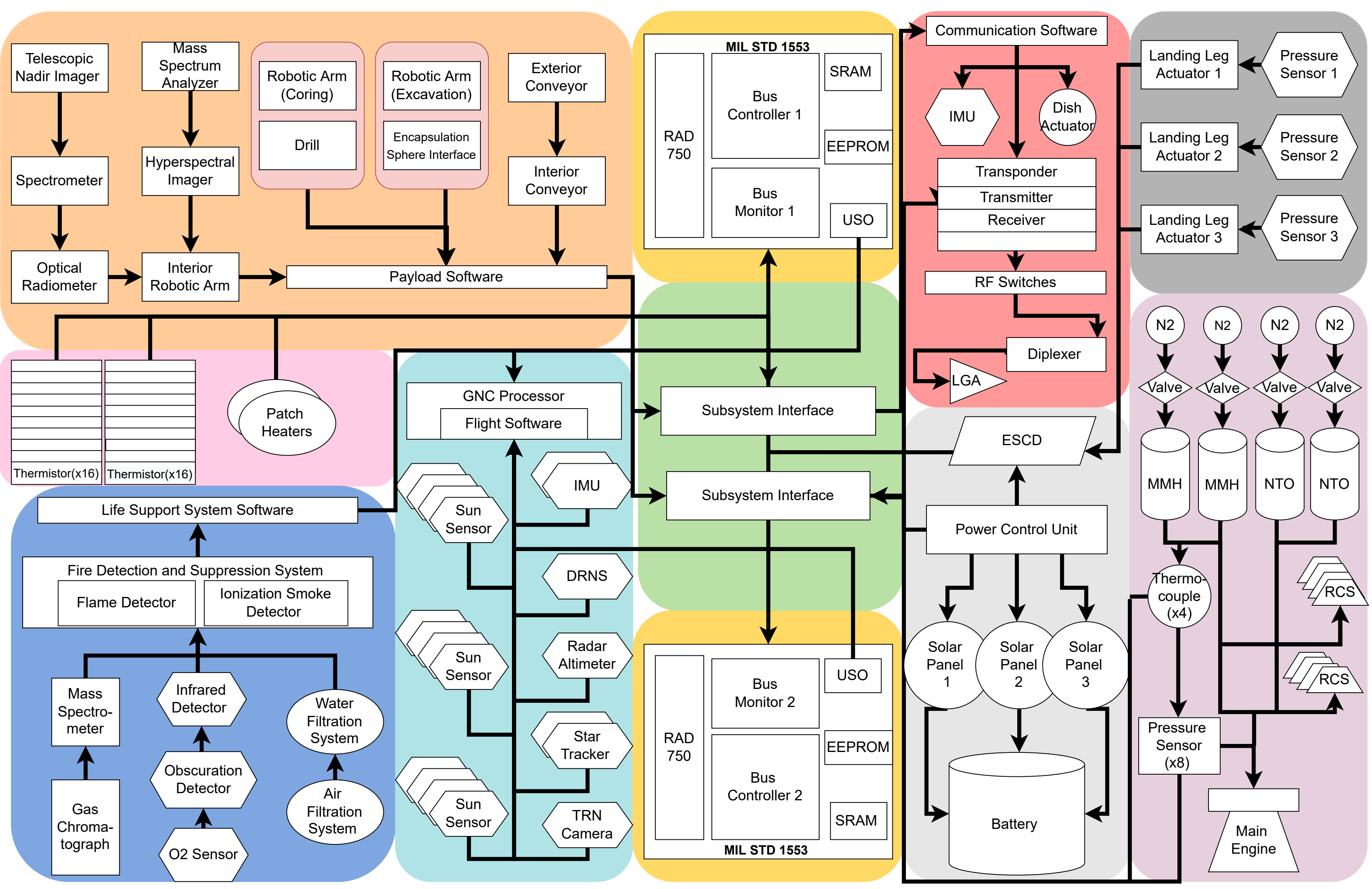
# EEV

## Exploration Excursion Vehicle



The EEV is a crewed next-generation spacecraft that will bring two humans to the surface of the Martian Moons.





The power budget for the EEV and its different modes (see section 4.9.3) is below.

| Subsystem | Maximum power mode [kW] | Minimum power mode [kW] | Afterlife mode [kW] | Critical power mode [kW] |
|-----------|-------------------------|-------------------------|---------------------|--------------------------|
| GNC       | 0.14                    | 0.026                   | 0.14                | 0.14                     |
| CDH       | 0.0155                  | 0.01                    | 0.003               | 0.0155                   |
| COMM      | 0.05                    | 0.01                    | 0.05                | 0.05                     |
| PROP      | 1.423                   | 0.1944                  | 0.1944              | 0.1944                   |
| POW       | 0.03                    | 0.03                    | 0.03                | 0.03                     |
| STRUC     | 0.01                    | 0.002                   | 0.002               | 0.002                    |
| LSS       | 1.15                    | 0.115                   | 0                   | 0                        |
| TCS       | 0.25                    | 0.15                    | 0.08                | 0.08                     |

Figure 4.5: Power Budget.

### 4.1.2 Launch Vehicle Selection

The Falcon Heavy is selected as the launch vehicle for the EEV [17]. With an estimated launch cost of 178 million dollars based on heritage from the Europa Clipper mission [18], the Falcon Heavy lies within a 1 billion dollar mission budget. The Falcon Heavy is flight-proven and capable of lifting a maximum of 16,800 kg to Martian orbit. The current fairing size has an inner length of 11 meters and an inner diameter of 4.6 meters. These dimensions informed the EEV design. The EEV will sit entirely within the fairing in a complete state.

## 4.2 Guidance, Navigation, and Control

The Guidance, Navigation, and Control (GNC) System of the EEV is responsible for orbit determination, attitude determination, maneuver execution, and attitude control. To fulfill this responsibility, GNC will provide the suite of sensors necessary to perform state/momentum estimation, and actuators necessary to execute guidance commands. GNC will also provide the corresponding algorithms to utilize these sensors and actuators effectively.

### 4.2.1 System Architecture

GNC encompasses the Navigation, Guidance, and Control Subsystems. The Navigation system is responsible for state and momentum estimation. The difference between this estimate and the guidance command will

quantify the error in the EEV's position, attitude, and momentum. This quantity will determine the behavior of the control algorithm, which is tasked with minimizing this error.

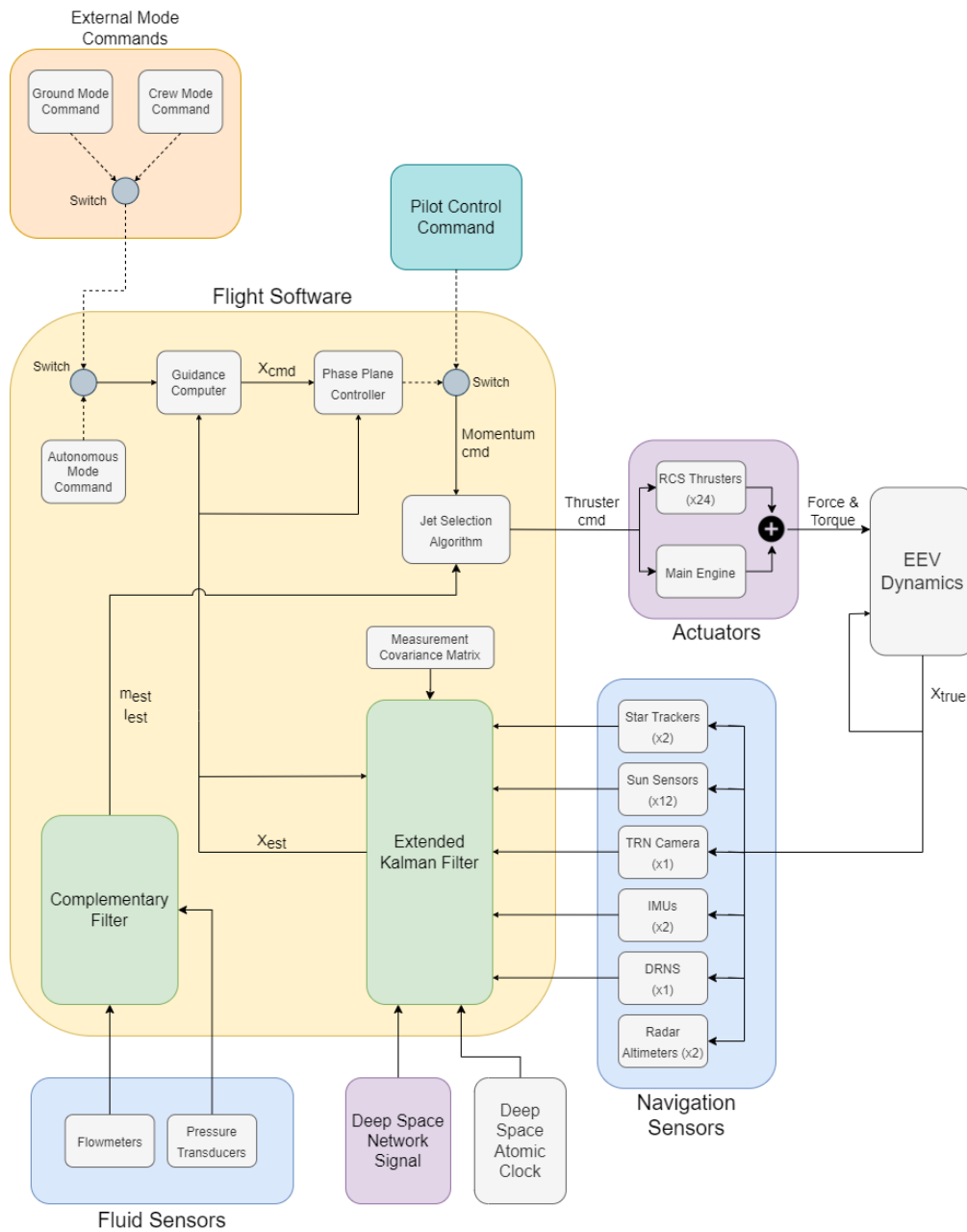


Figure 4.6: High-Level Architecture for the GNC System. Includes all the sensors and actuators that will be used on the vehicle.

Note that there are switches in the architecture. These switches allow for the crew, ground, and the flight software to change the spacecraft mode, depending on mission phase. The pilot can also override the internal



controller to directly control the spacecraft. This architecture allows humans to be in the loop to assist in operation of the GNC system.

#### 4.2.2 Navigation Sensors

This section provides details of the sensors being used by the Navigation Subsystem. Communication with the Deep Space Network (DSN) will be used to provide additional position measurements. An Extended Kalman Filter (EKF) will be used to generate the best estimation of the EEV's state and momentum from the sensor measurements. Models of each of these sensors were created for installation in the vehicle assembly.

**Inertial Measurement Unit (x2):** IMUs contain an accelerometer and gyroscope which measure linear acceleration and angular velocity, respectively. These measurements are integrated to acquire velocity, position, and attitude estimates. The product being used is a **STIM-377H**.

**Star Tracker (x2):** Star Trackers provide an estimate of attitude by measuring the position of the stars. The mission will use a new star tracker from Ball Aerospace, the **CT-2020**.

**Radar Altimeter (x2):** Radar Altimeters provide estimates of altitude relative to a surface, which is essential for landing. The mission is using the **GRA 5500** from Garmin for this mission, which provides 16.5 km of range.

**Sun Sensor (x12):** Sun Sensors can provide information about the EEV's attitude the location of the Sun. The mission is using the NFSS-411 from NewSpace Systems for this mission, a modern Fine Sun Sensor.

**Docking Relative Navigation System (DRNS):** The DRNS is a suite of sensors that contains LIDAR and an Optical Camera, which will provide the EEV with high accuracy and precision in a relative state for autonomous docking. The DRNS is heavily inspired by the STORRM system, which was successfully tested in space for the Orion project.

**Terrain Relative Navigation (TRN) Camera:** The TRN Camera will provide images such that the EEV can determine its position relative to the surface of Phobos and Deimos. This camera is heavily inspired from the Perseverance lander.

**Deep Space Atomic Clock (DSAC):** The DSAC provides a high precision time estimate for the EEV.

This information allows for the vehicle to process ranging information from the DST and DSN onboard for position and velocity estimates.

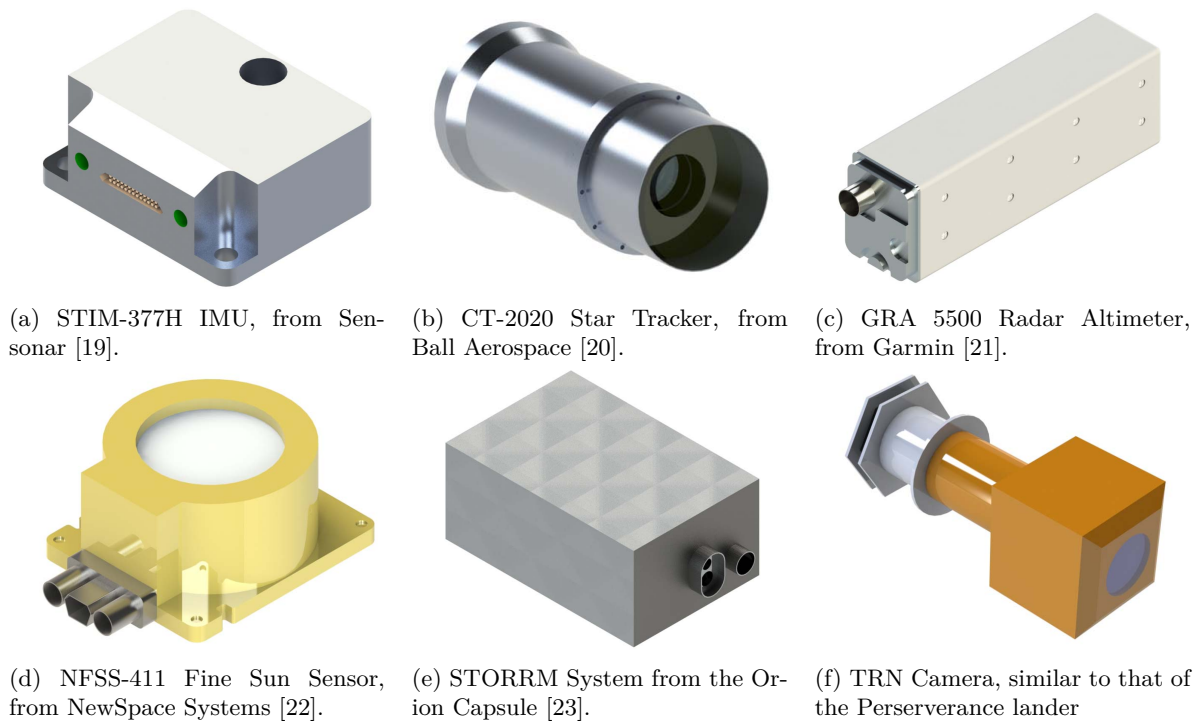


Figure 4.7: Chosen Navigation Sensors for the EEV.

### 4.2.3 Reaction Control System

#### Actuator Selection Trade Study

There are many permutations of actuators that can be used on the vehicle for different purposes. Therefore, a trade study was conducted to assess the benefits and drawbacks of different attitude and momentum control (AC and MC) actuators. Reaction/Momentum wheels, chemical thrusters, and electric thrusters were considered in the design process. Ultimately, chemical thrusters were chosen for both attitude and momentum control due to the significant control authority and comparatively simple design.

| Design Factors (scale 0.1 to 1)<br>Alternatives                                  | Control Authority (x3) |     | Simple Design (x2) |     | Fuel Consumption (x3) |     | Power Consumption (x2) |     | Monetary Cost (x1) |     | Total (out of 11) |
|--|------------------------|-----|--------------------|-----|-----------------------|-----|------------------------|-----|--------------------|-----|-------------------|
|  | U                      | W   | U                  | W   | U                     | W   | U                      | W   | U                  | W   |                   |
| <b>AC:</b> Reaction Wheels<br><b>MC:</b> Chemical Thrusters                      | 0.3                    | 0.9 | 0.6                | 1.2 | 0.9                   | 2.7 | 0.6                    | 1.2 | 0.7                | 0.7 | <b>6.7</b>        |
| <b>AC:</b> Chemical Thrusters<br><b>MC:</b> Chemical Thrusters                   | 0.9                    | 2.7 | 0.8                | 1.6 | 0.2                   | 0.6 | 0.8                    | 1.6 | 0.8                | 0.8 | <b>7.3</b>        |
| <b>AC:</b> Chemical Thrusters<br><b>MC:</b> Momentum Wheels & Chemical Thrusters | 1.0                    | 3.0 | 0.5                | 1.0 | 0.4                   | 1.2 | 0.7                    | 1.4 | 0.6                | 0.6 | <b>7.2</b>        |
| <b>AC:</b> Chemical Thrusters<br><b>MC:</b> Electric Thrusters                   | 0.8                    | 2.4 | 0.3                | 0.6 | 0.5                   | 1.5 | 0.3                    | 0.6 | 0.4                | 0.4 | <b>5.5</b>        |
| <b>AC:</b> Electric Thrusters<br><b>MC:</b> Chemical Thrusters                   | 0.1                    | 0.3 | 0.3                | 0.6 | 0.8                   | 2.4 | 0.2                    | 0.4 | 0.3                | 0.3 | <b>4.0</b>        |

Figure 4.8: Design decision matrix used to select the actuator type for this mission.

## Configuration

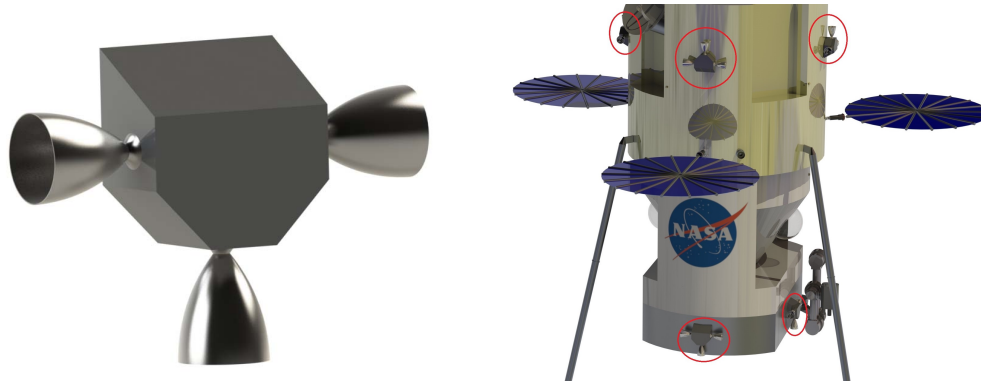
The EEV is equipped with 24 small bipropellant thrusters to execute control commands. Section 4.4.2 contains details of the hardware used. This thruster can provide anywhere from 378-511 Newtons of thrust, and has the ability to pulse quickly.

These thrusters will be grouped in pairs of three, for eight total RCS assemblies. Four RCS assemblies will be placed near the bottom of the vehicle, while four will be placed near the top of the vehicle. This RCS system will not have throttle. It is worth noting that for the assemblies on the bottom, the robotic arms (see section 4.6) will be positioned (rotated) such that they are not in the way of the RCS jet plumes.

## Control Algorithm

Autonomous operations require a controller for the RCS. To test control algorithms, developed an in-house Six Degree of Freedom (6DOF) environment to simulate the spacecraft. A nonlinear phase plane control law was selected for a high level controller as the RCS does not have throttle. This controller has varying deadbands and rate limits depending on the spacecraft mode.

A jet selection algorithm is required to determine which thrusters, and for what amount of time, must be turned on to fulfill the momentum command of the high level controller. The algorithm used on the



(a) RCS Assembly using three Aerojet R-4D-11 thrusters (b) Locations of the RCS assemblies around the vehicle.

Figure 4.9: Configuration of the Reaction Control System.

EEV will be a Linear Program (LP) that minimizes the mass consumption required for fulfilling momentum commands,

$$\begin{aligned}
 & \text{minimize } \Sigma c^T t \\
 & \text{s.t. } \mathbf{A}t = [p_{ref} \ h_{ref}]^T \\
 & \quad t \geq 0
 \end{aligned} \tag{4.1}$$

where  $c^T$  is a vector containing the mass flow rates of each thruster,  $t$  is a vector containing the on-time of each thruster, and  $\mathbf{A}$  is a matrix that maps the time vector to the corresponding changes in linear momentum  $p_{ref}$  and angular momentum  $h_{ref}$ . This matrix changes depending on the current mass and inertia tensor of the EEV, which is estimated by the fluid levels in each tank.

This algorithm was tested in several scenarios. One example, shown in Figure 4.10, is a scenario where the EEV is initialized in a tumbling state. The controller is quickly and effectively able to detumble the spacecraft and restore the commanded attitude of the spacecraft.

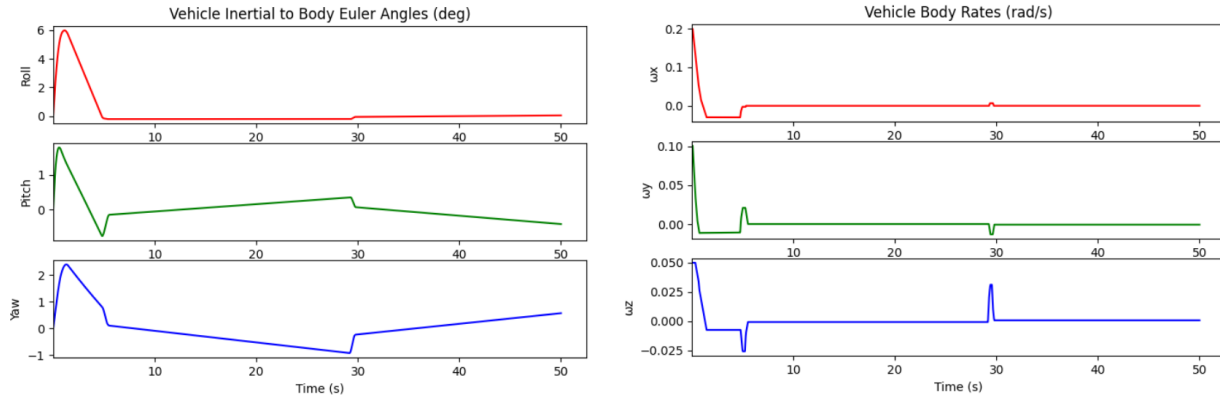


Figure 4.10: Plots demonstrating the effectiveness of the RCS controller in reducing body rates and restoring a desired attitude.

## 4.2.4 Maneuvers

In this section, the most prominent spacecraft maneuvers and their relation to the GNC system will be detailed.

### Autonomous Docking

The DRNS, Sun Sensors, and Star Trackers will initialize the EEV's relative state to the DST. The RCS will be used to orient the spacecraft and control a slow trajectory towards the DST, with accurate state information being provided by the DRNS and IMUs. The thrusters can also be used for an abort if necessary.

### Landing

The landing sequence will be executed by a pilot, rather than autonomously. There are two reasons for this. First, autonomous landing has never been attempted with a crew, and hence poses an unacceptable safety concern for the astronauts. Second, there is insufficient terrain map resolution on the majority of the surfaces of Phobos and Deimos [24]. This provides an unnecessary constraint on the landing locations on each moon, a constraint easily avoided by the use of a pilot.

The pilot will use the RCS to control a slow descent towards the surface. The main engine does not need to be used due to the micro-gravity environment. Approximately 20 meters off the ground, the pilot

will observe the surface of the moon and select an landing site; then, they will slowly guide the EEV to the surface at less than 0.5 m/s.

From the combination of the Radar Altimeters, Star Trackers, IMUs, and TRN Camera, the pilot will have an estimate of the EEV's altitude and attitude at all times during descent. The pilot will also have a visual of the surface through their semi-spherical window.

### **Traverse**

The EEV will have multiple sites to visit on each moon, so a methodology to travel from one point to another has been established. The EEV will "hop" from one location to another; to do this, the pilot will first use the RCS to climb to an altitude at which the terrain will not interfere with lateral motion. Next, the EEV will travel horizontally at 5 m/s to its next landing site.

### **Takeoff**

The takeoff sequence for the EEV is less involved. Due to the micro-gravity environment, the EEV will launch directly into its next transfer orbit without attempting to orbit Phobos or Deimos first. This maneuver will be done using the main engine, with the RCS providing attitude control.

## **4.3 Command and Data Handling**

The Command and Data Handling (CDH) subsystem is charged with the collection, processing, and management of data on board the EEV. Responsibilities include autonomous monitoring of subsystem health, carrying out on board and off board commands, data storage and organization, and providing accurate calculations of locations and orientations of the spacecraft's surroundings and proper mission time. This section will discuss the detail of the CDH subsystem involving architecture, hardware, software, and the Electrostatic Charge Defense system (ESCD).

### 4.3.1 System Architecture

The CDH system's on board processing includes both software and hardware. The following subsections review these two classes in greater detail.

#### Software

CDH software is separated into five classes:

- (1) Operating system.
- (2) Subsystem software that ensures the proper operation of subsystems and supervises and services subsystem health.
- (3) Software management that is responsible for the storage and processing of mission data.
- (4) Control system software that makes orientation, orbit, attitude, and time calculations using GNC and CDH instrumentation and data. Control system software also assists in autonomous docking and low gravity landing.
- (5) Payload management software operates the instruments used for sample collection and storage. Information gathered by the payload management system is shared with software management for proper data storage and processing. [25]

Software management (3) utilizes static random access memory (SRAM) and (EEPROM). SRAM and EEPROM are volatile and non-volatile forms of memory storage respectively. Using both memory forms allows for efficient storage usage, redundancy, and data security in the event of power loss. It is assumed that the specific software selected will be the most recent version that complies with the hardware discussed below.

#### Hardware

The EEV uses a distributed bus architecture with two buses and two central processors to transport information between components. The specific hardware selected is two Military Standard 1533 data bus (*MIL-STD-1533*), two RAD750 processors, and an ultra stable oscillator (*USO*).

The *MIL-STD-1533* data bus for this mission has 31 terminals for subsystems with two connection cables

on each terminal for redundancy purposes. Along with these subsystem terminals are the two RAD750 processors, two bus monitors, and two bus controllers. These components also have two cable connections. The *MIL-STD-1553* is well known for its' redundancy on a variety of crewed, heritage missions. Proper CDH function is essential for completion of the mission and survival of the crew, thereby making the fail safe nature of the MIL-STD-1533 highly desirable for a deep space spacecraft like the EEV.

The bus controller, 31 terminals, and bus monitor have specific functions:

- 1) The bus controller controls the flow of data throughout the system using a command/respond procedure.
- 2) The remote terminals connect the data bus to the subsystems and their instruments.
- 3) The bus monitor collects and stores data received and processed by the bus.

The *MIL-STD-1553*'s has a 80% efficiency with a 20-bit word as the smallest unit exchange. Three bits are allocated for synchronization and one bit for a parity check. Leaving 16/20 bits available. Drawbacks include a signal loss of 1dB per 100 ft of wire in the connector cables and a data-throughput of 1 Mbps. The Federal Communication Commission recommends a data throughput greater than 25 Mbps for data-heavy operations. [26] [25]

Looking to heritage missions such as the Mars Reconnaissance Orbiter and JUNO, BAE System's *RAD750* processor was selected for the on board processor. The *RAD750*, while costly, is equipped with radiation resistance, strong arithmetic capabilities, and fast processing speeds. The *RAD750* performs between 32 and 64 bit arithmetic and processes at speeds greater than 260 million instructions per second. Two *RAD750* processors will be used in the EEV CDH as outlined in the block diagram.

The *RAD750* offers four memory types. Two of which are SRAM and EEPROM. SRAM and EEPROM will be utilized for this mission as defined in software section of the CDH system.

To keep mission time, the EEV uses an USO. The extremely low gravity effects felt on Phobos and Deimos creates an unstable landing and sampling environment, enforcing strict stability and precision requirements. An USO's consideration of frequency and vibration impacts on the CDH electronics will help ensure proper mission time is kept.[25]



### 4.3.2 Risk and Risk Mitigation

The greatest risk to the CDH system is the electrically charged surfaces of Phobos and Deimos causing a semi-permanent loss in power. Without a functional CDH system, mission success and crew safety is threatened. Planetary surfaces become electrically charged as solar radiation excites surface features such as dust. There is little knowledge on how charged dust particles behave in low gravity environments such as those on the Martian moons. Using heritage missions and research as a guide, the mission is expected to experience some level of discharge due to the triboelectric effect of Martian moon dust [27] [28]. To mitigate the risk of power loss due to surface contact - discharge, the EEV maintains an Electrostatic Charge Defense system (ESCD). The ESCD system can be categorized by its location on the EEV: Solar panels, landing legs, and surface features. Specific mitigation tactics are addressed further in the power and structure subsections.

## 4.4 Propulsion

The goal of the main propulsion system is to provide thrust to the EEV for its trajectory-changing maneuvers between the Deep Space Transport and the Martian moons, and to provide thrust for landing and ascent on the moons. As the only way to significantly alter trajectory, it is vital for the propulsion system to be as reliable as possible. For this mission's high  $\Delta v$  requirements, it also will need to be highly efficient to reduce the required fuel mass.

Due to the very low gravity field on both moons, it is impractical to use a high-thrust engine for landing or ascent. It is also impossible to orbit either moon due to their low masses. The process of landing on the surface is more similar to an orbital rendezvous and docking than it is to a traditional landing. Therefore, the landing phase of the mission will be performed by the attitude-controlling reaction control system thrusters. For the higher energy orbital maneuvers, it would be impractical, inefficient and slow to use the RCS thrusters. Therefore, a separate main engine with higher thrust is the best design.

## 4.4.1 Propulsion Requirements

### Main Engine Requirements

The initial engine design criteria can be derived from the mission and system requirements. The RFP requires that the excursion to both moons be completed within thirty days. This eliminates the use of electric propulsion, which is highly efficient, but very low thrust and would lead to very slow maneuvers. Also, the engine should be able to be controlled and throttled to ensure more precise burns.

Since the engine will not be used during landing and ascent phases, the engine will be placed on the top of the spacecraft, opposite the landing legs. This allows more room on the bottom of the spacecraft for scientific tools and crew working space. Main engine thrust can vary, but the ceiling on thrust is determined by the amount of acceleration that the crew and instruments can take. To protect instruments and the crew, the acceleration experienced from the engine should not exceed 0.1g. In the trajectory calculations on page 19, a  $\Delta v$  requirement of 2,400 m/s was determined for the orbital maneuvers. The engine chosen should be the most efficient engine possible while requiring the least mass. This will be a significant factor in fuel choice, which will be discussed later on.

### Reaction Control Thruster Requirements

The reaction control system thrusters will primarily be used for attitude control and the landing and ascent. To maintain attitude in multiple directions, multiple thrusters must be mounted at different points of the vehicle. On page 37, it was determined that multiple thrusters were needed, with three nozzles in three different directions for each RCS assembly. The same section also shows where they will be placed on the spacecraft and how the control system will operate them.

For attitude control, it is important that the thrusters can fire at a range of low thrusts for very short periods of time, differing from the high thrust and long burn requirements of the main engine. For RCS thrusters, it is possible to use cold-gas, monopropellant or bi-propellant fuels. Either one is very reliable, but bi-propellant is most efficient. If the thrusters use the same fuel as the main engine, the spacecraft can eliminate the need for additional fuel tanks.

## 4.4.2 Propulsion Design

### Design for Engine Reliability and Risk Mitigation

Reliability is a key factor for this mission, as engine failure can lead to total crew loss and mission failure. Highly reliable engine design and engine parts must be chosen to ensure that the engine will not fail. To ensure the most reliable engine, proven, high-TRL level technologies with significant heritage are preferred. Several design decisions that increase reliability will be described. Instead of a turbopump-fed staged combustion cycle engine or another more complex engine cycle that would be seen on first stages of launch vehicles, a pressure-fed engine cycle has fewer points of failure and is better suited for in-space propulsion.

Reliable ignition is also an essential part of a reliable engine. If an igniter fails, the engine will "hard start", exploding and endangering the entire crew. Hypergolic, which ignite on contact with each other, are a reliable way to [29]

Propulsion reliability also depends on the number of engines. [30] Every engine has a possibility of failure, and in the case of one engine failure, other engines could still be used to complete the mission or return to the DST. However, the RCS fuel system will be given extra margin, and will be suitable enough to return the crew safely if engine failure should occur. Therefore, more than one main engine is unnecessary.

For both RCS and main engines, it is also possible for the system to fail due to a fluids component failure. To mitigate this risk, redundancies can be put into place in the system. Multiple valves and sensors will be used to ensure system functionality if one component fails. The system will also have multiple fuel tanks to mitigate the risk of fluid system failure.

### Trade Study: Propellant Choice

Choosing the propellant is an important step that will affect the rest of the engine design. Although the RCS propellants can vary, modern high thrust engines are universally liquid bi-propellant engines. From bi-propellants, the fuel and oxidizer should be storable, efficient, flight-proven and have a high energy density. Below in Figure 4.11, the properties of some of the most common bi-propellants are compared in a decision matrix to determine the optimal propellant choice.

| Design Factors<br>Propellant Options | I <sub>sp</sub> (efficiency)<br>(Weight=3) |      | Oxidizer/fuel ratio<br>(Weight=2) |      | Storability (boil-off)<br>(Weight=4) |     | Density<br>(Weight=2) |     | Design heritage<br>(Weight=3) |     | Total (out of 14.0) |
|--------------------------------------|--|------|-----------------------------------|------|--------------------------------------|-----|-----------------------|-----|-------------------------------|-----|---------------------|
|                                      | U  | W    | U                                 | W    | U                                    | W   | U                     | W   | U                             | W   |                     |
| RP-1, LOX                            | .8   | 2.4  | .90                               | 1.8  | .4                                   | 1.6 | .9                    | 1.8 | 1.0                           | 3.0 | <b>10.6</b>         |
| CH <sub>4</sub> , LOX                | .9   | 2.7  | .7                                | 1.4  | .3                                   | 1.2 | .5                    | 1.0 | .3                            | .9  | <b>7.2</b>          |
| H <sub>2</sub> , LOX                 | 1.0  | 3.0  | .1                                | .2   | .1                                   | .4  | .3                    | .6  | .9                            | 2.7 | <b>6.9</b>          |
| MMH, NTO                             | .75  | 2.25 | .95                               | 1.90 | .95                                  | 3.8 | 1.0                   | 2.0 | 1.0                           | 3.0 | <b>12.95</b>        |
| UDMH, NTO                            | .70  | 2.1  | 1.0                               | 2.0  | 1.0                                  | 4.0 | .95                   | 1.9 | .9                            | 2.7 | <b>12.7</b>         |

Key: U=Unweighted W=Weighted 1.0=Best .1=Worst

Figure 4.11: Decision Matrix: Propulsion System Propellant choice [29] [31] [32]

From figure 4.11 above, the most optimal fuel is MMH (monomethyl hydrazine) with NTO (nitrogen tetroxide) oxidizer. The first three fuels in Figure 4.11 (RP-1, CH<sub>4</sub> and H<sub>2</sub> with liquid oxygen) are cryogenic, which is highly efficient but will also boil off very quickly, which is not optimal for long term missions. These three fuels are primarily used for launch vehicles and first stages. Monomethyl hydrazine and unsymmetrical-dimethyl-hydrazine (UDMH) are both very efficient propellants when combined with dinitrogen tetroxide. They can be stored at much higher temperatures and therefore do not boil off as significantly. Another significant benefit of hydrazine and NTO fuel combinations is that they are hypergolic, and will ignite very reliably. Hydrazine fuel combinations have significant heritage for in-space propulsion [29] [31] and have been used on many interplanetary transfer stages and crewed missions.

### Main Engine Heritage

The propulsion system can be designed completely from the ground up, but it will be more reliable if it uses a commercially available design that has already been significantly tested and flight-proven. For the main engine, one of the most prominently used in-space propulsion systems for crewed missions is the Aerojet AJ-10 thruster, which has been used on Apollo, Space Shuttle, multiple interplanetary transfer stages and

will be used on Orion. The AJ-10 uses MMH/NTO fuel, is simple and reliable pressure fed design and can be throttled. It has an  $I_{sp}$  of 316s and produces 26.689 kN of thrust. The engine weights 118kg.

An AJ-10-190 engine can be modified to provide different thrust for different needs, and one can be modified to fit the EEV’s needs as a main engine.

### Reaction Control Thruster Heritage

For low-thrust attitude control thrusters, a prominently-used option is Aerojet Rocketdyne’s R-4D-11. This thruster has the benefit of using the same fuel as the AJ-10, and has been used reliably in crewed and uncrewed spaceflight. For this thruster, it would not be necessary to modify or scale down. The R-4D-11 has a thrust range of 378-511N and an  $I_{sp}$  of 311 s. It has been used in Apollo, Shuttle and many other heritage spacecraft.

### Engine Sizing and Calculations

In the earlier trajectory calculations on page 19, a required 2.4 km/s was calculated, with the biggest maneuver requiring approximately 1km/s. The targeted accelerations during burns is around 0.1g. Using the Rocket Equation and Newton’s Second Law with the earlier estimated dry mass of 7,300kg and the AJ-10-190’s  $I_{sp}$  of 316s, the EEV Propulsion System specifications are calculated and displayed in Table 4.2

$$\text{Tsiolkovsky Rocket Equation: } \Delta v = I_{sp} \cdot g_0 \cdot \ln\left(\frac{m_{wet}}{m_{dry}}\right) [33]$$

| Main Engine Specifications    | Value            |
|-------------------------------|------------------|
| Isp                           | 316 s            |
| $\Delta v$                    | 2.4 km/s         |
| Propellant Mass (main engine) | 8938 kg          |
| Wet (Total) Mass              | 16,596 kg        |
| Main Engine Mass Flow         | 51 kg/s          |
| Thrust                        | 16 kN [3596 lbf] |

Table 4.2: Data for EEV Propulsion System, Scaled from AJ-10 [34]

## Engine CAD Models

Both propulsion systems were designed based on the decided specifications and constructed in Solidworks. Their designs are shown and discussed below.

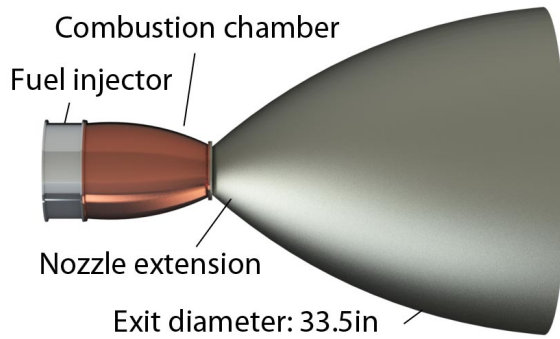


Figure 4.12: CAD Model of the main engine, created using reference material from Aerojet Rocketdyne [35] and other references on liquid rocket engines [31] [34]

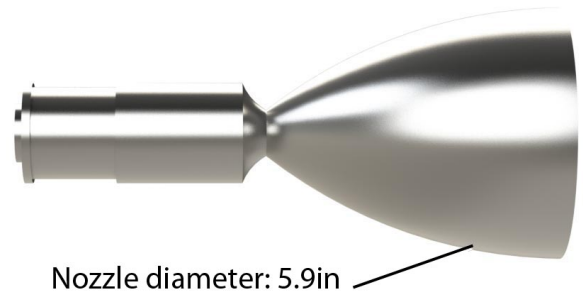


Figure 4.13: CAD Model of the R-4D-11, created using reference material from Aerojet Rocketdyne [35].

## Main Engine Design

The EEV main engine is a modified AJ-10-190, shown in Figure 4.12. The AJ-10-190 was designed to propel the space shuttle, but the EEV is a lighter spacecraft, and the engine doesn't need to produce as much thrust. The mass flow rate and throat area can be scaled down to determine the dimensions of the EEV engine. The same expansion ratio of 55 is kept to maintain the same  $I_{sp}$ . The thrust chamber will be stainless-steel and nickel with regenerative cooling channels. Regenerative cooling is when the cold fuel is fed through tiny channels in the wall of the thrust chamber before entering the injector, allowing the thrust chamber to absorb heat easily [31]. The thrust chamber will be cooled with cooling channels within it, but the nozzle will not be regeneratively cooled, and only be passively cooled by an ablative applied to the inside of the nozzle. This is because it is difficult to manufacture cooling channels in a thin nozzle, and the exhaust temperature drops significantly after entering the nozzle.

## Reaction Control Thruster Design

The RCS uses an R-4D-11 thruster, shown in Figure 4.13. The EEV is equipped with 24 of these small thrusters in groups of three to execute its control commands. It has the ability to pulse rapidly for small attitude adjustments. The placement and control system is discussed in the GNC section on page 37.

### 4.4.3 Propulsion Fluids System

The fluids system will reliably provide fuel to the engine and RCS thrusters. Both systems draw from the same fuel tanks, but there are multiple fuel tanks and multiple valves to ensure fluids system redundancy. There are four pressurant tanks that drive the propulsion system: two oxidizer tanks, two fuel tanks. The full fluids system is laid out in the Spacecraft Block Diagram.

The fuel lines are filtered upstream of the engine or RCS system because it needs to flow through the thin regenerative cooling channels. Valves are positioned to allow for the individual control of the engine, RCS, and pressure vessel. To support refuelling from the DST, each tank has the capacity to be vented, and minimal quick disconnect ports are used to reduce the necessary connections during refuelling. The refuelling capability would involve using the DST as a propellant depot with a specialized refuelling apparatus that interfaces with EEV fuel ports. The refuelling apparatus is covered in the DST section on page 82.

The ability to refuel in space is a technology still in development [15]. There is difficulty with refuelling due to space environment factors that are covered in the DST section. It is near-future technology and will likely be reliable when this mission takes place. The propulsion system benefits from the ability to refuel from the DST, because it allows the EEV to have less propellant mass and not carry all its fuel from the beginning.

#### Tank Sizing

The fuel tanks are designed for the calculated fuel mass with sufficient margin and redundancy. By using the density of the fuel and oxidizer and the expected pressures and temperatures, tank mass and volume can be calculated. The values are in Table 4.4.3. Note that while the data is for individual tanks, there are two

of the propellant and oxidizer tank for redundancy. The tank data was calculated based on the new SMAD [16].

| Tank                        | Material         | Mass     |
|-----------------------------|------------------|----------|
| MMH (fuel) Tank             | Ti6AlV4          | 27.17 kg |
| NTO (oxidizer) Tank         | AlZnMg1          | 45.94 kg |
| N <sub>2</sub> (pressurant) | Carbon/Epoxy CFK | 13.32kg  |

Table 4.3: Propulsion Fluids Tank Data

## 4.5 Structures

### 4.5.1 Structures Design

The EEV structure will provide micro-meteoroid and orbital debris protection, and will be capable of sustaining landing forces, extreme temperatures, and radiation. The structure consists of the physical material encapsulating the crew and EEV contents and the landing legs.

The structural material will determine the EEV’s strength and durability against environmental factors. Materials research has been primarily sourced from previous Martian Rovers as well as lunar landers. The materials for the EEV main structure are: high modulus carbon fiber, Flex-core aluminum vented honeycomb structure, BTCy-1A Toughened Resin, and Super Light Ablator SLA-561V.

The structure will be made up of a flex-core aluminum vented honeycomb core, with layers of high-modulus carbon fiber. The aluminum will create a strong base structure[36], and the carbon fiber will add strength and stiffness [37]. The toughened resin has advantages over other materials such as epoxy, as it is serviceable in vacuum, has low moisture absorption and is has no significant volatile emission in space. The last layer, SLA-561V, will act as thermal protection for the structure [36] [38].

The TEST-RAD system will also be incorporated into the junctures of the EEV. This system is a CDH dust mitigation tactic that prevents discharge due to the electrostatic charge of the martian moons detailed in section 4.3.2. TEST-RAD repels charged dust particles via repulsive fibers embedded in regolith and chinchilla fur. It is important to prevent contamination and discharge in the junctures of the EEV as a defense between the habitable interior and essential electric equipment, and the outside environment. Initial



testing shows the TEST-RAD is only 30% effective in repelling dust particles [39] . It is assumed this efficiency will reach 80% by the year 2035.

The second part of the structure is the landing legs, whose purpose is to protect the vehicle from the terrain of the landing site and to absorb landing loads. Due to the extremely low gravity on the moons, the landing legs will implement RCS to assist and push the vehicle towards the surface. The crush angle of a material is the angle of the applied landing load on a material. Materials that have directional strength will decrease in strength depending on crush angle, and have the highest strength along the main axis of the material. The capability to constrain the crush angle can allow for maximum material strength [40]. Due to the extremely low landing forces, the current design choice is based on simplicity and thus will be rigid, non telescoping legs.

The materials for the landing legs will consist of an aluminum honeycomb core with carbon based graphite fiber fabric and 7178 Aluminum Alloy for the poles, with aluminum honeycomb foot pads. Aluminum honeycomb has high energy absorption, which will be crucial for landing loads. Carbon based graphite fiber fabric is lighter than aluminum but retains high rigidity and will support the leg poles along with the aluminum.

Incorporated into the landing leg's foot pads will be the HOMES system. This is one of the CDH mitigation tactics for potential discharge due to electrostatic charge of moon's surfaces described in section 4.3.2. HOMES has four phase wire electrodes that create alternating electric fields to move charged particles with variable charges. This system repels roughly 91% of 0.45-0.50 micrometer particles and roughly 98% of 0.45-560 micrometers particles [41] . HOMES can currently withstand a weight of the average astronaut. It is assumed that HOMES will have a successful upscale by 2035 and can withstand the force between the EEV and martian moon terrain upon landing.

Lastly, the landing gear will have the capability to be stored in a compact position and deployed once separated from the DST. The deployment mechanism will be primarily mechanical and utilize a system of springs. Locking mechanisms will hold the legs in the deployed position. The landing gear will be stored in the launch vehicle. Once deployed, the legs will remain in this position for the duration of the mission. Additionally, there will be pressure sensors on the foot pads to detect ground contact during landing. [42]

## 4.5.2 Landing Legs Analysis

A structural analysis test was done on the landing legs. A load of 1600 N was applied to the bottom of the landing leg, with the connection to the EEV being a fixed area.

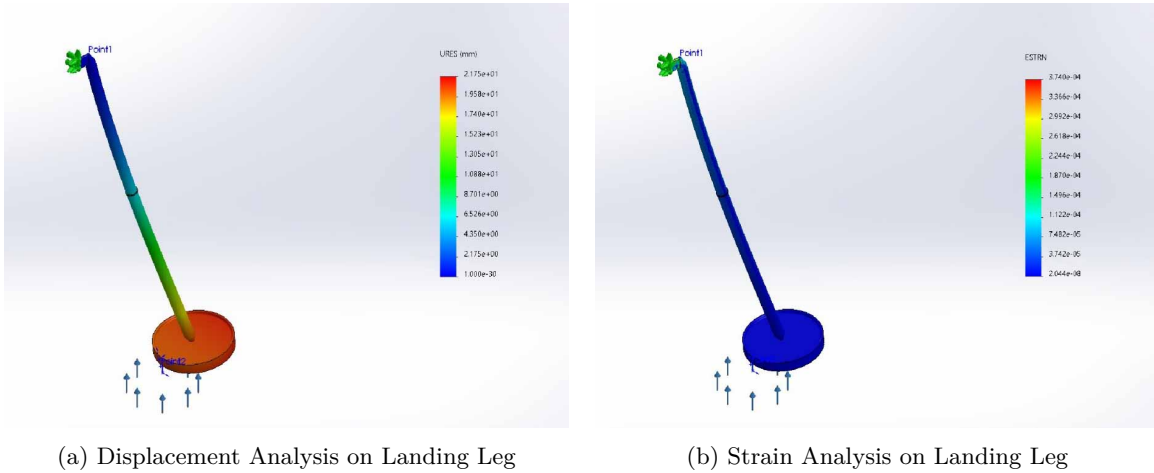


Figure 4.14: Structural Analysis done on the Landing Leg in Solidworks

As shown in figure 4.14a and 4.14b, maximum displacement on the legs is at this load is 21 mm, and the maximum strain is shown to be  $3.7\text{e-}4$  mm/mm. These results show that the landing legs will be suitable for the mission, and will remain structurally intact.

## 4.6 Payload & Sampling Systems

### 4.6.1 Sampling Procedures and Sample Containment

To achieve the mission's scientific goals of investigating the origins of the Martian moons and to assess their viability to support future missions in the Martian region, two sampling methods are employed onboard the EEV. The first is a complex sample coring and hand-off system similar to that of the *Perseverance's*, and the second is a more archaic excavation method in which the pilots capture large rocks and the surrounding area using spherical encapsulating mechanisms. Although differing in complexity, both sample collection systems have their own methods of sample collection and quarantine to ensure that the crew can collect anything of interest that is identified both during and prior to their mission. The backbone of these sampling systems are dependent on the payload module – home to an assortment of sensors and robotics necessary to

support navigation, attitude control and sample transport/organization during the mission. The expected and max-potential mass collection from each moon for each sampling system are found in Tables 4.4, 4.5 and 4.6 below:

| Sampling Method [Phobos] | Max Collection [Kg] | Expected Collection [Kg] |
|--------------------------|---------------------|--------------------------|
| <b>Coring</b>            | 79.5                | 63.6                     |
| <b>Excavation</b>        | 115.8               | 57.9                     |

Table 4.4: Phobos - Max and Expected Collection Masses for each Sampling System

| Sampling Method [Deimos] | Max Collection [Kg] | Expected Collection [Kg] |
|--------------------------|---------------------|--------------------------|
| <b>Coring</b>            | 63.0                | 50.4                     |
| <b>Excavation</b>        | 91.2                | 45.6                     |

Table 4.5: Deimos - Max and Expected Collection Masses for each Sampling System

| Sampling Method [Both] | Max Collection [Kg] | Expected Collection [Kg] |
|------------------------|---------------------|--------------------------|
| <b>Coring</b>          | 142.5               | 114.0                    |
| <b>Excavation</b>      | 207.0               | 103.5                    |
| <b>Total</b>           | 349.5               | 217.5                    |

Table 4.6: Both Moons - Max and Expected Collection Masses for each Sampling System

Both the coring and excavation sampling systems use similar exterior robotic arms but the two sampling systems each have different end interfaces - the coring system has a drill interface while the excavation has an interfacing mechanism specific for utilizing the encapsulating spheres. Both sampling systems utilize a 6-DOF robotic arm, each of which have a radial reach of approximately 3.15 meters - allowing for coring and collection of surface minerals in an expansive envelop. The only notable difference between the two arms, aside from their respective end effectors, is the degree of autonomy that is associated with piloting each. The crew member operating the coring system arm can submit a request to the robotic systems to move to the drill to specific locations and can submit further request to make small adjustments; However, all other coring system maneuvers are automated for safety and precision during interfacing on the EEV. On the other hand, the excavation sampling system robotic gives much more freedom to crew members - only

restricting the crew with a set envelop of motion and only requiring autonomy during encapsulation sphere reattachment to the exterior belt.

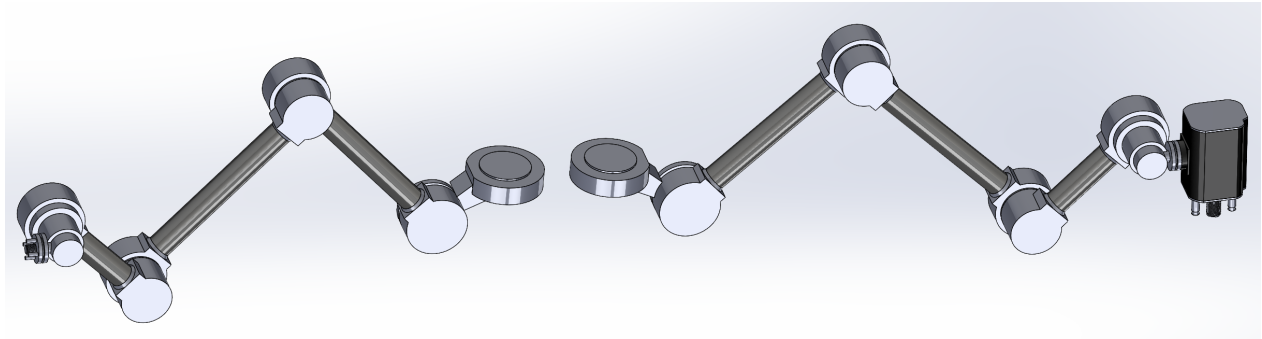


Figure 4.15: Robotic Arms for Excavation Sampler Interface (left) and Coring Drill (right)

#### 4.6.2 Coring Sampling System Architecture (C-Sampling)

The basis of the coring sample system is heavily influenced by the *Perseverance* mission, because, although the mission is not strictly an autonomous mission, the lack of EVA during mission operations makes autonomy a must for precision-required operations. The EEV drill is the most identical to the *Perseverance* mission's drill, as it has the same look and proportions; However, the heritage drill was scaled to meet mission sampling mass targets while staying within a strict mission timeline. The *Perseverance* drill was chosen because it has mission heritage with autonomously interfacing with a spacecraft main body and has utilized with a bit reloading and transport system - a necessity for collecting and, most importantly, transporting core samples in this EVA-restricted mission.

For context, the *Perseverance* drill was equipped with a 2.2 cm diameter drill barrel which collected 1.3 cm diameter by 6 cm length cores from the Martian surface. In consideration of the mission timeline, the team has had to upscale the components of that drill in order to collect 6 cm diameter by 30 cm length cores from the moons. In order to make more comprehensive estimates on the power and performance metrics of this drill, the drill was scaled according to the factor of approximately 5, which describes the increase from the collected sample core diameters (different from drill barrel diameter) of *Perseverance* to the EEV, for all drill dimensions aside from the drilling barrel depth and diameter. The drilling depth was increased by equipping the upscaled drill with a drill barrel capable of drilling 30 cm deep core with a 7.8 cm barrel diameter - which implies a 0.9 cm barrel thickness betwixt the barrel-interior sample bit and the exterior of the barrel. Notice

that this drill barrel is 0.15 cm thicker than the perseverance drill barrel - this increased thickness is presented to mitigate any potential barrel yielding during the deeper portions of drilling operations. Additionally, the higher barrel length-to-diameter portion (compared to *Perseverance*) was implemented in order to avoid the large losses in torque and higher power requirements for operation which are inherent from increasing diameter and moving along the Torque-Speed and Speed-Diameter curves [43]. Each 6 cm diameter by 30 cm length sample bit is sized to collect at maximum  $848 \text{ cm}^3$  of sample, and by using estimates of Phobos and Deimos surface densities from [44], the mission will have an estimated maximum of 1.59 and 1.26 kilograms of core sample per core from Phobos and Deimos, respectively.

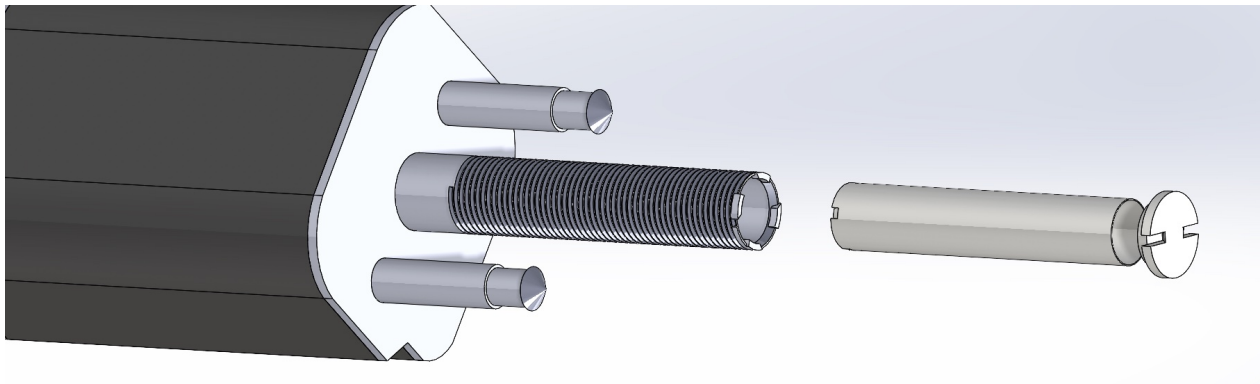


Figure 4.16: Drill Barrel, Sample Collection Bit/Tube and Hermetic Seal Cap

Because the Payload module and mass budget allow, the vehicle will store 100 corer sample bits and 4 core sample collection racks (Figure 4.17) which have room to store 25 sample bits each within the Payload module. Assuming each sample tube is filled to at least 80% volume (a 20% volume loss margin in consideration of top layer micro-gravity ejection), and assuming 50 tubes are filled at each moon, the core sampling is estimated to collect 63.6 Kg and 50.4 Kg of sample mass from Phobos and Deimos respectively. Although the collection mass from this sampling system alone already exceeds the mass collection target of 50 kg for each moon, the possibility of unexpected mishaps and failure modes requires a heavy margin when providing resources to collect samples.

As mentioned earlier, the drill is an upscaled version of *Perseverance*'s drill, which is a model of Honeybee's ROTary PERcussive Coring (ROPEC) drill. For context, this heritage drill consumes approximately 110 watts of power and drills 27 mm diameter holes [45]. With these parameters, a comprehensive estimate of the power

consumption of the upscaled drill used in the mission can be calculated by using the square of the diameter increase factor and the proportion of the feed rate increase factor according to [43]. Assuming the feed rate remains identical to the heritage drill, and considering that the system drills a 7.8 cm diameter hole (*Perseverance* drills a 2.2 cm diameter hole), the drill sampling procedures can be expected to consume a nominal 918 watts of power. Note that this is an average/nominal number which will be targeted by control loops but can be exceeded when more torque is required and at the discretion of the crew members. Variations are expected and additional margins have been provide to account for power allocations increases during sampling procedures.

| Parameter                       | Perseverance | Equipped Drill |
|---------------------------------|--------------|----------------|
| Drill Barrel Diameter (mm)      | 27           | 78             |
| Drilled Drill Barrel Depth (mm) | 60           | 300            |
| Power Consumption (W)           | 110          | 783            |

Table 4.7: *Perseverance* v EEV Drilling

As stated before, the micro-gravity environment can cause large fractional losses in sample mass (primarily, through ejections during transport), especially during sample transportation, if not adequately handled. This environment and the mission EVA restrictions renders some complex heritage drilling systems ill-equipped for mission implementation. In considerations of the micro-gravity, the team has implemented caretaking robotics which physically hand-off the core samples to other robotics systems until the sample reaches its containment unit - to ensure that samples in transit aren't ejected away from the spacecraft.

To mitigate micro-gravity effects on collected samples and avoid sample loss, after collecting a core sample, the coring drill docks at the deposition port on the Payload Module for a choreographed sample hand-off sequence which ensures that the sample bit is secured at all times. At the deposition port, the sample bit in the drill is handed-off to an interior robotic system in the payload module which transports the core sample to a sample containment rack sitting at the loading position (see Foldout at the end of the section for more in-depth procedures).

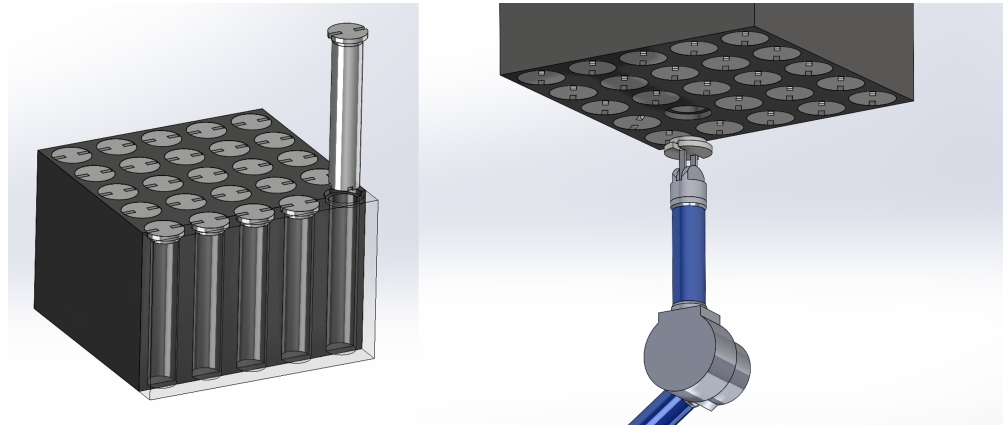


Figure 4.17: Core Sample Containment Racks

Notice in Figure 4.17 above, that the Sample Containment Racks are sized to hold 25 samples - this number was decided because the racks must enter the tunnel betwixt the crew module and docking adapter for post-mission retrieval. With 25 samples each, four of these containment racks will be stored in the Payload Module for the 100 total sample bits equipped in the EEV (discussed earlier in this section). To move each rack across the payload module, each of the four Sample Containment Racks are interfaced with a conveyor system which moves them from their **(1)** initial storage location to the **(2)** loading station location and, finally, to their **(3)** final storage location where they are pulled out by the crew after final rendezvous with the DST.

### 4.6.3 Excavation/Encapsulating Sampling System Architecture (E-Sampling)

The second sampling system is the Excavation sampling system, which uses an encapsulating sphere to capture large volumes of samples on the surface's of the moons. It is a simplistic yet effective way to collect large masses of rocks and loose gravel on the micro-gravity bodies. The encapsulating sphere encapsulates with strictly mechanical input and the interfacing mechanisms and sphere can be seen in Figure 4.18 below:

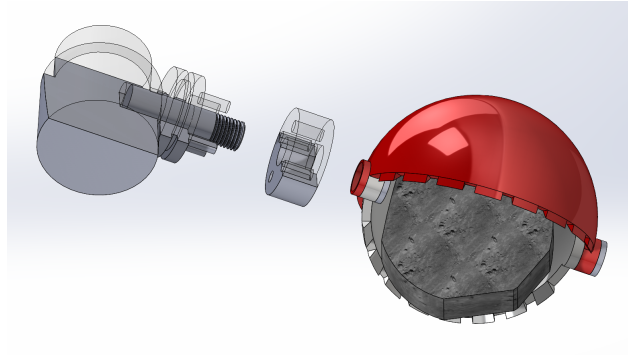


Figure 4.18: Excavation Arm Interface, Encapsulation Sphere Connector, and Encapsulation Sphere

The Excavation sampling system uses its system-allocated robotic arm to take an encapsulation sphere from the exterior conveyor and capture surface rocks and loose surface minerals within the robotic reach envelop. After capturing a sample volume, the robotic arm places the sphere back onto the exterior conveyor and the sphere is transported to the exterior containment cylinder where it will wait until it is transferred to the DST at final rendezvous (see Foldout at the end of the section for more in-depth procedures).

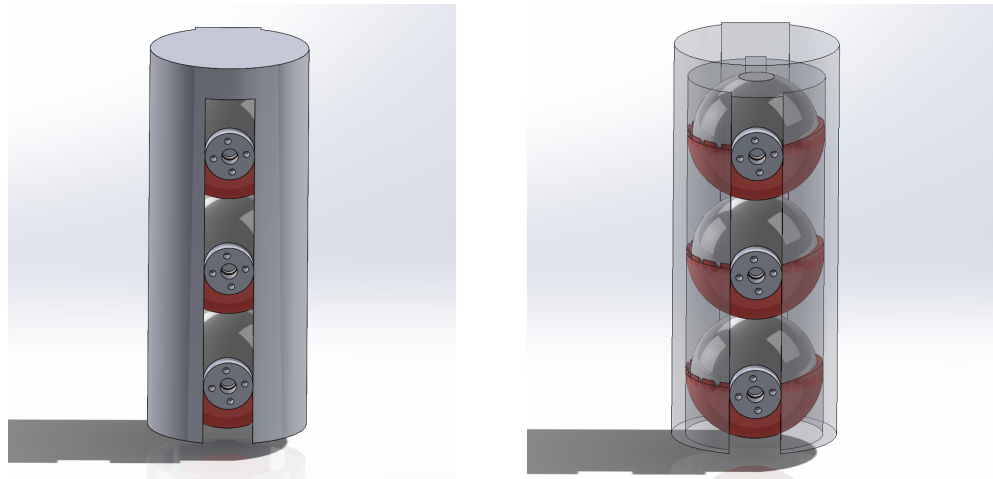


Figure 4.19: Excavation Sample Sphere Containment Cylinders

The encapsulation spheres are sized with an inner diameter of 34 cm, providing a total encapsulation volume potential of  $0.021 \text{ m}^3$ . Using the surface density estimates from [44], the maximum potential mass collection is 38.6 kg and 30.4 kg per encapsulation sphere for Phobos and Deimos, respectively. However, due to the impossible chances of filling the entirety of the sphere, 50% of the volume for failure modes and operational expectations are shaved off, which leaves an expected 19.3 kg and 15.2 kg per encapsulation sphere for



Phobos and Deimos, respectively. Equipping the EEV with three spheres per moon, a maximum potential mass collection of 115.8 kg and 91.2 kg per encapsulation sphere is calculated for Phobos and Deimos, respectively, and an expected mass collection of 57.9 kg and 45.6 kg is calculated per encapsulation sphere for Phobos and Deimos, respectively.

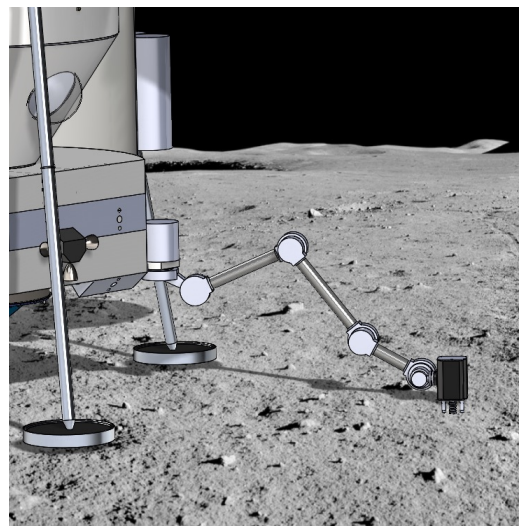
#### 4.6.4 Additional Scientific Instruments and Imagers

In order to analyze sampling sites and investigate geographical features to explore while on the surface, the EEV is additionally equipped with the following imagers. All of the tools below, except for the cameras on the robotic arms, are not needed for mass collection during the mission, but they are equipped to the EEV in order to support comprehensive analysis of the moons' geologies:

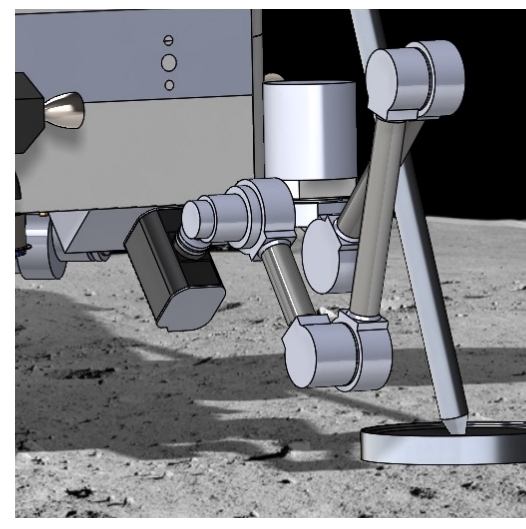
| Scientific Instruments   | Purpose  |
|--|--|
| <b>Hyperspectral Imager (Mac-rOMEGA)</b>                         | Uses high resolution imagery and spectroscopy to identify hydrated minerals, water molecules, and organic materials which will support the investigation of the evolution and formation of the Martian moons (Scientific Objective 2,3)            |
| <b>Telescopic Nadir Imager for Geomorphology</b>                 | Camera-interface system composed of optics, image sensor, AFE, ADC function, and TENG00-E to analyze geological features on the Martian moons (Scientific Objective 1)   |
| <b>Optical Radiometer Composed of Chromatic Imagers (OROCHI)</b> | Imaging system used for multi-band observations (includes 7 band-pass filters, with 7 optics and 7 CCD image sensors) which will be used to investigate geological Features, hydrated minerals, and space weathering (Scientific Objectives 1,2,3) |
| <b>Mass Spectrum Analyzer (MSA)</b>                              | Organizes samples based on mass-charge ratio which will support investigation of the space Ion Environment and possible ice inside moon materials (Scientific Objective 2,3)   |
| <b>Robotic Arm Camera</b>  | Allow for visuals during manual control of Payload Module robotic arms - during coring and excavation sampling (Scientific Objective 1,2,3)  |

Table 4.8: List of Payload Scientific Instruments NOT Used for Mass Collection

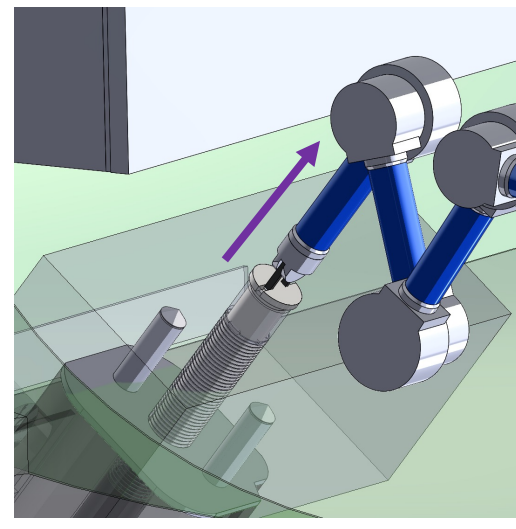
Coring Sampling System



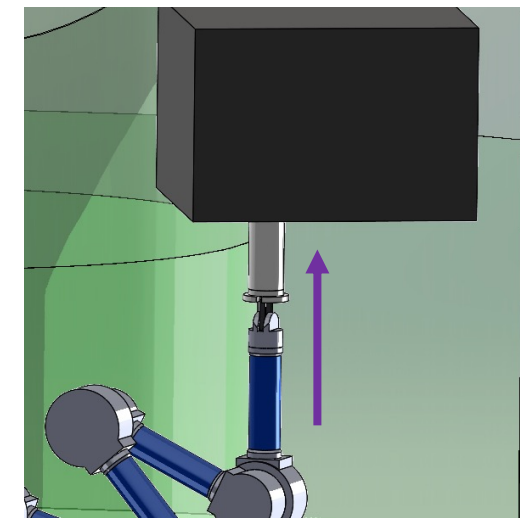
(1) 6-DOF arm extends down to sampling site after command and drills core sample



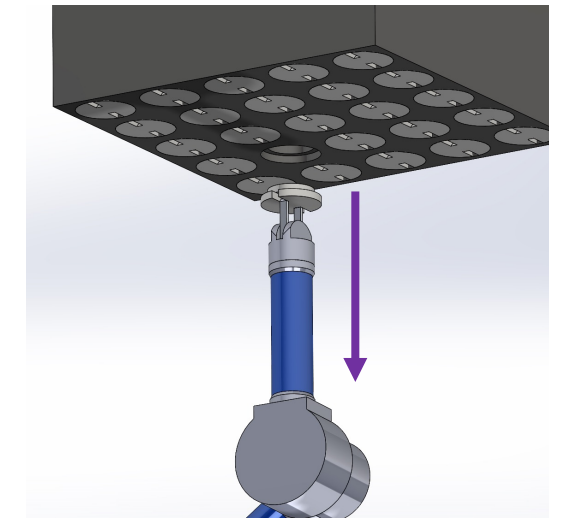
(2) After sample collection the drill docks at the deposition port to access processing station on the EEV



(3) At the processing station, the drill hands off the sample bit to the interior robotic system where it is hermetically sealed

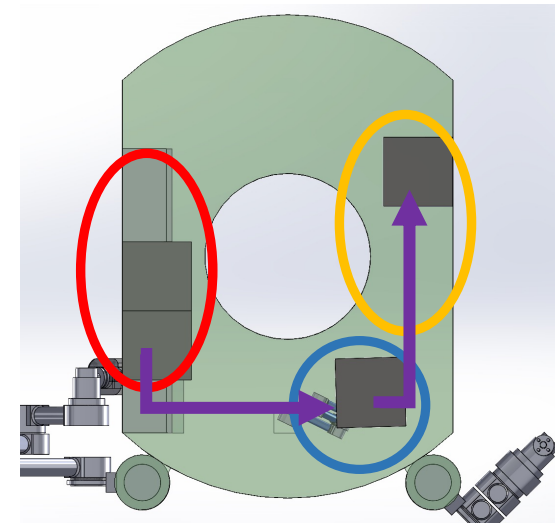


(4b) Interior robotic deposits sample bit in the sample containment service rack. If the sample rack is filled, another rack is conveyed to the loading position

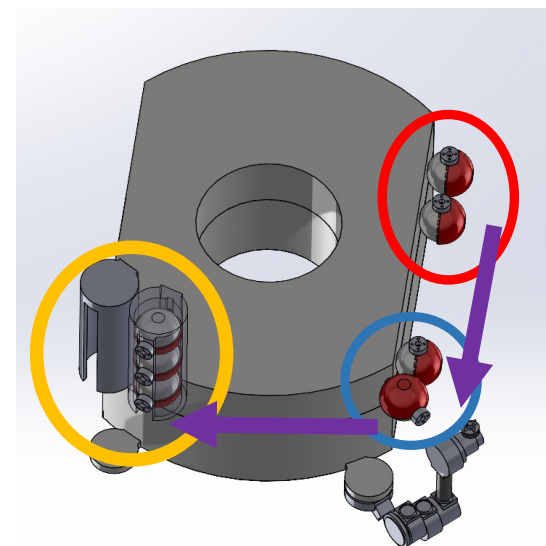


(5b) Interior robotic grabs another sample cap/seal and returns to deposition port, awaiting another sample deposit

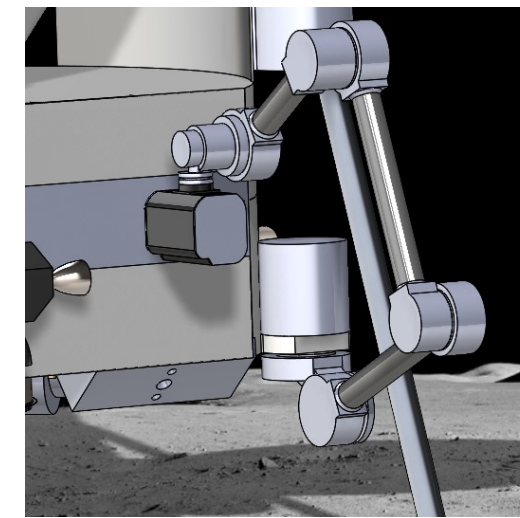
Sampler Conveyors



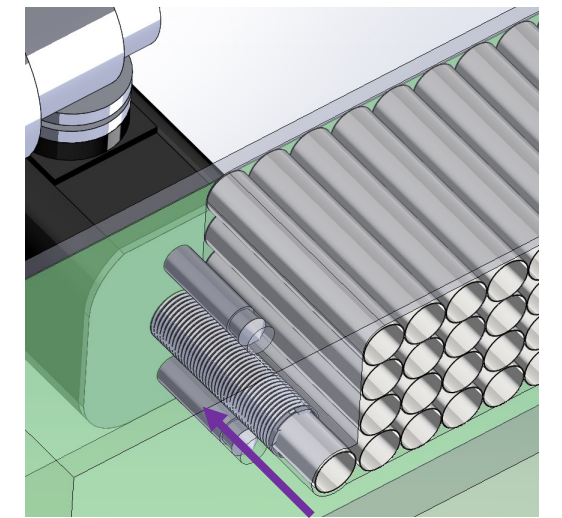
(Coring) Diagram of Sample Tube Service Rack Conveyor: {red} Initial Storage, {blue} Loading Position, and {yellow} Final Storage



(Excavation) Diagram of Encapsulation Sphere Conveying {red} Initial Storage {blue} Interfacing location {yellow} Final Storage

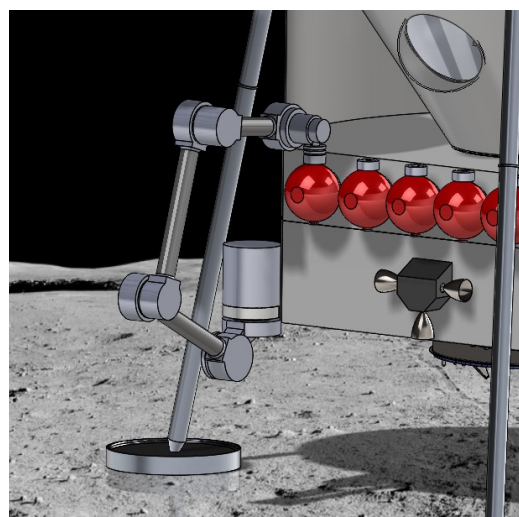


(4a) Drill undocks from sample deposition port and docks at sample bit dispenser port

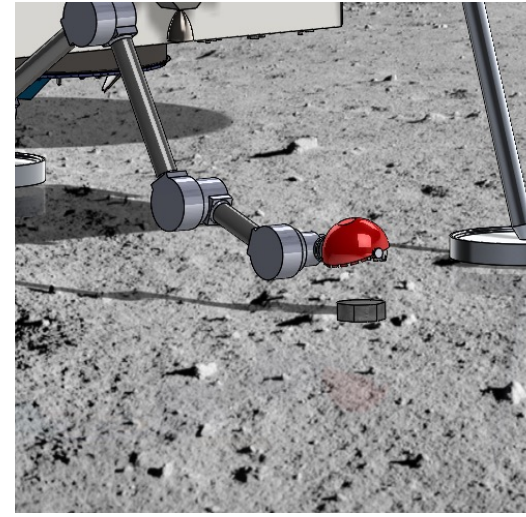


(5a) The bit dispenser port provides the drill with another sampling bit as it enter the port. After drill departure, the dispenser magazine readies another bit, awaiting the next reload

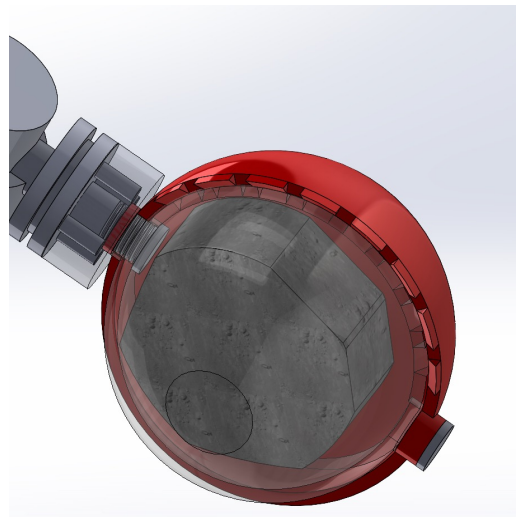
Excavation Sampling System



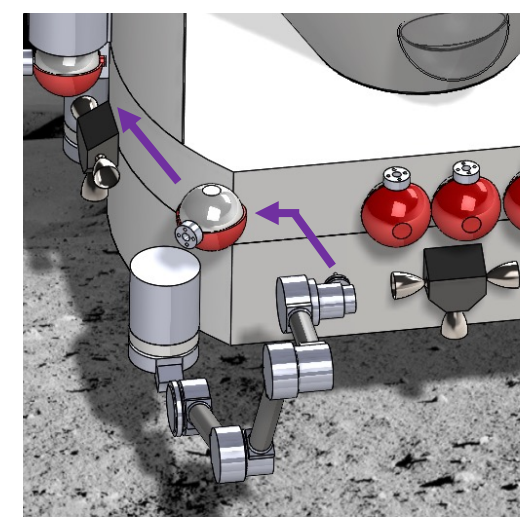
(1) Arm extends upwards towards exterior conveyor and interfaces with encapsulation sphere



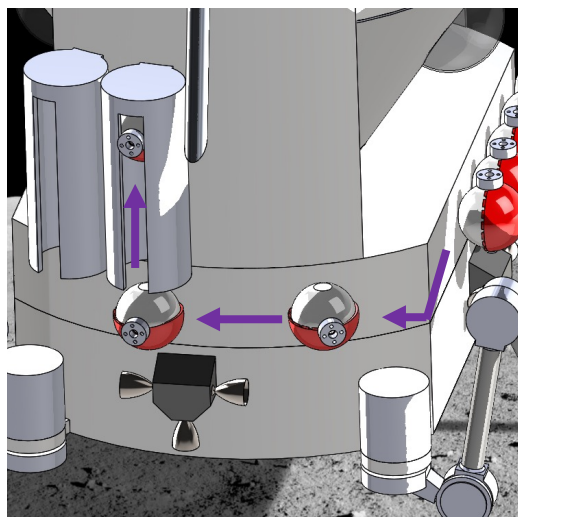
(2) Encapsulation sphere hovers above target and uses cameras, sensors, and crew visuals to confirm the target is in encapsulation area



(3) The encapsulation sphere lowers to sampling area/target and captures it, locking the sphere after full closure



(4) The locked sphere is then moved and reattached back to the exterior conveyor and disconnected from the robotic arm's interface



(5) The sphere is then conveyed to its external storage on the EEV where it is kept until transfer to the DST at final rendezvous

## 4.7 Environmental Control and Life Support System

The Environmental Control and Life Support System, ECLSS, is responsible for maintaining a habitable and comfortable environment in the EEV where the crews lives and works during the HAMMER mission.

### 4.7.1 Requirements and Consumables

The ELCSS must support two crew members for a total mission duration of 30 days. In the event issues arise at any point during the mission, the ECLSS shall continue life support functions until the EEV rendezvouses with the DST. A margin of six earth days has been allotted to allow time for mission aborts, troubleshooting, and transfer maneuvers. Thus, the ECLSS is designed to provide life support for a total of 72 [CM-d] (crew member days) or 36 days per individual. To support the crew for this amount of time, the ECLSS will provide the consumables and their amounts listed in the table 4.9 below and are based on the Baseline Values and Assumptions Document. [46, 47]:

| Group        | Consumable            | Mass per day [ $kg/d$ ] | Mass (with Packaging) [ $kg$ ] |
|--------------|-----------------------|-------------------------|--------------------------------|
| Air          | Oxygen                | 1.84                    | 66.24                          |
| Air          | Nitrogen              | 0                       | 8.61                           |
| Water        | $H_2O$                | 3.94                    | 141.84                         |
| Food         | Food                  | 7.33                    | 263.88                         |
| Misc.        | Clothing, Wipes, etc. | 0.69                    | 24.84                          |
| <b>Total</b> |                       | <b>13.80</b>            | <b>505.41</b>                  |

Table 4.9: Consumables Required by the Crew on the Life Support System [46]

### 4.7.2 ECLSS Architecture

The ECLSS is divided into a total of four subsystems, each handling a distinct aspect of maintaining crew life. Each subsystems interfaces with the crew and other subsystems to achieve the desired functions. The four subsystems are Air Revitalization, Water, Food, and Waste Management. In figure 4.20, the roles of each subsystem are introduced in greater detail and the interactions between subsystems are listed:

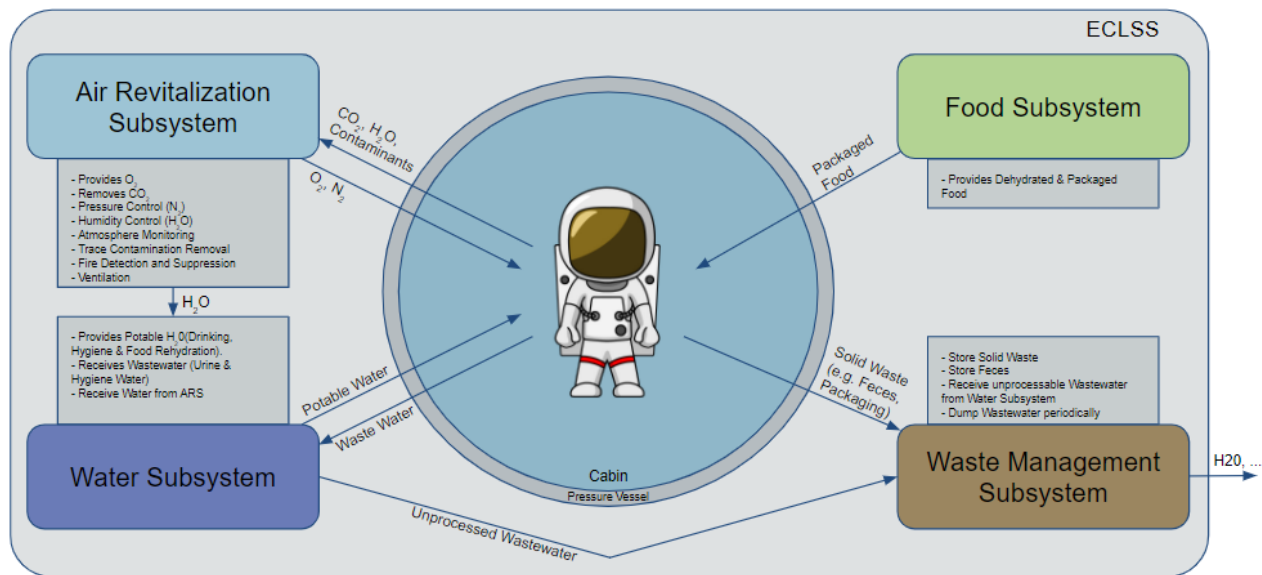


Figure 4.20: The EEV Life Support System Architecture [48]

In the sections below, each subsystem will be introduced and discussed in more detail.

### Air Revitalization

It is desirable to maintain conditions at a short-sleeve atmosphere to provide maximum comfort to the crew. Maximum comfort helps the crew function best. To achieve this, cabin air is circulated through the air revitalization system (ARS). Here, excess  $CO_2$  is removed, humidity and air temperature are controlled, trace contamination is managed, and fire detection and prevention is achieved.

| Parameter              | Units       | Lower Bound | Upper Bound | Nominal Value |
|------------------------|-------------|-------------|-------------|---------------|
| Habitable Volume       | $m^3$       | 8.00        | 10.00       | <b>9.50</b>   |
| Leakage Rate           | $\%/d$      | 0.00        | 0.10        | <b>0.05</b>   |
| Ventilation Rate       | $m^3/min$   | 1.80        | 2.60        | <b>2.20</b>   |
| Air Temp.              | $^{\circ}K$ | 291.00      | 300.00      | <b>296.00</b> |
| Rel. Humidity          | $\%$        | 25.00       | 70.00       | <b>40.00</b>  |
| Total Pressure         | $kPa$       | 100.00      | 102.00      | <b>101.00</b> |
| $O_2$ Partial Pressure | $kPa$       | 20.20       | 22.20       | <b>21.20</b>  |
| $N_2$ Partial Pressure | $kPa$       | 77.38       | 79.38       | <b>78.38</b>  |

Table 4.10: Parameters of the Cabin Atmosphere [46]

The ARS has been designed using Baseline Values and Assumptions Document (BVAD) values. [46]. The

necessary properties of the cabin atmosphere are defined in table 4.10 above. A number of monitoring and control steps are performed by the subsystem sketched below in figure to maintain these variables. 4.21.

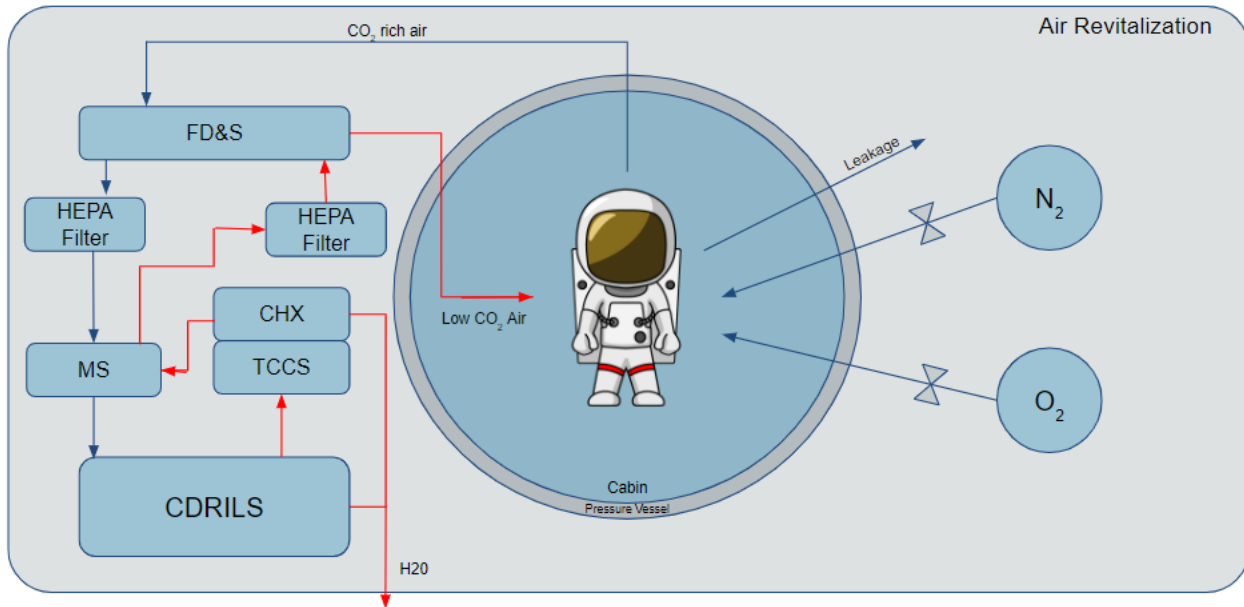


Figure 4.21: The The Air Revitalization System Architecture [49]

On the right side of figure 4.21, air is lost from the pressurized cabin to the outside environment due to imperfections in the pressure vessel. Shown in table 4.10, lost air is almost negligible on a day to day basis. However, over longer periods of time similar to a Mars transits, this effect becomes noticeable. The ECLSS system will operate during this transit period to avoid possible malfunctions when the system is accessed by the crew. Several of the ARS modules will have exceeded their respective maintenance times and will need to have components replaced by the crew upon arrival to avoid a toxic atmosphere. The combination of atmospheric leakage and possible toxins in the cabin when the crew arrives at the EEV will be resolved using the DST's ARS system. ARS will re-pressurize and decontaminate the EEV's atmosphere when the two crafts are docked and before the crew boards. Once the EEV's atmosphere is deemed safe by the DST's ECLSS system, the crew will then board the EEV, perform all required maintenance on the ARS, and fully power up the EEV's ECLSS system. The EEV also must be able to survive a depressurization and re-pressurization without sustaining damage. The required gas to perform a re-pressurization has been considered in the consumables mass budget. Nitrogen ( $N_2$ ) is provided to the cabin atmosphere straight from a storage tank, in order to re-pressurize the cabin as well as to provide pressure control. This system

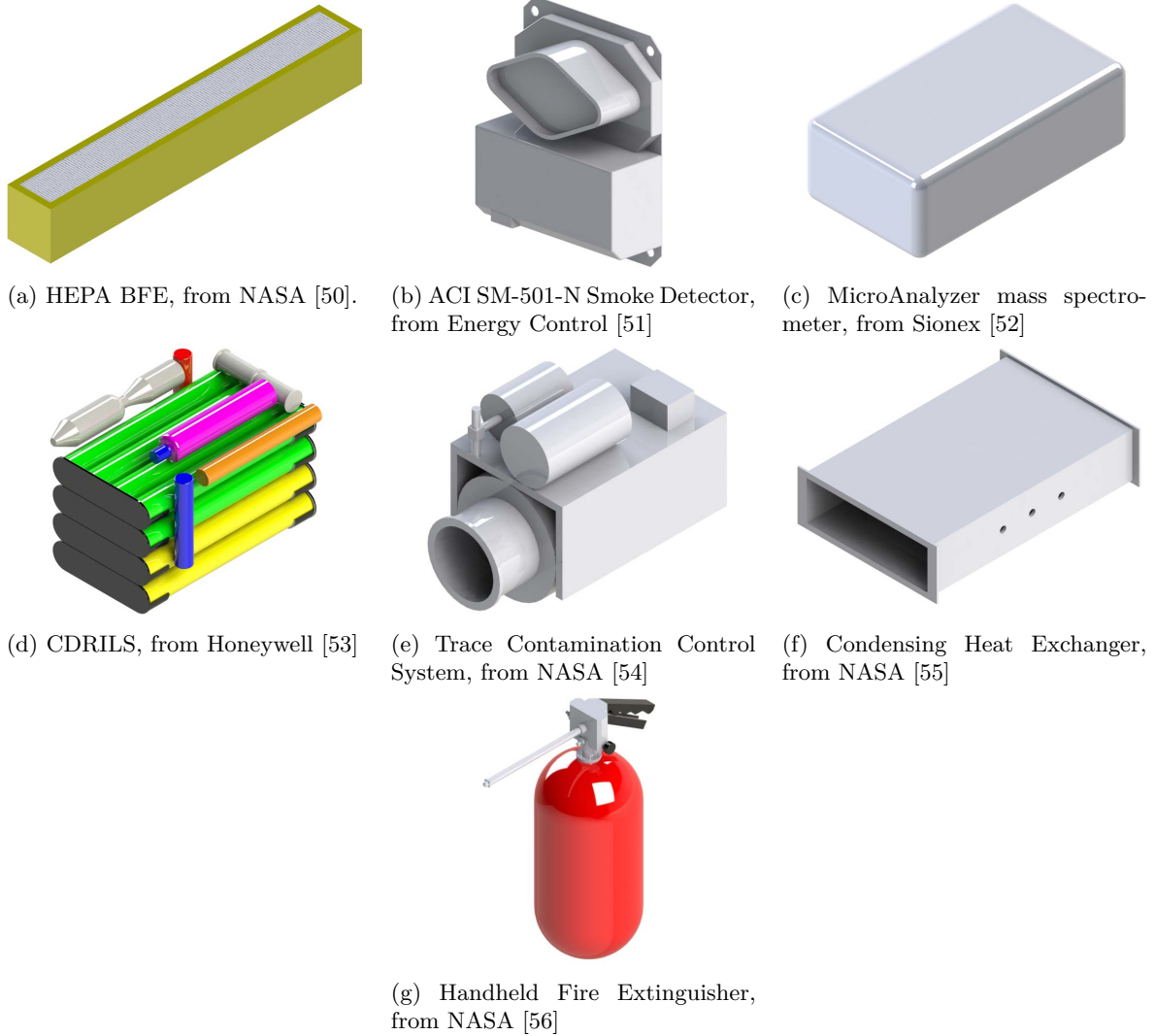


Figure 4.22: Chosen components for Air Revitalization System (ARS)

is responsible for keeping the total cabin atmosphere at the desired level. Oxygen ( $O_2$ ) is also provided to the cabin atmosphere straight from a storage tank, and is required to keep partial pressure at a desired level and to replace breathable air lost to leakage. On the left side of the diagram, the Atmospheric Monitoring, Control and  $CO_2$  scrubber assembly is depicted. In order to allow cabin fires to be detected quickly and allow for a swift response, the Fire Detection and Suppression (FD&S) system is the first assembly passed by the  $CO_2$  rich air circulated through the ARS. To allow for detection of fires or issues within the ARS, the FD&S system is passed once again by the low  $CO_2$  air reentering the cabin. The FD&S system specifically detects smoke (using ionization smoke detectors)[51], and fire prevention will be achieved with a handheld fire extinguisher that has been charged with water and nitrogen[56]. Excess water and nitrogen expelled into

the cabin from the extinguisher would be removed by the ARS. Directly after air passes the FD&S system, it encounters the first stage of filtering, a HEPA grade Bacterial Filter Element (BFE). The purpose of this filter is to ensure the removal of any potentially harmful particulate matter larger than 0.3 microns[50]. Air then passes through a Sionex microAnalyzer mass spectrometer which will analyze the molecular composition of the atmosphere passing through it, and allow the crew to be aware of any possible buildups or leaks of dangerous substances in the air [52]. Next is the removal of  $CO_2$  from the air. Due to the high mass of a closed system such as a 4 Bed Molecular Sieve (4BMS) and of the spare filters required for a Lithium Hydroxide scrubber (LiOH), a much lighter Carbon Dioxide Removal by Ionic Liquid Sorbent (CDRILS) system is used. This system requires no replaceable or rechargeable filters like the other aforementioned options, and if the liquid sorbent does begin to lose effectiveness due to aging or contamination, the fluid can easily be removed and replaced by crew. The system includes a built in dehumidifier, but due to the mass, volume, and power restrictions of the mission, this water can not be properly treated and will be handled by the waste management subsystem. CDRILS systems allow heat to be easily regulated due to the scrubber solution being a working fluid and through the use of heaters and coolers. Although this system has yet to be used in a space environment, similar technology has been used in submarines since the 1950's, and it is currently slated to be tested in space very soon [53]. Once the  $CO_2$  has been removed from the air using the CDRILS scrubber, the now low  $CO_2$  air is fed through a Trace Contaminant Control System (TCCS). The TCCS utilizes several different layers of solid chemical sorbent filters, and when air passing through these filters is heated to approximately 400 degrees Celsius, chemical reactions occur to remove any remaining toxins or contaminants in the air. The use of solid chemical sorbents dictates the need to periodically replace or recharge these filters, which will occur upon crew entry of the EEV as described earlier[54]. Before air can return to the cabin, it is cooled back to room temperature by a Condensing Heat Exchanger (CHX). The air then passes back through another microAnalyzer mass spectrometer to ensure that the previous modules have successfully completed their tasks within the ARS. A second HEPA filter is the final step before air returns to the cabin, and will help contain any contaminants that are still present or help prevent any possible smoke caused by the ARS from entering the cabin. However, if any smoke from the ARS does make it through the HEPA filter, the air will once again pass the smoke detector and alert the crew of danger.

## **Water**

The main responsibility of the water subsystem is to provide potable water to the crew. Water is required for several uses such as drinking water, to re-hydrate food, and for hygiene. Based on experiences from the ISS and Space Shuttle, the total water consumption was estimated in table 4.9 [46]. To maintain a simple system, the water subsystem was chosen to be identical for all use-cases and inherited from the ISS. To maintain redundancy, two access points are available in the cabin in case one connector fails. While the water subsystem is generally kept as simple as possible, one added complexity is the provision of hot water to aid in food re-hydration and this will be accomplished through heaters along the water lines. Water is transported by an electrically actuated centrifugal pump, and in case of failure, the pump can also be actuated manually. Due to the high weight of a urine/water processing assembly, the recycling of water has been eliminated from the water processing subsystem for the EEV. Instead, any excess water is transferred to the waste management subsystem.

## **Food**

Due to the limited mission duration, all food will be provided as dehydrated food in plastic packaging to the crew. This system is the same as the food packaging used aboard the ISS [57]. To heat up and re-hydrate food, hot water is transferred directly into the food packaging by the water subsystem, as described above. The crew can then eat directly from the food packaging. Once finished, the packaging and any remaining food waste is directly moved to the waste subsystem. Similar to the ISS, beverage packages are available to provide the crew with flavoured drinks which can also provide required vitamins and minerals[57]. These packages are also disposed of in the waste subsystem.

## **Waste**

The waste subsystem is responsible for storing and/or disposing of any waste produced by the crew or other subsystems. In general, the waste subsystem is used to handle solid wastes (wipes, clothing, food packaging, feces,...) as well as liquid wastes (hygiene water, urine,...). Due to the relatively short mission duration as well as the desire to leave the surrounding environment largely unpolluted, solid waste is stored aboard the



EEV in the trash compartment. To reduce the required volume for storage and increase room for the crew, the trash generated during the first sortie to Deimos is placed back into the DST during the resupply. Here, solid waste is stored until the EEV returns from the second sortie. Before final separation from the DST at the end of the mission, the solid waste from both sorties as well as the inbound transfer with the DST is loaded into the EEV for disposal. The solid waste will act as a mass replacement for science equipment and crew during the uncrewed landing attempt on the Phobos surface. Liquid waste will be transferred to the wastewater tank via a Soyuz-inspired toilet that consists of a simple bucket and hose apparatus. This apparatus will be stowed in a compartment of the crew cabin and is shown below.



Figure 4.23: Soyuz-Inspired Waste Receptacle

As can be seen in table 4.9 on page 60, a large amount of water is consumed by the crew throughout the mission. This results in large amounts of wastewater being produced. When considering EEV performance, it is simply not viable to store such amounts of wastewater. For this reason, a smaller wastewater tank is used which will be dumped in regular intervals [58], and this practice allows for large mass savings to the EEV. To prevent contamination of landing sites on the moons, wastewater dumps are to be performed during orbital maneuvers between the moons and the DST or during periods where the EEV is a significant distance from the moons.

### **Life Support Trade Off Tool (LiSTOT)**

To compare different possible designs of the EEV ECLSS, a publicly available automated tool written by the Chair of Aeronautics of the Technical University of Munich has been used [47]. The Life Support Trade Off

Tool (LiSTOT) is modular and allows users to create, simulate and compare different Life Support Systems to ensure the chosen system is optimal. Next to Equivalent System Mass (ESM), the tool also allows a Multi-Criteria-Approach (MCA) to consider further parameters such as Technology Readiness Level (TRL) and Reliability and Maintenance effort. A sample EEV Life Support System used during Trade Off Studies is depicted in figure 4.24 below:

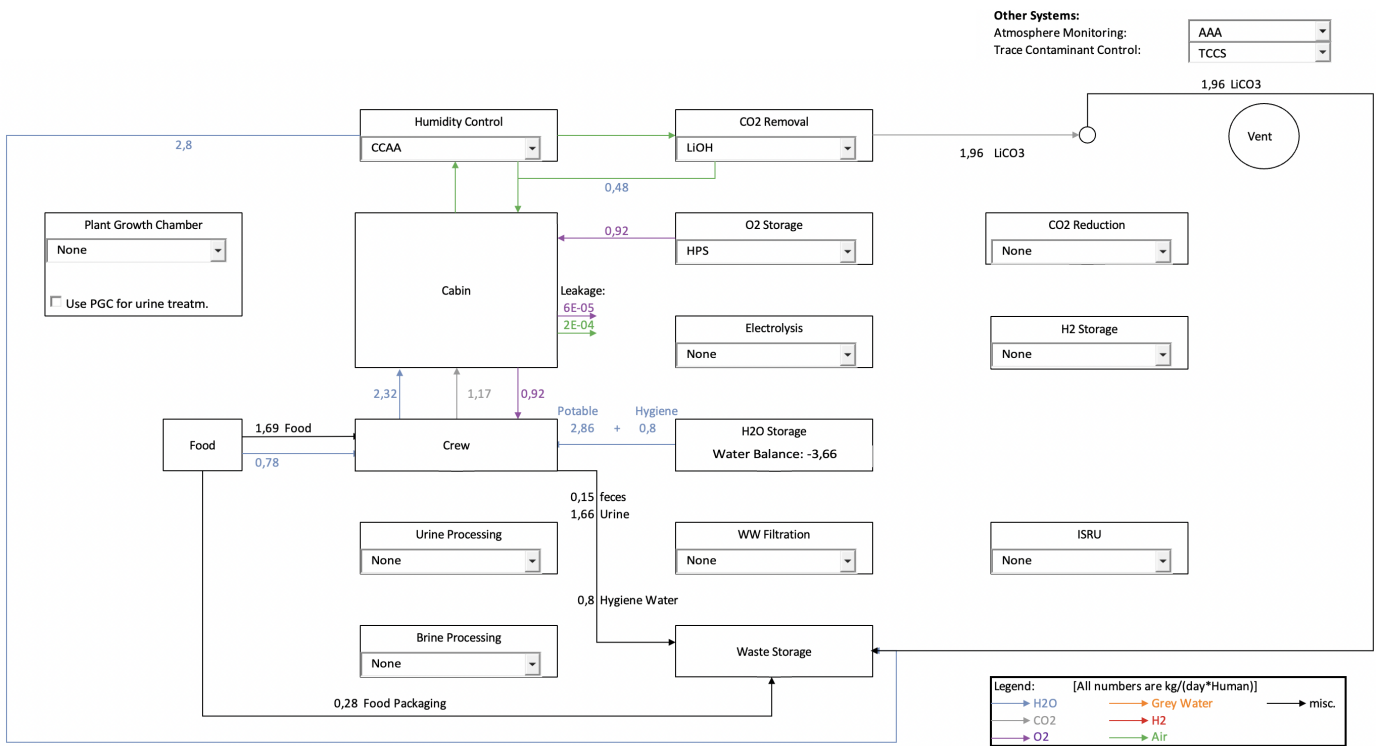


Figure 4.24: The EEV Life Support System in LiSTOT [47]

Using the LiSTOT Tool, the total system mass, volume, power consumption, heat release, and crew time requirement can be calculated. Some of these values were used to assist in budget calculations.

## 4.8 Communications

### 4.8.1 System Requirements & Architecture

The purpose of the communication subsystem is to ensure that data can be transmitted and received between mission control, the DST, and the EEV. By maintaining communication between all elements of the mission it

will minimize risk to the crew, maximize the ability to collect and analyze science, and provide the necessary means to maintain proper attitude and position for the duration of the mission.

The EEVs communication subsystem has been designed to transmit and receive scientific and telemetry data at a rate of 4 Mb/s with the DST. The EEV shall communicate on the S-band frequency with the DST, maintain a direct link with the DST, and have different power modes during communications blackouts.

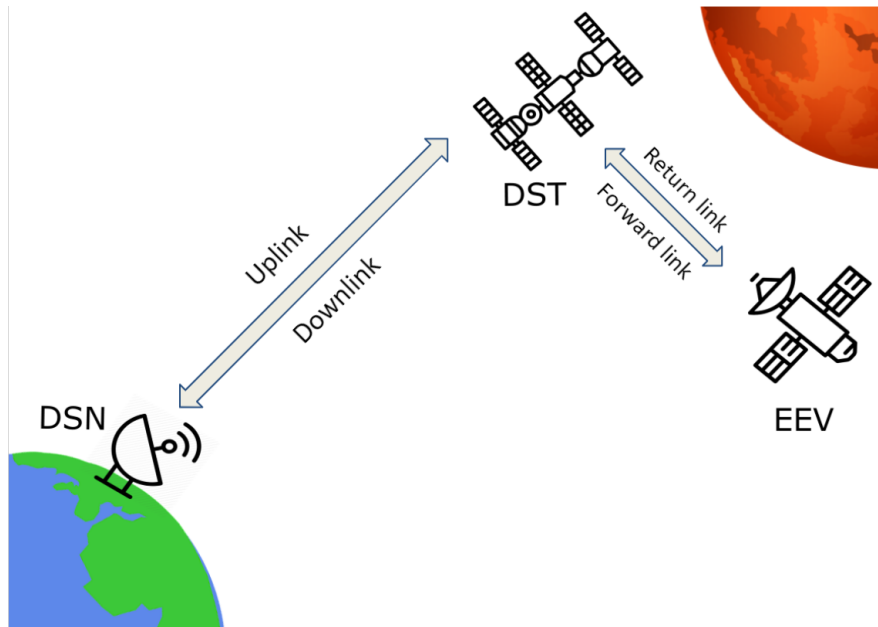


Figure 4.25: Proposed System Architecture

From Figure 4.25, it is shown that the EEV shall communicate with the the DST on a shorter range S-band frequency, while the DST acts as a relay satellite to communicate with the Deep Space Network on the longer range Ka-band frequency. By employing this method of communication, it allows for the EEV to have a smaller communications array, with the DST taking the burden transmitting at higher frequencies across the interplanetary distance between the Martian system and Earth.

#### 4.8.2 EEV Communications Trade Study

Many antenna types exist for transmitting data between satellites. They all vary in size, shape, mass, performance, and complexity. By choosing an antenna type that lines up best with the requirements for the communications subsystem, it ensures that the communications subsystem has maximum efficiency with minimal impact to the complexity and cost of using the selected antenna. The following choices will be

analyzed and compared to find the optimum choice of antenna type: Parabolic Reflector, Helix, Horn, Array. Each choice will be analyzed against the following criteria, outlined below. With each criteria defined, will compare each choice in a weighted decision matrix.

Technology readiness level (x2) - According to NASA [1], TRL is defined as “Technology Readiness Levels (TRL) are a type of measurement system used to assess the maturity level of a particular technology.” TRL is measured on a 1 to 9 scale, with 1 being the lowest maturity level, and 9 being the highest maturity level. For the COM subsystem considering TRL in this decision is important because employing lower TRL technological solutions incurs more risk, such as risk of failure. To avoid introduce unnecessary risk to this crucial subsystem, the TRL criteria has been weighted as slightly more than the others. For this project TRL is also modified by the use of each antenna type in the space environment.

Mass (x3) - Mass is a crucial decision factor when deciding a potential component for the EEV. Because the total craft must be able to traverse the entire Martian System, being as light as possible in critical to maintain maneuverability. As such, the mass component of this decision is weighted most heavily.

Volume/Size (x1) - Because the Antenna shall be able to have separate attitude from the main craft, having a low volume is necessary to ensure its mobility without running into the EEV’s main hull. By limiting the decision by size, it also ensures that the EEV has a lower moment of inertia when performing attitude adjustments. These features were deemed not as mission critical as the others, and has been given the lowest weighted value of all the decisions.

Max Gain (x2) - The max gain of the chosen antenna is linked to its’ “efficiency” and thus is very relevant to the overall communications subsystems efficiency. By choosing an antenna shape with high max gain, it ensures that the communications subsystem operates at the lowest power consumption mode. Therefore, a weight of 2 has been applied to this decision factor.

Complexity (x2) - The complexity of each antenna type is a function of its overall shape, manufacturing process, and ability to employ the chosen type of antenna in the space environment. To ensure an antenna that adds the lowest mission complexity, a weight of 2 has been applied to this decision criteria.

| Decision Factors:<br>(scale out of 10) | TRL     |     | Mass |     | Volume |    | Max Gain |     | Complexity |     | Weighted<br>Total |
|--|---------|-----|------|-----|--------|----|----------|-----|------------|-----|-------------------|
|  | Weight: |     | 3    |     | 1      |    | 2        |     | 2          |     |                   |
|  | U       | W   | U    | W   | U      | W  | U        | W   | U          | W   |                   |
| Parabolic Reflector<br>Antenna         | .9      | 1.8 | .6   | 1.8 | .4     | .4 | .8       | 1.6 | .7         | 1.4 | <b>7</b>          |
| Helical Antenna                        | .7      | 1.4 | .7   | 2.1 | .2     | .2 | .7       | 1.4 | .5         | 1.0 | <b>6.1</b>        |
| Horn Antenna                           | .5      | 1.0 | .6   | 1.8 | .6     | .6 | .6       | 1.2 | .8         | 1.6 | <b>6.2</b>        |
| Antenna Array                          | .5      | 1.0 | .7   | 2.1 | .1     | .1 | .7       | 1.4 | .5         | 1.0 | <b>5.6</b>        |

Key: U = Utility Value ; W = Weighted Value

Figure 4.26: Antenna Type Decision Matrix

Of the listed design considerations, the parabolic antenna is the best decision for the medium gain antenna aboard the EEV. Because of the extensive heritage of parabolic antennas, their ability to be incredibly directional, and due to having the highest max gain of the analyzed antenna types, it makes sense that this should be the chosen antenna. The only detriment that the parabolic antenna has, is its potential to be incredibly massive. This can be mitigated by limiting the diameter of the antenna, while increasing the power transmitted to maintain performance.

### EEV Link Budget and CAD

Because the EEV must receive and transmit data to and from the DST, a simple proposed communications block diagram for the EEV was derived as follows.

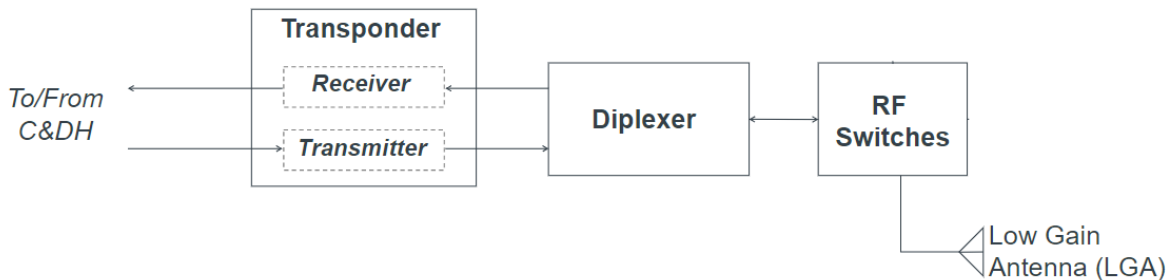


Figure 4.27: Proposed Communication System Architecture

As shown from the above block diagram for the on board communication array, the EEV shall be capable of transmitting and receiving data with one low gain antenna. This is made possible with the addition of a suitable combination of RF switches and a diplexer. The transponder is also capable of amplifying, filtering, and modulating the transmitted and received signals to command and data handling subsystem.

The antenna aboard the EEV shall be designed to have separate attitude control from the main spacecraft. This designed mechanism will minimize pointing losses for the communication subsystem. The satellite dish assembly will thus have two axial pistons that tilt the assembly by extending and retracting, giving the satellite dish an arc of 60 degrees to align itself with the receiving dish aboard the DST.

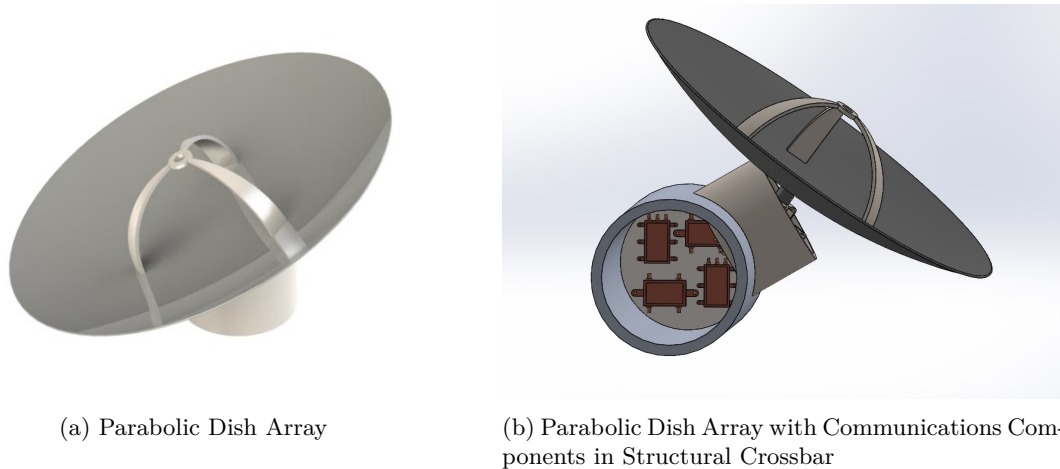


Figure 4.28: Parabolic Dish Array CAD

Knowing the specifications of the components of the EEV communication array, a preliminary link and mass budget for the EEV to DST communication network can be generated, and is detailed below in Figure 4.29.

| Link                           | Value          | Units       | Notes:   |
|--------------------------------|----------------|-------------|--|
| Power to Transmitter           | 50.000         | Watts       | Power Source: <u>_Solar Panels &amp; Batteries_</u>        |
| Transmitter efficiency         | 0.550          |             | Amplifier Type: <u>_Travelling Wave Tube Amplifier_</u>    |
| Transmitted power              | 14.393         | dBW         |  |
| Transmitter ant gain           | 25.765         | dB          | Transmitting Antenna Type: <u>_Parabolic Antenna_</u>      |
| Signal Strength at Transmitter | 40.158         | dBW         | Transmitting Antenna Dimensions (m): <u>_1m diameter_</u>  |
| Space Loss                     | -195.072       | dB          | Average Distance from trans to rec (km): <u>_54137_</u>    |
| Signal Strength upon arrival   | -154.914       | dBW         | Max Distance from EEV to DST (km) <u>_129402_</u>          |
| Atmospheric Loss               | 0.000          | dB          | Min Distance from EEV to DST (km) <u>_0.885_</u>           |
| Signal Strength after atm loss | -154.914       | dBW         | Assumed Elevation ( $\beta$ ) <u>_90 degrees_</u>          |
| Pointing Loss                  | -0.001         | dB          | Avg Pointing Error ( $\theta$ ): <u>_0.01 degrees_</u>     |
| Signal Strength after pointing | -154.916       | dBW         | Ant Half-power Beamwidth ( $\delta$ ): <u>_82 degrees_</u> |
| Receiver ant gain              | 85.870         | dB          | Receiver Antenna Type: <u>_DST Parabolic_</u>              |
| <b>RECEIVED POWER</b>          | <b>-69.046</b> | <b>dBW</b>  | Receiver Antenna Dimensions (m): <u>_2 m_</u>              |
| Energy per bit: Eb             | -120.807       | dBW/Hz      | Reference Temperature (K): <u>_290_</u>                    |
| System Noise Density: No       | -189.568       | dBW/Hz      | System Noise Temp (K): <u>_80_</u>                         |
| Received Eb/No                 | 68.762         | dB          | MRO Heritage Bandwidth (kHz): <u>_20_</u>                  |
| Implementation Loss            | -1.000         | dB          | MRO Heritage Implementation Loss (db): <u>_-2.5db_</u>     |
| Link Margin (dB)               | 3.700          | dB          | MRO Heritage Link Margin (db): <u>_3.7_</u>                |
| <b>Required Eb/No</b>          | <b>66.062</b>  | <b>dB</b>   |  |
| Bandwidth, B (Hz)required      | 4038088.609    | Hz          |  |
| <b>Bit rate</b>                | <b>4.038</b>   | <b>Mbps</b> |  |

Figure 4.29: EEV to DST Link Budget

As seen from figure 4.29 above, a simple link budget calculation can be done. The inputs to this calculation are the distance between the EEV and DST, the efficiencies of the components, and the power supplied to the transmitter. Using the average distance between the EEV and DST, it was determined that the communications subsystem is able to maintain a stable data transmission rate of 4.038 Mb/s. To determine the range of bit rate transmission, input the maximum and minimum distance between the EEV and DST over the mission span into the above calculation to find that EEV will transmit and receive data at a rate of 5.021 Mb/s when both crafts are closest, and 2.801 Mb/s when both crafts are at their farthest. To compensate for the space loss incurred at this maximum distance, a new long range transmission power mode is to be implemented, increasing the power to the transmitter to 100 watts, thus increasing the lower bound of transmission rates to 4.008 Mb/s.

### Chosen Communications Components

This section provides descriptions for each of the components of the communications subsystem. The components shall be arranged according to Figure 5.27 and will ultimately communicate with the command and data handling subsystem to ensure that received data is properly interpreted. The efficiencies and specifications have been included in the link budget constructed earlier.

**Transponder:** The product chosen is a **C/TT-520 S-Band transponder** [59], a popular transponder choice for spacecraft operating in the S-band frequency.

**Diplexer:** The mission is using a diplexer from Southwest Antennas, the **Dual Band Diplexer 4.4 - 12.0 GHz 3x SMA(f) RF Connector** [60]. This diplexer fits the required specifications for the communication subsystem.

**RF Switch:** The mission is using the **RFoF 12.0GHz high frequency ODL modules** [61] from RFOptic for this mission.

### Communication Blackouts

Because of the highly elliptical orbit of the DST, the motion of the Martian moons, topographical impedance of landing sites, and the constantly changing position of the EEV, it is unrealistic to maintain two way communication between the EEV and the DST without an established Martian communications infrastructure. The following graphic illustrates that communication blackouts will be frequent and often extensive in duration.

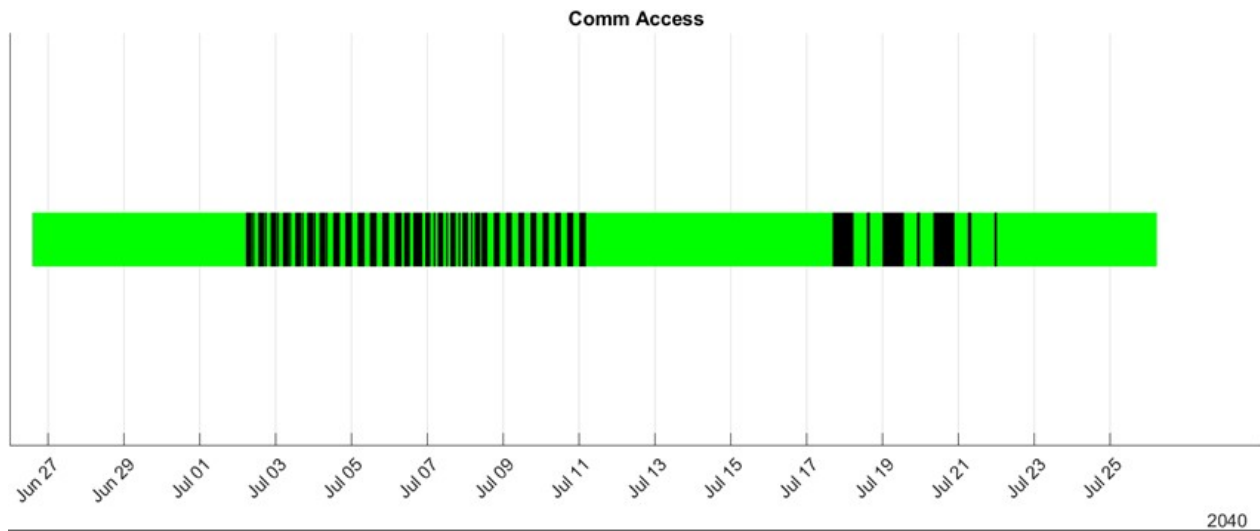


Figure 4.30: Times of EEV-to-DST-to-DSN Communications Link (green), and Communications Blackout Events (Black)

As shown can see from Figure 4.30 above, if nothing is done to avert the communication blackout problem it is not possible to maintain continuous two way communication between the DST and EEV. A total of 48 blackout events will occur over the course of the mission. The three longest blackout events occur during



the Deimos operation and last over 13 hours. The Phobos operation has more frequent blackout events, but with an average blackout time of only 4 hours. To mitigate communication blackouts the following methods will be explored and employed by the EEV.

1. Before each blackout event, the crew must perform a safety check on each of the EEV subsystems to minimize the probability of catastrophic failure during a blackout event.
2. Conserve power by turning off the communications subsystem during the longer blackout times.
3. Increase power to transmitter to mitigate atmospheric loss when DST and EEV communicate through upper Martian atmosphere.

## **4.9 Power**

### **4.9.1 System Requirements Overview**

The power system must supply power at the proper voltage and amperage though out the mission to support all mission operations and the vehicle must sustain power in order to sustain human life and accomplish the science objectives. As with all on board systems, the power system must pose minimal risk to the crew of the EEV.

### **4.9.2 Design And Sizing**

In order to size and choose the appropriate method of power generation, HAMMER needs an estimate of power draw for the whole system. This has been created from every system's power estimates. In order to support the power draw and impose minimal effects on other systems, the EEV will use solar panels. Solar panels do not produce radiation that could be harmful to humans and require no propellants - which would induce additional mass. There is rich heritage for the use of solar panels in space and in high vibration environments. The use of solar panels also come with some difficulties. Their major drawback is the requirement of sunlight availability. This can be mitigated by quality solar panel aiming mechanisms; However, this mechanism can not collect solar energy during black out periods.

## **Solar Panel Sizing**

The size of the solar panels are determined by the power draw of the EEV. The solar panels are assumed to be capable of converting thirty percent of solar radiation into electrical energy. The intensity of solar radiation around Mars is estimated at 700 Watts per square meter. To provide margin for shade expectations on the panels, the solar arrays have been sized to include 15 square meters of panel. Three ultra-flex design solar panels of 5 square meters of area each will be deployed in a triangular formation around the space craft. The three solar panels will initially be folded and held flush to the space craft while it is being launched. Upon exiting the launch vehicle, the solar panels supports will be extended and the ultra flex panels will unfold. Through out the mission the solar panels will be rotated around the axis of the support, such that they are catching as much sunlight as possible.

## **Battery Technology And Sizing**

The size of the battery is determined by the power requirements of the data acquisition system and the black out periods expected. As described in the power budgets by mode, the battery must supply 2.5 KW of power for at least 30 minutes of sustained operation. And then be capable of recharging back to those levels with in 33 hours. The Battery must also be able to support the maintenance of spacecraft systems during black out periods. The largest black out period expected based on trajectory is 15 hours. This black out requirement is much larger than the data acquisition mode's requirement on battery capacity. So the batteries were sized exclusively on the blackout requirement.

Lithium ion batteries remain the best choice for battery technology due to their heritage in space and high power storage capacity with relatively little mass. The energy density of lithium ion batteries is estimated to be 180 Wh/kg. including some initial capacity losses. Using this estimate the battery system was sized to support 3kw draw for the longest blackout period of 15 hours. With a small margin, that yields a requirement of 272 kilograms. For Physical symmetry, the battery system is divided into three 84 kg batteries.

### **4.9.3 Modes**

In order to accomplish the requirements of the power system with minimal mass, the EEV is employing the use of three power modes. The three modes are nominal, data collection and uncrewed. Data collection will be employed to support high power draw science equipment. The uncrewed mode will be employed while the EEV is in transport with no crew.

While the modes enable valuable savings in the design they introduce new requirements. In order to support the higher power draw of data-collection mode, an on board battery will be charged during nominal operation and discharged during data-collection mode. The uncrewed mode will draw far less power than the manned mode, in order for this to be useful the power generation system must be capable of not only distributing less power but producing less power. For the uncrewed mode to be useful for power generation system must be capable of throttling.

#### **Nominal**

This mode will be employed for the great majority of the time the EEV is crewed. In this mode the power system is supporting the entire rest of the craft except for some of the high power draw science equipment. During nominal mode, the power system will support the power needs of the following systems: life support, propulsion, GNC, communications, low power draw science equipment, active thermal control and the battery to be used to support data collection mode. This mode will be used for a majority of the mission, and as such, the power system is designed primarily around the needs of this mode. Specifically the generator is designed to be most efficient at the power-draw of the mode.

#### **Data-Collection**

Data-Collection mode is employed to enable the simultaneous operation of high power draw science equipment while not compromising the operation of the rest of the vehicle. While this mode is active the battery that was being charged during nominal operation will discharge.

This mode is designed to be employed at a maximum once every 2000 minutes, approximately 33 hours.

This infrequency is required in order to allow the battery to charge back up to sufficient levels to support the vehicle operating in Data-Collection mode for at least 30 minutes.

Without the use this power mode, the power generation system would have to be larger. Employing this mode allows a reduction in the nominal wattage that the power system must generate. The added complexity of implementing this mode is justified by the mass savings of designing a smaller power generation system.

## **Uncrewed**

The Uncrewed mode is to be employed primarily while the vehicle is in transit, from Earth to Mars before it docks with the DST to pick up the crew. During the Uncrewed mode, the power system will support the power needs of the following systems: propulsion, active thermal control, GNC, and communications. The following systems will remain un-powered: life support and science equipment. Communications, GNC, propulsion, and active thermal control are all powered during this mode because they are necessary to keep the vehicle on course and intact.

As the life support system and science equipment draw a large amount of power, this mode enables the vehicle to operate on much less power. Since the vehicle is running on less power, less power needs to be generated.

### **4.9.4 Human Safety Design Considerations**

If the power system fails, the craft will quickly lose the ability to support human life let alone complete any science objectives. For this reason the entire power system must be robust. The solar panels will be well tested for longevity and potential environmental stresses. All wiring will adhere to strict human spaceflight standards as described by NASA-STD-8739.4

To help ensure the crew safety, CURVES is implemented along the solar panel surfaces. The system is a portion of the CDH dust mitigation tactics described in section 4.3.2. CURVES uses piezoelectric excitation via actuators at frequencies between 19 kHz and 7 MHz. CURVES redeems 49% of power lost due to dust accumulation along solar panels. 154 MJ/kg of energy per mass of CURVES is also reclaimed. This system prevents build up of dust kicked up by the EEV in the low gravity landings. This system will stay in

effect when the EEV enters its end-of-life cycle as a permanent communication relay on Phobos. The power reclamation provided by CURVES will help ensure a long life cycle for the communication relay [62].

## 4.10 Thermal Control

Thermal environments in space, near Phobos, and near Deimos were used to determine the thermal requirements of the EEV. Both active and passive thermal control methods were selected to keep all EEV systems and the crew within safe operating temperature ranges - Because the various components of the spacecraft have different operating temperature ranges, a variety of thermal control solutions are needed. There are four main categories of processes that change the temperature of the EEV: (1) Environmental Heat Loss, (2) Internal Heat Generation, (3) Active Thermal Control, and (4) Passive Thermal Control.

### 4.10.1 TCS Calculations & Environmental Conditions

The governing equation used to do all thermal calculations is as follows:  $Q_{Sun} + Q_{Albedo} + Q_{BlackBody} - Q_{Space} = Q_{InternallyGenerated} + Q_{ThermalControl}$ . The terms on the left were calculated using spacecraft and planet properties. Afterwards, the value for  $Q_{InternallyGenerated}$  was estimated using the total power consumption of all systems inside the spacecraft. The value for  $Q_{ThermalControl}$  was the remaining amount of heat that was necessary to balance the equation.

### 4.10.2 TCS Subsystem Architecture

Here the various subsystem architectures of the TCS are described. The subsystems that will be explored in detail are the fluid cooling loops, multi-layer insulation, thermal coatings, and heaters.

The fluid cooling loop architecture can be seen above. The purple arrows represent the physical pipes and movement of the fluids. The red boxes represent heat sinks and the blue boxes represent heat sources. The idea behind the fluid cooling loop is to take heat from high-temperature regions of the spacecraft (where the electronics are) and transfer them to the crew cabin and space. This design was picked to minimize power consumption by recycling unwanted heat to colder areas of the spacecraft.

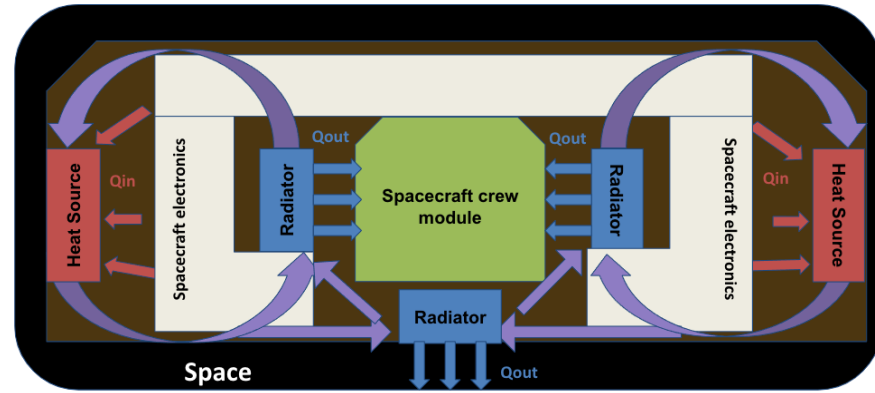


Figure 4.31: Fluid Cooling Loop Architecture

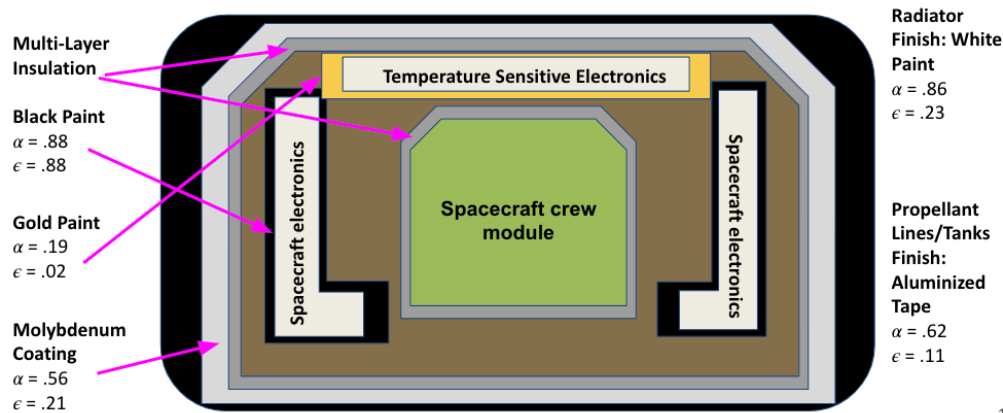


Figure 4.32: Thermal Coating and Insulation Architecture

The thermal coating architecture can be seen above. The specific materials are represented by a color pertaining to the material the coating is made out of. The first layer of interest is the external spacecraft coating. This coating was chosen to be a molybdenum alloy coating and was chosen for its specific absorptivity and emissivity values. These values were optimized to allow for the right amount of heat transfer. The next layer of interest is the multi-layer insulation. That insulation surrounds the entire spacecraft directly adjacent to the interior of the hull along with surrounding the crew cabin. The purpose of this insulation is to prevent any unplanned heat loss to the exterior environment and allow all heat to be utilized or recycled. The final layer of interest is the coating on the electronics. Generally, the electronics will have a black paint coating on them in order to radiate as much heat as possible (that will then be recycled by the fluid loops.) The

temperature sensitive electronics will be coated with gold paint. This is to ensure that they do not over or under heat.

### 4.10.3 Thermal Heater Architecture

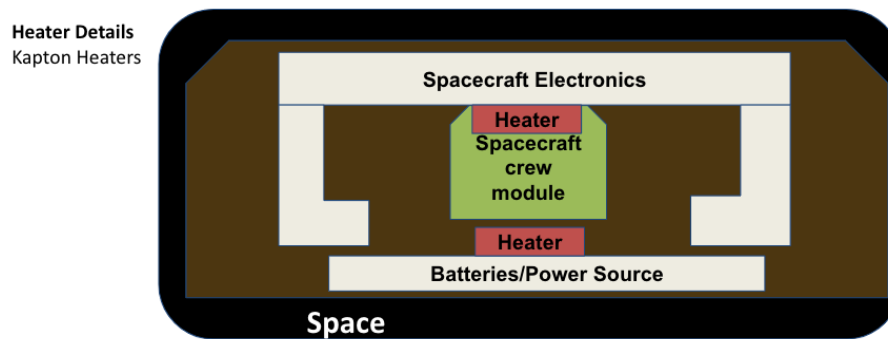


Figure 4.33: Thermal Heater Architecture

The thermostatic heater architecture is quite simple. There are heaters in the crew module and near the batteries/power sources. The heater in the crew module is mainly for redundancy. The heater in the battery compartment is to satisfy the higher temperature range requirement for batteries.

# Chapter 5

## Deep Space Transport

### 5.1 DST Requirements

The DST has been given the following requirements to fit it into the mission architecture. These requirements were implicitly derived from the RFP, or proposed to facilitate the needs of the DST to act as a propellant depot and communications relay for the EEV.

| ID     | Requirement   | Rationale   |
|--------|---|---|
| DST-01 | The DST shall have a docking module the extends at least 2.5 meters and a maximum diameter of 3 meters.   | These dimensions are required for the EEV to safely dock with the DST.  |
| DST-02 | The DST shall maintain two-way communication contact with the DSN and EEV for the <b>majority</b> of the mission  | Two way communication is vital to crew safety and nominal operations.   |
| DST-03 | The DST shall be capable of acting as a propellant depot for the EEV, and shall carry an additional 10,700 kg of fuel to refuel the EEV during docking. | Using the DST as a propellant depo allows for the EEV to be designed with greater freedom to complete the proposed mission architecture |
| DST-04 | The DST shall have the capacity to transport three crew members to Mars orbit and back to Earth.  | Two crew members will be on the EEV, while one crew member will stay behind on the DST.   |

Table 5.1: Requirements for the DST

### 5.2 Refuelling in Space

Because the current mission includes refueling with the DST, the the DST shall have the capability to act as a propellant depot for duration of the mission. This means that the DST must be capable of storing and



transferring propellant in a low-G environment. Transferring fluids comes with several challenges, a few of which are explored in the following:

1. **Propellant Settling:** The low-G environment of space means that the distribution of liquids stored in tanks is uncertain at any given time. In order to drain or fill a pressurized container in space the first problem to overcome is propellant settling, or reducing the uncertainty of the liquids distribution in the specified container. According to heritage research, the most logical solution to this problem is by employing a centrifugal propellant settling method [63]. This involves spinning the tank to be drained, and applying a known centrifugal force to the liquid inside, thus reducing the uncertainty of the distribution of the contained liquid. The mission will apply centrifugal propellant settling on board the DST to ensure that fuel transfers smoothly between the two vehicles.
2. **Propellant Transfer:** The mission will plan to apply the propellant transfer technology demonstrated by Orbit Fab's Tenzing-001 mission [64], in combination with NASA's Robotic Refueling Mission 3 [65], to construct a proposed refueling apparatus detailed below. CAD models of the propellant transfer system developed are detailed below in Figure 5.1a.

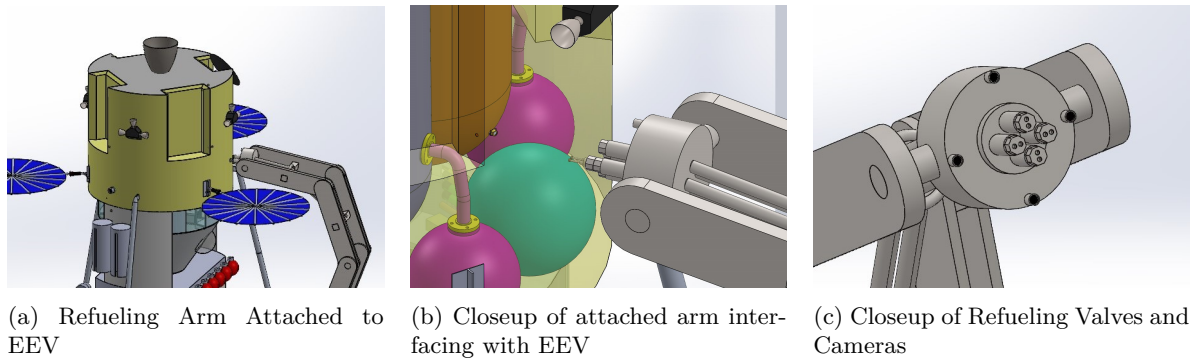


Figure 5.1: Refueling Apparatus

With a fully extended length of three meters, and the ability to rotate three hundred and sixty degrees, the refueling assembly pictured above is more than capable of bridging the gap between the DST and EEV to refuel. The assembly features four main flow tubes that end with four RAFTI valves used on the Tenzing-001 mission [64]. By using the above designed refueling assembly, can transfer up to four different liquids at a rate of 1 L/min to minimize the amount of time needed to completely refuel the EEV. This flow rate is made

possible by utilizing Orbit Fab's RAFTI Valve [64] in combination with the Robotic Refueling System NASA used for the RRM3 mission [15]. The combination of these two technologies makes the refueling assembly act similarly to a small docking adapter, as the RAFTI valve operates in much the same way. To remotely operate the refueling arm, the crew members on the DST will use the four high resolution cameras on the tip of the arm (Figure 5.1c) to guide the valves to their ports on the EEV. Alignment markers shall be present on the EEV to ensure the valves are aligned for optimum docking.

### 5.3 Communications

To minimize the total mass and size of the EEV, it was deemed necessary for the DST to act as a relay satellite to communicate between the EEV and NASA's Deep Space network. This additional purpose for the DST means that in addition to being able to communicate with the EEV, the DST needs a sufficiently large communications array to transmit and receive data across interplanetary space. A preliminary link budget that takes into account communication between the Martian system and the DSN was constructed to assess the expected data transmission rate between the DST and the DSN.

| Link Budget for Deep Space Transport to Deep Space Network |                    |              |                                     |                     |
|--|--------------------|--------------|-------------------------------------|---------------------|
| Type of Link:  | Downlink           |              | Atmospheric Loss                    | -0.200 dB           |
| Channel:   | Ka                 |              | Signal Strength after atm loss      | -193.526 dBW        |
| Frequency:   | 20 GHz             |              | Pointing Loss                       | -0.001 dB           |
| Wavelength:  | 0.014989623 meters |              | Signal Strength after pointing loss | -193.527 dBW        |
|  |                    |              | Receiver ant gain                   | 85.870 dB           |
|  |                    |              | <b>RECEIVED POWER</b>               | <b>-107.657 dBW</b> |
| <b>Link</b>  | <b>Value</b>       | <b>Units</b> | Energy per bit: Eb                  | -120.668 dBW/Hz     |
| Power to Transmitter                                       | 160.000            | Watts        | System Noise Density: No            | -189.568 dBW/Hz     |
| Transmitter efficiency                                     | 0.550              |              | Received Eb/No                      | 68.900 dB           |
| Transmitted power  | 19.445             | dBW          | Implementation Loss                 | -1.000 dB           |
| Transmitter ant gain                                       | 60.437             | dB           | Link Margin (dB)                    | 3.700 dB            |
| Signal Strength at Transmitter                             | 79.882             | dBW          | <b>Required Eb/No</b>               | <b>66.200 dB</b>    |
| Space Loss   | -273.208           | dB           | Bandwidth, B (Hz)required           | 4169160.301 Hz      |
| Signal Strength upon arrival                               | -193.326           | dBW          | <b>Bit rate</b>                     | <b>4.169 Mbps</b>   |

Figure 5.2: DST to DSN Down-Link Budget with Design Considerations

With a proposed power supply of 160 watts and a 2 meter parabolic antenna, the DST is capable of transmitting data to the DSN at a rate of 4.169 Mb/sec.

# Chapter 6

## Mission Management

### 6.1 Research, Development & Integration Schedule

The mission schedule is constrained by the deadline for arrival at Mars being the Summer of 2040. The corresponding launch window constraint, therefore, is October 2039. The system design cycle starts in 2026 with Phase B after Preliminary Design Review, and ends in 2030 with a Critical Design review for the EEV. Once CDR is passed, Phase D begins, with parts being sourced and manufactured, with priority dependent on lead time. Significant margin (30%) is added to this phase to ensure that the 2038 launch window is met. When assembly is complete, system testing will be performed on the individual spacecraft to ensure the spacecraft is functional. After testing is complete, the spacecraft will be integrated with launch vehicle at Kennedy Space Center. Integration testing and launch final testing will be performed to ensure the spacecraft is prepared for the launch window.

Phase E includes all primary mission operations, starting with the launch of the EEV, Martian orbit and Phobos/Deimos ops, and then ending with the return of the crew to the DST. Phase F includes the return of the EEV to Phobos for long term uncrewed science operations as the spacecraft eventually meets the end of its lifespan.

The mission mostly uses mature and flight-proven technology, so the development time is not expected to deviate too far from schedule. The primary technology that still needs developing is in-space fuel transfer. This technology is expected to reach Technology Readiness Level (TRL) 9 in 2024 after its use in a Dynetics Lunar Lander Mission [66]. Therefore, this technology has a high probability of achieving TRL 9 prior to the beginning of the design cycle in 2026.

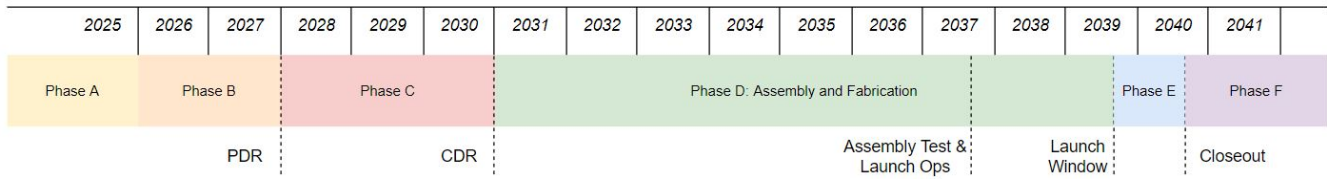


Figure 6.1: Development and Operations Schedule for the EEV.

## 6.2 Cost Analysis

Cost analysis was performed using the automated NASA PCEC [67] (NASA Project Cost Estimating Capability) tool. The tool uses CER (Cost Estimating Relationship) data from previously designed spacecraft to predict the cost of a project based on its subsystems and scope. The mission has a budget limit of \$1 billion, so accurate forecasting is essential to the project’s development. The RFP requires cost prediction for all elements of the vehicle design, including all hardware, ground systems, testing and other requirements. PCEC has CERs for all of these systems, and provides the full cost over the project’s WBS (Work Breakdown Structure). The cost analysis was performed based on the estimated subsystems for the EEV, with considerations made for parts that would be purchased COTS (Commerical Off-The-Shelf) to reduce costs.

| FY2021 SM |       | Units Conversion Factor: 1.000                 |          |                      |                      |             |            |               |            |          |
|-----------|-------|--|----------|----------------------|----------------------|-------------|------------|---------------|------------|----------|
|           |       | Inflation Factor: 1.116                        |          |                      |                      |             |            |               |            |          |
| WBS #     | Level | Line Item Name/Description                     | DDT&E    | Design & Development | System Test Hardware | Flight Unit | Production | Non-Allocated | Operations | TOTAL    |
| 0         | 1     | System Name                                    | \$ 892.5 | \$ 693.8             | \$ 120.3             | \$ 142.6    | \$ 103.8   | \$ -          | \$ -       | \$ 996.3 |
| 1.0       | 2     | Project Management                             | \$ -     | \$ -                 | \$ -                 | \$ -        | \$ -       | \$ -          | \$ -       | \$ -     |
| 2.0       | 2     | Systems Engineering                            | \$ -     | \$ -                 | \$ -                 | \$ -        | \$ -       | \$ -          | \$ -       | \$ -     |
| 3.0       | 2     | Safety and Mission Assurance                   | \$ -     | \$ -                 | \$ -                 | \$ -        | \$ -       | \$ -          | \$ -       | \$ -     |
| 4.0       | 2     | Science/Technology                             | \$ -     | \$ -                 | \$ -                 | \$ -        | \$ -       | \$ -          | \$ -       | \$ -     |
| 5.0       | 2     | Payload(s)                                     | \$ -     | \$ -                 | \$ -                 | \$ -        | \$ -       | \$ -          | \$ -       | \$ -     |
| 6.0       | 2     | Flight System \ Spacecraft                     | \$ 747.4 | \$ 693.8             | \$ 120.3             | \$ 142.6    | \$ 103.8   | \$ -          | \$ -       | \$ 851.2 |
| 6.01      | 3     | Crewed Vehicle Management                      | \$ 76.0  | \$ 76.0              | \$ -                 | \$ 12.6     | \$ -       | \$ -          | \$ -       | \$ 76.0  |
| 6.02      | 3     | Crewed Vehicle Systems Engineering             | \$ 5.6   | \$ 84.4              | \$ -                 | \$ 17.0     | \$ -       | \$ -          | \$ -       | \$ 5.6   |
| 6.03      | 3     | Crewed Vehicle Product Assurance               | \$ -     | \$ -                 | \$ -                 | \$ -        | \$ -       | \$ -          | \$ -       | \$ -     |
| 6.10      | 3     | Crewed Vehicle                                 | \$ 558.1 | \$ 429.1             | \$ 120.3             | \$ 92.5     | \$ 83.4    | \$ -          | \$ -       | \$ 641.5 |
| --        | 4     | Primary Crew Structures                        | \$ 225.8 | \$ 202.6             | \$ 23.2              | \$ 17.9     | \$ 17.9    | \$ -          | \$ -       | \$ 243.6 |
| --        | 5     | Fuselage/Body                                  | \$ -     | \$ -                 | \$ -                 | \$ -        | \$ -       | \$ -          | \$ -       | \$ -     |
| --        | 5     | Capsule Structures                             | \$ 225.8 | \$ 202.6             | \$ 23.2              | \$ 17.9     | \$ 17.9    | \$ -          | \$ -       | \$ 243.6 |
| --        | 4     | Tanks  | \$ 27.5  | \$ 20.0              | \$ 7.5               | \$ 5.8      | \$ 5.8     | \$ -          | \$ -       | \$ 33.2  |
| --        | 5     | Fuel Tank                                      | \$ 12.4  | \$ 9.0               | \$ 3.4               | \$ 2.6      | \$ 2.6     | \$ -          | \$ -       | \$ 15.0  |
| --        | 5     | Oxidizer Tank                                  | \$ 15.1  | \$ 11.0              | \$ 4.1               | \$ 3.2      | \$ 3.2     | \$ -          | \$ -       | \$ 18.2  |
| --        | 4     | Mechanisms                                     | \$ -     | \$ -                 | \$ -                 | \$ -        | \$ -       | \$ -          | \$ -       | \$ -     |
| --        | 5     | Thrust Vector/Flight Control                   | \$ -     | \$ -                 | \$ -                 | \$ -        | \$ -       | \$ -          | \$ -       | \$ -     |
| --        | 5     | Mechanisms-Other                               | \$ -     | \$ -                 | \$ -                 | \$ -        | \$ -       | \$ -          | \$ -       | \$ -     |
| --        | 4     | Main Propulsion Systems                        | \$ 15.7  | \$ 14.9              | \$ 0.8               | \$ 0.6      | \$ 0.6     | \$ -          | \$ -       | \$ 16.3  |
| --        | 4     | Propulsion                                     | \$ 17.7  | \$ 1.3               | \$ 7.7               | \$ 5.9      | \$ 5.9     | \$ -          | \$ -       | \$ 23.6  |
| --        | 5     | Liquid Engines                                 | \$ 11.2  | \$ -                 | \$ 2.4               | \$ 1.9      | \$ 1.9     | \$ -          | \$ -       | \$ 13.0  |
| --        | 5     | Reaction Control/Orb Maneuv Sys                | \$ 6.5   | \$ 1.3               | \$ 5.2               | \$ 4.0      | \$ 4.0     | \$ -          | \$ -       | \$ 10.5  |
| --        | 4     | Avionics                                       | \$ -     | \$ -                 | \$ -                 | \$ -        | \$ -       | \$ -          | \$ -       | \$ -     |
| --        | 5     | Guidance, Nav, & Control                       | \$ -     | \$ -                 | \$ -                 | \$ -        | \$ -       | \$ -          | \$ -       | \$ -     |
| --        | 5     | Telemetry & Tracking                           | \$ -     | \$ -                 | \$ -                 | \$ -        | \$ -       | \$ -          | \$ -       | \$ -     |
| --        | 5     | CCDH   | \$ -     | \$ -                 | \$ -                 | \$ -        | \$ -       | \$ -          | \$ -       | \$ -     |
| --        | 4     | Electric Power                                 | \$ 157.7 | \$ 145.7             | \$ 11.9              | \$ 9.2      | \$ -       | \$ -          | \$ -       | \$ 157.7 |
| --        | 4     | Crew Systems                                   | \$ 113.8 | \$ 44.7              | \$ 69.2              | \$ 53.2     | \$ 53.2    | \$ -          | \$ -       | \$ 167.1 |
| --        | 4     | Software                                       | \$ -     | \$ -                 | \$ -                 | \$ -        | \$ -       | \$ -          | \$ -       | \$ -     |
| --        | 5     | Flight Software                                | \$ -     | \$ -                 | \$ -                 | \$ -        | \$ -       | \$ -          | \$ -       | \$ -     |
| --        | 5     | Ground Software                                | \$ -     | \$ -                 | \$ -                 | \$ -        | \$ -       | \$ -          | \$ -       | \$ -     |
| 6.60      | 3     | Integration, Assembly, Checkout                | \$ 16.0  | \$ 16.0              | \$ -                 | \$ 20.4     | \$ 20.4    | \$ -          | \$ -       | \$ 36.4  |
| 6.70      | 3     | System Test Operations                         | \$ 67.1  | \$ 67.1              | \$ -                 | \$ -        | \$ -       | \$ -          | \$ -       | \$ 67.1  |
| 6.80      | 3     | Ground Segment                                 | \$ 24.6  | \$ 21.2              | \$ -                 | \$ -        | \$ -       | \$ -          | \$ -       | \$ 24.6  |
| 6.80.01   | 4     | Ground/Test Support Equip                      | \$ 19.0  | \$ 19.0              | \$ -                 | \$ -        | \$ -       | \$ -          | \$ -       | \$ 19.0  |
| 6.80.02   | 4     | Tooling  | \$ 5.6   | \$ 2.2               | \$ -                 | \$ -        | \$ -       | \$ -          | \$ -       | \$ 5.6   |
| 6.80.03   | 4     | Facilities                                     | \$ -     | \$ -                 | \$ -                 | \$ -        | \$ -       | \$ -          | \$ -       | \$ -     |
| 6.80.04   | 4     | Launch Operations                              | \$ -     | \$ -                 | \$ -                 | \$ -        | \$ -       | \$ -          | \$ -       | \$ -     |
| 6.80.05   | 4     | Flight Operations                              | \$ -     | \$ -                 | \$ -                 | \$ -        | \$ -       | \$ -          | \$ -       | \$ -     |
| 7.0       | 2     | Mission Operations System (MOS)                | \$ -     | \$ -                 | \$ -                 | \$ -        | \$ -       | \$ -          | \$ -       | \$ -     |
| 8.0       | 2     | Launch Vehicle/Services                        | \$ 145.1 | \$ -                 | \$ -                 | \$ -        | \$ -       | \$ -          | \$ -       | \$ 145.1 |
| 9.0       | 2     | Ground Data System (GDS)                       | \$ -     | \$ -                 | \$ -                 | \$ -        | \$ -       | \$ -          | \$ -       | \$ -     |
| 10.0      | 2     | System Integration, Assembly, Test & Check Out | \$ -     | \$ -                 | \$ -                 | \$ -        | \$ -       | \$ -          | \$ -       | \$ -     |
| 11.0      | 2     | Education & Public Outreach                    | \$ -     | \$ -                 | \$ -                 | \$ -        | \$ -       | \$ -          | \$ -       | \$ -     |

|          |            |                  |
|----------|------------|------------------|
| Reserves | Reserves % | Total w/Reserves |
|          | 0%         | \$ 996.3         |

Figure 6.2: PCEC Work Breakdown Structure Results

The PCEC estimate is able to factor in the cost of RD in addition to testing, operations and launch vehicle. The analysis was done specifically considering data from previous crewed spacecraft with life support and hypergolic engine systems. PCEC also factors in inflation based on its own model for the FY2021. The final cost estimate for the entire EEV architecture was \$996 million. With this budget, the EEV's mission is feasible, however with very little reserve money, delays and additional costs down the line would be very difficult to work around.

# Chapter 7

## Conclusions

HAMMER is a crewed, sample collection mission to the Martian Moons Phobos and Deimos. HAMMER aims to push the envelop of long duration space missions in the Martian planetary region. The mission's architecture is inspired by *Perseverance*, *MMX*, *ISS*, *LEM*, and *Philae* missions to accurately and comprehensively propose a feasible spacecraft that can deploy, traverse, and sample on the Martian moons whilst sustaining two astronauts. The micro-gravity environment on the small-body moons is the key challenge of this mission. HAMMER's architecture attempts to mitigate the effects of the micro-gravity and potentially electrostatic-charged environment, while also utilizing these hurdles to incorporate original designs that use the unique environment towards the mission's advantage.

To fulfill HAMMER's scientific objectives, a coring and excavation sampling system is used to collect surface and subsurface mineral samples. The coring sampling system, derived from *Perseverance*, collects a core sample and hands it off to a choreographed robotic system which transports the sample to its containment unit. The excavation sampling system, an original system derived from various *NASA* and *Honeybee* robotics, employs a mechanized sphere which doubles as a sampler and containment unit as it encapsulates interesting mineral areas and rocks on the moons' surfaces.

HAMMER's contribution to the scientific community will outreach planetary geological information. The unique solutions implemented in HAMMER's EEV will provide knowledge and experience in crewed, long-duration missions. It will also supply insight on maintaining life support, propulsion, sampling, power, and communication subsystems in an low-gravity environment. In closing, HAMMER has the potential to serve the greater Space community by paving a path in deep space missions.

## 7.1 Compliance Matrix

| #     | Requirement  | Compliant? | Page Number                    |
|-------|--|------------|--------------------------------|
| RFP-1 | Design an Exploration Vehicle (EEV) for the Martian Moons: Phobos and Deimos   | Yes        | 26                             |
| RFP-2 | Research and define appropriate scientific objectives for the crew to during the mission sortie, to include the sample retrieval at the destination  | Yes        | 8                              |
| RFP-3 | Design and define the mission operations, including orbit transfer, station keeping, and other maneuvers necessary for mission sortie  | Yes        | 14                             |
| RFP-4 | Perform trade studies on vehicle system options at the system and subsystem level to demonstrate the fitness of the chosen vehicle design. It is highly desirable to use technologies that are already demonstrated on previous programs or currently in the NASA technology development portfolio | Yes        | 36, 45, 70                     |
| RFP-5 | Describe in detail how the vehicle will be deployed to Mars in preparation for the crew arrival.   | Yes        | 14                             |
| RFP-6 | Discuss selection of subsystem components and the values of each of the selection and how the design requirements drove the selection of the subsystem   | Yes        | 35, 41, 46, 49, 58, 63, 66, 72 |
| RFP-7 | The cost for the vehicle shall not exceed \$1 Billion US Dollar (in FY21), including the launch cost.  | Yes        | 85                             |

Table 7.1: Compliance Matrix showing adherence to all Design Requirements and Constraints from the RFP

| Required Deliverables                | Page(s) Location |
|--------------------------------------|------------------|
| (1) Requirements Definition          | 7                |
| (2) Concept of Operations            | 13               |
| (3) Trade Studies                    | 36, 45 70        |
| (4) Design Integration and Operation | 29, 32, 84       |
| (5) Cost Estimate                    | 86               |
| (6) Schedule                         | 19               |
| (7) Executive Summary                | 1                |
| (8) References                       | iv               |

Table 7.2: Location of all deliverables required by the RFP

# References

- [1] Fujiya, Wataru et al., ‘Analytical protocols for Phobos regolith samples returned by the Martian Moons eXploration (MMX) mission’, in: *Earth, Planets and Space* 73 (Dec. 2021), DOI: 10.1186/s40623-021-01438-9.
- [2] Eberhardt, P. et al., ‘Trapped Solar Wind Noble Gases, Kr<sup>81</sup>/Kr Exposure Ages and K/Ar Ages in Apollo 11 Lunar Material’, in: *Science* 167.3918 (1970), pp. 558–560, DOI: 10.1126/science.167.3918.558.
- [3] Wieler, Rainer et al., ‘Secular changes in the xenon and krypton abundances in the solar wind recorded in single lunar grains’, in: (1996).
- [4] Nagao, Keisuke et al., ‘Irradiation history of itokawa regolith material deduced from noble gases in the hayabusa samples’, English, in: *Science* 333.6046 (Aug. 2011), pp. 1128–1131, ISSN: 0036-8075, DOI: 10.1126/science.1207785.
- [5] Park, Jisun et al., ‘40 Ar/ 39 Ar age of material returned from asteroid 25143 Itokawa’, in: *Meteoritics Planetary Science* 50 (Nov. 2015), n/a–n/a, DOI: 10.1111/maps.12564.
- [6] Jourdan, F. et al., ‘Collisional history of asteroid Itokawa’, in: *Geology* 45 (Sept. 2017), pp. 819–822, DOI: 10.1130/G39138.1.
- [7] Rivkin, Andrew S. et al., ‘Hydrated Minerals on Asteroids: The Astronomical Record’, in: 2003.
- [8] Greenwood, James et al., ‘Hydrogen isotope evidence for loss of water from Mars through time’, in: *Geophysical Research Letters - GEOPHYS RES LETT* 35 (Mar. 2008), DOI: 10.1029/2007GL032721.
- [9] Rochette, Pierre et al., ‘Pyrrhotite and the remanent magnetization of SNC meteorites: A changing perspective on Martian magnetism’, in: *Earth and Planetary Science Letters* 190 (July 2001), pp. 1–12, DOI: 10.1016/S0012-821X(01)00373-9.
- [10] “Moon Surface Wallpapers (used in renderings)”, URL: <https://wallpaperaccess.com/moon-surface>.
- [11] *Trajectory Browser*, URL: [https://trajbrowser.arc.nasa.gov/..](https://trajbrowser.arc.nasa.gov/)
- [12] Committee on the Planetary Science and Astrobiology Decadal Survey, *Origins, Worlds, and Life: A Decadal Strategy for Planetary Science and Astrobiology 2023-2032*, URL: <https://nap.nationalacademies.org/catalog/26522/origins-worlds-and-life-a-decadal-strategy-for-planetary-science>.
- [13] Pratt, William and Hopkins, Joshua, *Comparison of Deimos and Phobos as Destinations for Human Exploration and Identification of Preferred Landing Sites*, 2011.
- [14] G., Kitmacher, *Reference guide to the International Space Station*, 2006.
- [15] "Breon, S R", *Robotic Refueling Mission 3 overview*, 2018.
- [16] Wertz Everett, Puschell, *Space Mission Engineering: The New SMAD (Space Technology Library, Vol. 28), First Edition*.
- [17] *2080<sub>A</sub>STC*ompendium, URL: [https://www.faa.gov/about/office\\_org/headquarters\\_offices/ast/media/2018\\_AST\\_Compndium.pdf](https://www.faa.gov/about/office_org/headquarters_offices/ast/media/2018_AST_Compndium.pdf).
- [18] Witt, Monica, ‘NASA Awards Launch Services Contract for Europa Clipper Mission’, in: (2021), URL: <https://www.nasa.gov/press-release/nasa-awards-launch-services-contract-for-europa-clipper-mission>.



- [19] Sensoror., *STIM-377H*. URL: <https://www.sensoror.com/products/inertial-measurement-units/stim377h/>.
- [20] Aerospace., Ball, *Star Trackers*, URL: <https://www.ball.com/aerospace/markets-capabilities/capabilities/technologies-components/star-trackers>.
- [21] Garmin, *GRA 5500*, URL: <https://www.garmin.com/en-US/p/135561#specs>.
- [22] Systems, NewSpace, *Sun Sensors*, URL: <https://www.newspacesystems.com/portfolio/sun-sensors/>.
- [23] EO, *ISS Utilization: STORRM (Sensor Test for Orion RelNav Risk Mitigation)*, URL: <https://earth.esa.int/web/eoportal/satellite-missions/i/iss-storrm>.
- [24] al, Wählisch et, 'Phobos and Deimos Cartography', in: *Planetary and Space Science* 102 (2014), DOI: 10.1016/j.pss.2013.05.012, URL: <https://www.sciencedirect.com/science/article/pii/S0032063313001293>.
- [25] Barker, S., *Command and Data Handling (CDh) Subsystem*.
- [26] *What is MIL-STD-1553?*, 2021, URL: [https://www.milstd1553.com/..](https://www.milstd1553.com/)
- [27] Toth Rajupet, Squire Volbers Zhou Li Sankaran Jacks, *Electrostatic charging of wind-blown dust and implication on dust transport*. URL: [https://www.e3s-conferences.org/articles/e3sconf/pdf/2019/25/e3sconf\\_caduc2019\\_02011.pdf](https://www.e3s-conferences.org/articles/e3sconf/pdf/2019/25/e3sconf_caduc2019_02011.pdf).
- [28] Krauss Horanyi, Robertson, *Modeling the formation of electrostatic discharges on Mars*, URL: <https://agupubs-onlinelibrary-wiley-com.ezproxy.lib.utexas.edu/doi/pdfdirect/10.1029/2004JE002313>.
- [29] Clark, John D., *Ignition!: An informal history of liquid rocket propellants*, 1972.
- [30] Steincamp, Lee, 'Reliability analysis techniques for engine-out failures in main propulsion systems', in: (2012), URL: <https://arc.aiaa.org/doi/pdf/10.2514/6.1992-1337>.
- [31] Huzel and Huang, *Modern Engineering for Design of Liquid Propellant Rocket Engines, Revised*, AIAA (American Institute of Aeronautics Astronautics), 1992.
- [32] Dodd', 'Tim, 'Is SpaceX's Raptor Engine the king of rocket engines?', in: (2019), URL: <https://everydayastronaut.com/raptor-engine/>.
- [33] Tsiolkovsky, Konstantin, 'Reactive Flying Machines', in: (1954).
- [34] Sutton, George P. and Biblarz, Oscar, *Rocket Propulsion Elements, Ninth Edition*, Wiley, 2016.
- [35] Rocketdyne, Aerojet, *In-Space Propulsion Data Sheets*, URL: [https://www.rocket.com/sites/default/files/documents/In-Space%20Data%20Sheets\\_7.19.21.pdf](https://www.rocket.com/sites/default/files/documents/In-Space%20Data%20Sheets_7.19.21.pdf).
- [36] *Composites carry the Curiosity rover to a safe Mars landing 2014*, 2014, URL: <https://www.compositesworld.com/articles/composites-carry-the-curiosity-rover-to-a-safe-mars-landing..>
- [37] *The Lander Structure*, URL: <https://mars.nasa.gov/mer/mission/spacecraft/entry-descent-and-landing-configuration/lander-structure/>.
- [38] *SLA-561*, URL: <https://www.lockheedmartin.com/content/dam/lockheed-martin/space/documents/thermal/SLA-56120Product20Information.pdf>.
- [39] University, Brown and Design, Rhode Island School of, *TEST-RAD: Tufted Electrostatic Solution to Regolith Adhesion Dilemma*, URL: <https://bigidea.nianet.org/wp-content/uploads/Brown-RISD-Final-Technical-Paper-2021-BIG-Idea.pdf>.
- [40] Sahinoz, Ahmet, 'Landing gear design and stability evaluation of a lunar lander', in: (2012), DOI: 10.13140/RG.2.2.13160.83202, URL: [https://www.researchgate.net/publication/338209202\\_Landing\\_Gear\\_Design\\_and\\_Stability\\_Evaluation\\_of\\_a\\_Lunar\\_Lander](https://www.researchgate.net/publication/338209202_Landing_Gear_Design_and_Stability_Evaluation_of_a_Lunar_Lander).

- [41] Team, CalTech, *Habitat Orientable Modular Electrodynamical Shield*, URL: <https://bigidea.nianet.org/wp-content/uploads/CalTech-Final-Technical-Paper-2021-BIG-Idea.pdf>.
- [42] Rogers, William F., *APOLLO EXPERIENCE REPORT - LUNAR MODULE LANDING GEAR SUBSYSTEM*, 1972, URL: <https://citeseerx.ist.psu.edu/viewdoc/download?doi=10.1.1.448.7199&rep=rep1&type=pdf>.
- [43] Malcolm M, Paul Sellmann, *GENERAL CONSIDERATIONS FOR DRILL SYSTEM DESIGN*, 1975.
- [44] R Ramsley, James W Head kenneth, *The Origins and Geological Histories of Deimos and Phobos: Hypotheses and Open Questions*, 2021.
- [45] Philip C, Justin S Kris Z, *ROPEC – ROTary PErussive Coring Drill for Mars Sample Return*, 2014.
- [46] *Life Support Baseline Values and Assumptions Document - NASA Technical Reports Server (NTRS)*, URL: <https://ntrs.nasa.gov/citations/20150002905>.
- [47] *LiSTOT - Technical University of Munich - Chair of Astronautics*, URL: <https://www.asg.ed.tum.de/en/lrt/research-at-the-chair-of-astronautics/exploration-technologies/listot/>.
- [48] *Astronaut Cartoon*, 2017, URL: <https://imgbin.com/png/GtwjRCEJ/astronaut-cartoon-png>.
- [49] Walter, Ulrich, *Bemannte Raumfahrt, Lecture 04: Life Support Systems 1*, 2020.
- [50] Green Robert, Agui Juan et al., *International Space Station (ISS) Bacterial Filter Elements (BFEs): Filter Efficiency and Pressure Drop Testing of Returned Units*, 2017.
- [51] *ACI SM-501-N Smoke Detector*, 2022, URL: [www.energycontrol.com](http://www.energycontrol.com).
- [52] Arkin R, Griffin T et al., *Space Applications of Mass Spectrometry*, 2010.
- [53] Yates Stephen, Kamire Rebecca et al., *Scale-up of the Carbon Dioxide Removal by Ionic Liquid Sorbent (CDRILS) System*, 2019.
- [54] Perry J, Cole H El-Lessy H, *An Assessment of the International Space Station's Trace Contaminant Control Subassembly Process Economics*, 2005.
- [55] Hasan M, Lutful K, *Conceptual Design of a Condensing Heat Exchanger for Space Systems Using Porous Media*, 2005.
- [56] Rodriguez, Branelle and Young, Gina, *Development of the International Space Station Fine Water Mist Portable Fire Extinguisher*, 2013.
- [57] *Space Food Packaging Facts*, URL: <https://www.eriesd.org/cms/lib/PA01001942/Centricity/Domain/1041/Space%20food%20packagingbrochure.pdf>.
- [58] *Apollo 11 Mission Report*, URL: <https://ntrs.nasa.gov/api/citations/19710015566/downloads/19710015566.pdf>.
- [59] *Spacecraft S-band Transponder*, URL: <https://www.l3harris.com/all-capabilities/spacecraft-s-band-transponder..>
- [60] *S amp; C dual band diplexers*, URL: <https://www.southwestantennas.com/products/filter-modules-diplexers-triplexers/s-c-dual-band-diplexers..>
- [61] *Optical delay line - ODL radar testing amp; calibrating solutions*, URL: [https://rfoptic.com/optical-delay-line-up-to-40ghz/?gclid=Cj0KCQiA15yNBhDTARIsAGnwe0UqF5ov8Z-8l2u8eUiiQ8D3o9-h-y97Tflm5t0EzhIEc6saK6cvnxUaA13AEALw\\_wcB..](https://rfoptic.com/optical-delay-line-up-to-40ghz/?gclid=Cj0KCQiA15yNBhDTARIsAGnwe0UqF5ov8Z-8l2u8eUiiQ8D3o9-h-y97Tflm5t0EzhIEc6saK6cvnxUaA13AEALw_wcB..)
- [62] Ainich Boeringa, Feld Koeing Reed Rittenhouse Thomasson Tomnek, *Contaminant Ultrasonic Removal via Vibration Ejection from Solar Cells*, URL: <https://bigidea.nianet.org/wp-content/uploads/Missouri-SandT-Final-Technical-Paper-2021-BIG-Idea.pdf>.

- [63] Kutter, Bernard, *A Practical, Affordable Cryogenic Propellant Depot based on ULA's Flight Experience*, URL: <http://www.ulalaunch.com/docs/publications/APracticalAffordableCryogenicPropellantDepotBasedonULAsFlightExperience20087644.pdf>.
- [64] Fab., Orbit, "*Products - Orbit Fab: Gas Stations in Space™.*"
- [65] NASA, *Robotic Refueling Mission (RRM)*.
- [66] Foust, Jeff, *Dynetics to use in-space refueling for NASA lunar lander*, URL: <https://spacenews.com/dynetics-to-use-in-space-refueling-for-nasa-lunar-lander/>.
- [67] *PCEC - Project Cost Estimating Capability | NASA*, URL: [https://www.nasa.gov/offices/ocfo/functions/models\\_tools/PCEC/](https://www.nasa.gov/offices/ocfo/functions/models_tools/PCEC/).

# Appendix A

## Definitions

**HAMMER:** Human Assisted Martian Moons Explore and Return  
**NASA:** National Aeronautics and Space Administration.  
**EEV:** Exploration Excursion Vehicle.  
**DST:** Deep Space Transport.  
**EVA:** Extravehicular Activity.  
**Ar:** Argon.  
**Rb:** Rubidium.  
**Sr:** Strontium.  
**U:** Uranium.  
**Pb:** Lead.  
**CM:** CM Grouping of Chondrites.  
**Ci:** Ci Grouping of Chondrites.  
**CR:** CR Grouping of Chondrites.  
**DSAC:** Deep Space Atomic Clock.  
**OIB:** Orbital Insertion Burn.  
**IDA:** International Docking Adapter.  
 **$\Delta V$ :** Change in velocity.  
**RCS:** Reaction Control System.  
**ISS:** International Space Station.  
**GNC:** Guidance, Navigation, and Control subsystem.  
**CDH:** Command and Data Handling subsystem.  
**PROP:** Propulsion subsystem.  
**STRUC:** Structures subsystem.  
**PAY:** Payload subsystem.  
**LSS/ECLSS:** Life Support Systems/Environmental Control and Life Support Systems subsystem.  
**COMM:** Communications subsystem.  
**POW:** Power subsystem.  
**TCS:** Thermal Control subsystem.  
**DSN:** Deep Space Network.  
**EKF:** Extended Kalman Filter.  
**IMU:** Inertial Measurement Unit.  
**DRNS:** Docking Relative Navigation System.  
**TRN:** Terrain Relative Navigation.  
**LIDAR:** Laser Imaging, Detection and Ranging.  
**LP:** Linear Program.  
**ESCD:** Electrostatic Charge Defence System.  
**HOMES:** Habitat Orientable Modular Electrodynamic Shield.  
**TEST-RAD:** Tufted Electrostatic Solution To Regolith Adhesion Dilemma.  
**SRAM:** Static Random Access Memory.  
**CURVES:** Contaminant Ultrasonic Removal via Vibration Ejection from Solar Cells.  
**EEPROM:** Electrically Erasable Programmable Read Only Memory.  
**USO:** Ultra-Stable Oscillator.  
**MMH:** Monomethyl Hydrazine.  
**UDMH:** Unsymmetrical Dimethyl Hydrazine.  
**NTO:** Dinitrogen Tetroxide.  
 **$I_{sp}$ :** Specific impulse [s], measures rocket engine efficiency.  
**QD:** Quick Disconnects.  
**MMX:** Martian Moons eXplorer (JAXA space probe in development).  
**AFE:** Analog Front-End Driver.  
**ADC:** Attitude Determination and Control.  
**TENGOO-E:** Telescopic Nadar Imager for Geomorphology  
**OROCHI:** Optical Radiometer Composed of Chromatic Imagers.  
**CCD:** Charged-Coupled Device.  
**MSA:** Mass Spectrum Analyzer.  
**CM-d:** Crew Member Days.  
**FD&S:** Fire Detection and Suppression.  
**HEPA:** High-Efficiency Particulate Absorbing Filter.  
**LiOH:** Lithium Hydroxide.  
**4BMS:** Four Bed Molecular Sieve.  
**CDRILS:** Carbon Dioxide Removal by Ionic Liquid Sorbent.  
**TCCS:** Trace Contaminant Control System.  
**CHX:** Condensing Heat Exchanger.  
**LiSTOT:** Life Support Trade Off Tool.  
**ESM:** Equivalent System Mass.  
**MCA:** Multi-Criteria-Approach.  
**TRL:** Technology Readiness Level.  
**CAD:** Computer Assisted Design.  
**RF:** Radio Frequency.  
**ODL:** Open and Distance Learning.  
**RFP:** Request For Proposal.  
**RAFTI:** Rapidly Attachable Fluid Transfer Interface.  
**RRM3:** Robotic Refueling Mission 3.